

UNIVERSITY OF TARTU
Faculty of Science and Technology
Institute of Physics

Helen Asuküla

**QUASINORMAL MODES OF SCHWARZSCHILD BLACK HOLES IN
1-PARAMETER NEW GENERAL RELATIVITY**

Master's thesis (30 ECTS)

Physics

Supervisors:
Manuel Hohmann, PhD
Christian Pfeifer, PhD
João Luís Rosa, PhD

Tartu 2021

Quasinormal modes of Schwarzschild black holes in 1-parameter New General Relativity

In this thesis, we examine quasinormal modes of Schwarzschild black holes in a theory of gravity called 1-parameter new general relativity. We start with an introduction to quasinormal modes and review how quasinormal modes of Schwarzschild black holes are derived in general relativity. There the axial and polar parity components of first-order metric perturbations are used to find the Regge-Wheeler and Zerilli equations. Then, the main concepts of teleparallel theories of gravity are introduced and we focus on 1-parameter new general relativity. The calculations involve first finding the background and first-order perturbed field equations. The background equations are then analysed to fix certain functions in the background tetrad. Finally, we find the axial and polar perturbed field equations in one branch of solutions, where we see that the symmetric quasinormal spectrum coincides with general relativity, the antisymmetric axial modes are generated by the symmetric perturbations and the antisymmetric polar modes remain undefined.

Keywords: quasinormal modes, teleparallel theories of gravity

CERCS: P190 – Mathematical and general theoretical physics, classical mechanics, quantum mechanics, relativity, gravitation, statistical physics, thermodynamics.

Schwarzschildi mustade aukude kvaasi-normaalsed režiimid 1-parameetriga uues üldrelatiivsusteoorias

Selles magistritöös me uurime Schwarzschildi mustade aukude kvaasi-normaalseid režiime gravitatsiooniteoorias, mida nimetatakse 1-parameetriga uueks üldrelatiivsusteooriaks. Me alustame sissejuhatusega kvaasi-normaalsesse režiimidesse ning seletame, kuidas Schwarzschildi mustade aukude kvaasi-normaalsed režiimid tuletatakse üldrelatiivsusteoorias. Selle raames kasutatakse meetrika esimest järku häirituse komponente, mis on aksiaalse ja polaarse paarsusega, Regge-Wheeleri ja Zerilli võrrandite leidmiseks. Seejärel antakse ülevaade teleparalleelsete gravitatsiooniteooriate põhiideedest ning me keskendume 1-parameetriga uuele üldrelatiivsusteooriale. Arvutused hõlmavad esmalt tausta ja esimest järku häiritud väljavõrrandite leidmist. Tausta võrrandeid analüüsitakse selleks, et fikseerida teatud tausta-tetraadi funktsioonid. Me lõpuks leiame aksiaalsed ja polaarsed häiritud väljavõrrandid ühes lahenduste harus, kus me näeme, et sümmeetriline kvaasi-normaalne spekter ühtib üldrelatiivsusteooriaga, antisümmeetrilised aksiaalsed režiimid tekivad sümmeetriliste häirituste kaudu ja antisümmeetrilised polaarsed režiimid jäävad defineerimata.

Märksõnad: kvaasi-normaalsed režiimid, teleparalleelsed gravitatsiooniteooriad

CERCS: P190 – Matemaatiline ja üldine teoreetiline füüsika, klassikaline mehaanika, kvantmehaanika, relatiivsus, gravitatsioon, statistiline füüsika, termodünaamika.

Contents

Introduction	4
1 Ringdown and quasinormal modes	5
2 Quasinormal modes in General Relativity	8
2.1 Linear perturbation theory	10
2.2 Perturbed field equations	13
2.3 Quasinormal frequencies	16
3 Quasinormal modes in New General Relativity	19
3.1 Expanding to linear perturbations	22
3.2 Calculating with SymPy in Jupyter Notebook	25
3.3 Finding the background field equations	26
3.4 Finding the perturbed field equations	30
3.4.1 Axial perturbed equations	31
3.4.2 Polar perturbed equations	33
3.5 Results and discussion	34
Summary	37
Acknowledgements	38
Bibliography	39
A Components of δv_μ, δa_μ and $\delta t_{\mu\nu\rho}$	42
B Equation coefficients $\mathcal{F}_{ij}(r)$	46
C SymPy code in Jupyter Notebook	48
Lihltitsents	64

Introduction

The physical phenomenon of gravity is a curious one – while it is extremely prevalent in our everyday lives, a complete mathematical description of its properties is yet to be found. The first rigorous description was Newton’s law of gravitation, which relates the force of gravitation between two bodies to their masses and inversely to the square of their distance. It is very successful in describing many physical situations, but ultimately proved to have its limits. General relativity (GR), first introduced in 1915, was the next outstanding theory of gravity. It made use of differential geometry and explained gravity as a geometrical property of spacetime, instead of a field on spacetime like the other fundamental interactions. This description states that spacetime is not flat, like assumed by Newton’s law of gravity, but instead curved by the presence of energy and matter. In GR, the curvature of spacetime is then the true nature of the gravitational field [1].

GR has proven itself successful in many experimental tests, where the gravitational field is relatively weak [2]. However, there are still problems that it fails to answer, such as questions regarding the cosmological constant, the mysterious nature of dark matter and dark energy, and the problem of finding a quantum theory of gravity. These lead to the idea that GR may not be the complete picture of gravity, but instead a very good approximation at certain energy levels. There are many different approaches to formulating a new theory of gravity. In order to navigate among them, the expected outcomes of physical observables must be found for all these theories that allow them to be distinguished experimentally [2]. The study of gravitational waves is a very promising avenue as they provide the unique opportunity to explore gravity in the strong-field regime. Gravitational waves are now regularly observed and offer a wide range of applications [3], and will undoubtedly provide even more possibilities in the coming decades [4]. The current gravitational wave measurements come mostly from mergers of binary black holes [3]. The final stage of such mergers is the ringdown, where the resulting distorted black hole relaxes to an equilibrium state. The gravitational waves emitted during this process are characterized by quasinormal modes, which describe the source of the waves. These quasinormal modes and the corresponding frequencies have very specific values in GR [5]. This then motivates the study of quasinormal modes in other theories of gravity to determine how they deviate from GR.

In this thesis, we will explore quasinormal modes of Schwarzschild black holes in the teleparallel theory of gravity called 1-parameter new general relativity (NGR). In Chapter 1, we will introduce the notions of ringdown and quasinormal modes in more detail. Then, Chapter 2 will outline the derivation of quasinormal modes in GR found in literature. Finally, in Chapter 3 we will first introduce the main concepts relevant to NGR. We will then follow the method laid out in Chapter 2 and find the background and perturbed gravitational field equations. We will then analyse them to determine whether any new quasinormal modes appear.

Chapter 1

Ringdown and quasinormal modes

Gravitational waves were first observed by the LIGO detector in 2015 from a merger of binary black holes [6]. Since then, the catalogue of gravitational wave events found by LIGO and Virgo has expanded to 50 events, and the regularity of detections is expected to continue to increase [3]. There are also plans to launch a space-based gravitational wave detector LISA around 2034, which would expand the available range of frequencies in order to observe new types of sources and make it possible to track these mergers far earlier than before [4]. Gravitational waves offer a lot of promise in the field of astronomy and astrophysics, where they can be used for multi-messenger astronomy and the study of neutron stars [3]. In terms of theory, gravitational waves provide a unique opportunity to observe gravity in the strong field regime. So far, tests of GR have been possible only in the weak field regime, so these strong field tests could uncover deviations from GR and offer experimental constraints for alternative theories of gravity [7].

The main source of gravitational wave events in the current catalogue are mergers of binary black holes [3]. The gravitational wave signal produced by these mergers consists of three stages: the inspiral stage describes the binary black holes when they are still separated from each other; the merger phase consists of the black holes fusing together, which forms the peak of the gravitational wave signal and can only be described by numerical simulations; the ringdown stage is the last part of the signal, where the resulting single perturbed black hole relaxes to an equilibrium state [8]. These three stages are indicated in Figure 1.1, which shows the reconstructed signal of the first observed gravitational wave event GW150914, from Ref. [6].

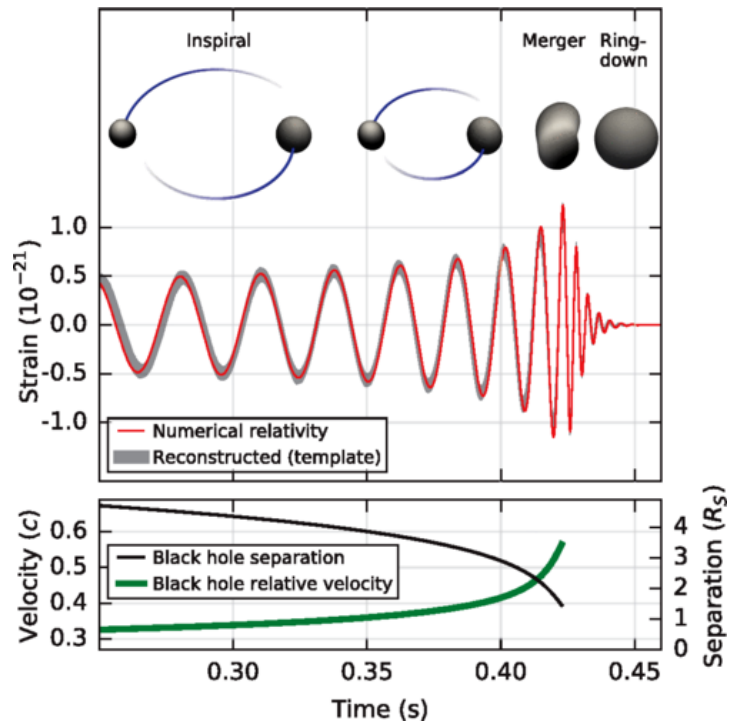


Figure 1.1: The gravitational wave strain amplitude from GW150914 with the three stages of the signal indicated (top), and the effective separation and effective relative velocity of the black holes (bottom) [6].

The ringdown signal is a valuable tool in studying black holes. The frequencies of the ringdown stage can be described in terms of quasinormal frequencies, which are entirely determined by the physical properties of their source. So, this quasinormal spectrum can truly be considered a characteristic of a black hole. This opens a new field of study, where quasinormal modes can be used to find the properties of black holes, sometimes called black hole spectroscopy [8]. Additionally, analysis of just the ringdown signal has certain advantages in terms of data when compared to the inspiral-merger-ringdown (IMR) signal analysis. For example, some tests with the IMR signal require a high signal-to-noise ratio specifically in the inspiral stage [9].

In order to investigate quasinormal modes in more detail, we first need to understand their meaning. Now, normal modes describe a classical oscillating system, where energy conservation is assumed. A general solution describing the system can be written as a superposition of normal modes: $\chi(t, x) = \sum_{n=1}^{\infty} a_n e^{i\omega_n t} \chi_n(x)$, where ω_n is the real-valued normal frequency, a_n is the expansion coefficient and $\chi_n(x)$ is the normal mode state of motion. If the system loses energy, for example by emitting gravitational waves, the oscillations decay in time and the system is instead described by quasinormal modes [10]. They differ from normal modes in a meaningful way as quasinormal modes do not form a complete set. This means that all oscillations of this system produced by some initial perturbations cannot generally be described as a superposition of quasinormal modes. Still, quasinormal modes can be analysed similarly to normal modes if proper boundary conditions are considered [11]. The time-dependent wave equation is [10]

$$\left(\frac{\partial^2}{\partial t^2} - \frac{\partial^2}{\partial x^2} + V(x) \right) \chi(t, x) = 0, \quad (1.1)$$

where $V(x)$ is the potential of the system. If the solution of this equation $\chi(t, x)$ is bounded, meaning that $|\chi(t, x)| < C$ for some finite value $C \in \mathbb{R}$, it can be written in terms of the Laplace transform $\hat{\chi}(\omega, x)$, where ω is complex. This Laplace transform can in turn be defined in terms of a Green function, which consists of two linearly independent solutions $y_1(\omega, x)$ and $y_2(\omega, x)$ to a homogeneous differential equation [10, 12]

$$\left(\frac{\partial^2}{\partial x^2} + \omega^2 - V(x) \right) y_{1,2}(\omega, x) = 0. \quad (1.2)$$

In finite spatial intervals and at late times, the system can be approximated with a finite sum of quasinormal modes in the form [10, 12]

$$\chi(t, x) \approx \sum_n^N a_n e^{-i\omega_n t} y_1(\omega_n, x). \quad (1.3)$$

A significant distinction from normal modes is the fact that the quasinormal frequencies are complex $\omega_n = \text{Re}(\omega_n) + i \text{Im}(\omega_n)$. The real part describes the physical oscillation frequency, and the imaginary part represents the inverse of the damping time of the waveform. For physically

meaningful quasinormal modes, the imaginary part must have the correct sign to ensure decay of the oscillations, which for (1.3) means $\text{Im}(\omega_n) < 0$ [10, 11]. The damping timescale, where the signal has decreased by a factor of e , is defined as $\tau_n = -1/\text{Im}(\omega_n)$ [8]. It is important to pay attention to the sign conventions as quasinormal modes are often introduced with the standard Laplace transformation parameter $s = -i\omega$, such as in [10] and [11]. This leads to the opposite sign in the exponent in (1.3) and consequently, the opposite demands for the sign of $\text{Im}(\omega_n)$.

As seen in (1.3), quasinormal modes form a discrete set with the index n . They are sorted in the order of n such that $n = 0$ stands for the least-dampened mode, called the fundamental mode. It is the longest lived mode and can therefore be used to characterize the entire quasinormal spectrum at sufficiently late times. The modes $n \geq 1$ are called the overtones, where higher values of n mean they are more highly dampened and thus have smaller values of the damping timescale τ_n [8].

The success of describing the quasinormal spectrum through only the fundamental mode relies on balancing finding an appropriately late start-time, when the overtones can be neglected and only the fundamental mode is relevant, but when the weak gravitational wave signal is still reliably accurate [8]. The fundamental frequencies predicted by GR for astrophysical Kerr black holes have been compared to the ringdown signal of GW150914 in [13], where the measured quasinormal oscillations and damping times agreed well with prediction for later start-times. Further late-time analyses of gravitational wave events in [9] also included the first overtone, and the general results were again consistent with GR.

The inclusion of overtones can additionally allow the use of the entire ringdown signal by providing a more accurate description of the waveform [8]. For example, the mass and spin of the final black hole from GW150914 were estimated in [5] and the first overtone was included starting at the peak of the signal. They found that this reduced uncertainty when compared to the late start-time analysis with just the fundamental mode, the reference values being the mass and spin calculated from the full IMR waveform.

In GR, the so-called “no-hair theorem” asserts that these quasinormal modes are fully determined by the mass and angular momentum of the black holes, and the quasinormal spectrum is therefore fixed [8]. Future observations of gravitational waves aim to improve the detection of the ringdown overtones [4], which would provide more accurate values of the quasinormal oscillation frequencies and damping times. It then becomes interesting to investigate quasinormal modes in other theories of gravity, since the properties of gravitational waves are quite diverse in different theories. Many theories find additional polarizations for gravitational waves for example [2]. The study of quasinormal modes would provide both experimental constraints for the theories and highlight fundamental differences in the behaviour of black holes [7]. This is the main motivation of this thesis. However, before we proceed to alternative theories, we are going to first familiarise ourselves with the formulation of quasinormal modes in GR.

Chapter 2

Quasinormal modes in General Relativity

General relativity is the current standard theory of gravity, where the gravitational field is described only by the geometrical curvature defined on the Riemannian spacetime. In this introductory section, we are going to briefly review the fundamentals of GR following the textbook [14]. We will use geometrical units, where the speed of light and Newton's gravitational constant are $c = G = 1$, and denote spacetime indices that run from 0 to 3 with Greek letters.

In GR, geometry of spacetime is described by the metric tensor $g_{\mu\nu}$, which is symmetric in its indices and defines the line element $ds^2 = g_{\mu\nu}dx^\mu dx^\nu$. A completely flat spacetime is described by the Minkowski metric $\eta_{\mu\nu} = \text{diag}(-1, 1, 1, 1)$ and allows the use of Euclidean geometry. This is not the case in general. Vectors and tensors exist in tangent spaces at each point of any spacetime and, for a curved spacetime, moving them between points is not trivial.

Parallel transport of a tensor means keeping it constant while moving it along a path. A connection $\Gamma^\rho_{\mu\nu}$ determines how exactly this is done by defining the covariant derivative ∇_μ , a generalization of the partial derivative. In a flat spacetime, a tensor remains constant along a curve if its components satisfy $\partial_\rho T^{\mu_1 \dots \mu_k}_{\nu_1 \dots \nu_k} = 0$. In a general spacetime, the meaning of remaining "constant" is different. A tensor remains constant in terms of the parallel transport if its components satisfy $\nabla_\rho T^{\mu_1 \dots \mu_k}_{\nu_1 \dots \nu_k} = 0$, where the covariant derivative is defined as

$$\begin{aligned} \nabla_\rho T^{\mu_1 \dots \mu_k}_{\nu_1 \dots \nu_k} = & \partial_\rho T^{\mu_1 \dots \mu_k}_{\nu_1 \dots \nu_k} + \Gamma^{\mu_1}_{\lambda\rho} T^{\lambda \dots \mu_k}_{\nu_1 \dots \nu_k} + \dots + \Gamma^{\mu_k}_{\lambda\rho} T^{\mu_1 \dots \lambda}_{\nu_1 \dots \nu_k} + \\ & - \Gamma^\lambda_{\nu_1\rho} T^{\mu_1 \dots \mu_k}_{\lambda \dots \nu_k} - \dots - \Gamma^\lambda_{\nu_k\rho} T^{\mu_1 \dots \mu_k}_{\nu_1 \dots \lambda}. \end{aligned} \quad (2.1)$$

A connection must therefore be defined on a spacetime for any meaningful physics to be done, because parallel transport is the means by which nearby tensors can be compared. A connection is called metric compatible if the metric is always parallelly transported with respect to it, meaning that $\nabla_\rho g_{\mu\nu} = 0$. This ensures that the inner product of two vectors, including the norm of vectors and orthogonality, is preserved under parallel transport. In a curved spacetime, parallel transport is path-dependent and parallelly transporting a tensor to the same point along different paths will not generally lead to same tensor.

The connection of the Riemannian spacetime is the Levi-Civita connection $\overset{\circ}{\Gamma}^\rho_{\mu\nu}$, which is symmetric in its lower indices, i.e. torsion free, and metric compatible. Its coefficients are uniquely constructed from the metric and are given by the Christoffel symbols

$$\overset{\circ}{\Gamma}^\rho_{\mu\nu} = \frac{1}{2} g^{\rho\kappa} (\partial_\mu g_{\nu\kappa} + \partial_\nu g_{\mu\kappa} - \partial_\kappa g_{\mu\nu}). \quad (2.2)$$

Curvature describes how the components change when a tensor is parallelly transported around an infinitesimal area. The Riemann curvature tensor vanishes only if the spacetime is flat and its components are defined in terms of the connection as

$$R^{\rho}{}_{\sigma\mu\nu} = \partial_{\mu}\overset{\circ}{\Gamma}{}^{\rho}{}_{\nu\sigma} - \partial_{\nu}\overset{\circ}{\Gamma}{}^{\rho}{}_{\mu\sigma} + \overset{\circ}{\Gamma}{}^{\rho}{}_{\mu\kappa}\overset{\circ}{\Gamma}{}^{\kappa}{}_{\nu\sigma} - \overset{\circ}{\Gamma}{}^{\rho}{}_{\nu\kappa}\overset{\circ}{\Gamma}{}^{\kappa}{}_{\mu\sigma}. \quad (2.3)$$

The gravitational interaction is given by field equations that relate curvature on one side, and the distribution of energy and matter, described by the energy-momentum tensor $T_{\mu\nu}$, on the other. The curvature terms are found by contracting the Riemann tensor to define the Ricci tensor and Ricci scalar

$$R_{\mu\nu} = R^{\kappa}{}_{\mu\kappa\nu} \quad \text{and} \quad R = g^{\mu\nu}R_{\mu\nu}. \quad (2.4)$$

They then compose the Einstein tensor $G_{\mu\nu} = R_{\mu\nu} - \frac{1}{2}g_{\mu\nu}R$, which defines Einstein's field equations. They are a set of second order partial differential equations for the metric in the form $G_{\mu\nu} = 8\pi T_{\mu\nu}$, which can be written as

$$R_{\mu\nu} - \frac{1}{2}g_{\mu\nu}R = 8\pi T_{\mu\nu} \quad \text{or} \quad R_{\mu\nu} = 8\pi\left(T_{\mu\nu} - \frac{1}{2}g_{\mu\nu}T\right), \quad (2.5)$$

where T denotes the trace of $T_{\mu\nu}$. The energy momentum tensor vanishes in the absence of energy and matter $T_{\mu\nu} = 0$, and so the field equations in vacuum are simply

$$R_{\mu\nu} = 0. \quad (2.6)$$

The unique non-trivial spherically symmetric solution to the vacuum field equations is the Schwarzschild metric, which describes the gravitational field created by any non-rotating and uncharged spherical body, and in spherical coordinates $x^{\mu} = \{t, r, \theta, \varphi\}$ is described by the line element

$$ds^2 = -\left(1 - \frac{2M_{\bullet}}{r}\right) dt^2 + \left(1 - \frac{2M_{\bullet}}{r}\right)^{-1} dr^2 + r^2 d\theta^2 + r^2 \sin^2 \theta d\varphi^2, \quad (2.7)$$

where M_{\bullet} is the mass of this body. The metric exhibits a true curvature singularity at $r = 0$ and a coordinate singularity at $r = 2M_{\bullet}$, which can be cleared up by choosing a different coordinate system. However, the Schwarzschild radius $r_S = 2M_{\bullet}$ is still significant as the motion of light and massive particles is different inside this radius, and they can never escape beyond this boundary without violating causality. This surface is called the event horizon and any body with a radius r_{\bullet} will collapse into a black hole if $r_{\bullet} = r_S$. The gravitational field of bodies with a radius $r_{\bullet} > r_S$ can also be described by the Schwarzschild metric, but only outside the body in the coordinate region $r > r_{\bullet}$. [14].

Astrophysical black holes have a non-zero angular momentum, and thus are not well described

by the Schwarzschild metric. Instead, they are analyzed with the use of the Kerr metric, which describes spacetime around uncharged black holes with angular momentum [15]. However, rotating bodies do not preserve spherical symmetry and, because of that, the Kerr metric is not diagonal, which leads to much more complicated field equations. Nevertheless, the Schwarzschild metric can be used to approximate relatively slowly rotating bodies, such as the Sun and the Earth [16].

So, we are going to limit ourselves to Schwarzschild black holes in this thesis. The spherical symmetry of the Schwarzschild geometry allows for a much simpler treatment of quasinormal modes as seen in overviews [10] and [11]. Additionally, the search for quasinormal modes requires a solution to the gravitational field equations, and spherically symmetric solutions are more readily available in alternative theories.

2.1 Linear perturbation theory

Gravitational waves are often analyzed in formalism of perturbation theory. The astrophysical situation is described as a superposition of an equilibrium state and a perturbation, which can be the source of gravitational waves [14]. Similarly, quasinormal modes of black holes can be analysed in terms of the metric perturbations. If one assumes that the perturbation is sufficiently small, the higher order terms can be neglected and one can consider only the linear order terms. This is called linear perturbation theory. Following [11], the metric is split into an unperturbed background $\bar{g}_{\mu\nu}$ and a small first-order perturbation $h_{\mu\nu}$

$$g_{\mu\nu} = \bar{g}_{\mu\nu} + h_{\mu\nu}. \quad (2.8)$$

The perturbed inverse metric is $g^{\mu\nu} = \bar{g}^{\mu\nu} - h^{\mu\nu}$. Inserting the perturbed metric into (2.1) and only considering terms linear in $h_{\mu\nu}$, the perturbed Christoffel symbols are

$$\overset{\circ}{\Gamma}{}^{\rho}{}_{\mu\nu} = \overset{\circ}{\Gamma}{}^{\rho}{}_{\mu\nu} + \delta\overset{\circ}{\Gamma}{}^{\rho}{}_{\mu\nu} \quad \text{with} \quad \delta\overset{\circ}{\Gamma}{}^{\rho}{}_{\mu\nu} = \frac{1}{2}\bar{g}^{\rho\kappa}(\bar{\nabla}_{\mu}h_{\nu\rho} + \bar{\nabla}_{\nu}h_{\mu\rho} - \bar{\nabla}_{\rho}h_{\mu\nu}). \quad (2.9)$$

The Ricci tensor can similarly be found in the form $R_{\mu\nu} = \bar{R}_{\mu\nu} + \delta R_{\mu\nu}$. The background Ricci tensor vanishes for the Schwarzschild metric, and so the background field equations are satisfied trivially. The perturbed Einstein's field equations in vacuum are

$$\delta R_{\mu\nu} = \overset{\circ}{\nabla}_{\nu} \delta\overset{\circ}{\Gamma}{}^{\rho}{}_{\mu\rho} - \overset{\circ}{\nabla}_{\rho} \delta\overset{\circ}{\Gamma}{}^{\rho}{}_{\mu\nu} = 0. \quad (2.10)$$

It is now necessary to find the components of the metric perturbation $h_{\mu\nu}$. The spherically symmetric background allows for a decomposition of $h_{\mu\nu}(t, r, \theta, \varphi)$ into separate functions of (t, r) and (θ, φ) [11]. It is useful to define the angular part in terms of the spherical harmonic functions $Y_{\ell m} = Y_{\ell m}(\theta, \varphi)$, which are the eigenfunctions of the Laplace operator ∇^2 on the

2-sphere. The eigenvalue equation and the spherical harmonic functions written explicitly are

$$\nabla^2 Y_{\ell m} = \frac{1}{\sin \theta} \frac{\partial}{\partial \theta} \left(\sin \theta \frac{\partial Y_{\ell m}}{\partial \theta} \right) + \frac{1}{\sin^2 \theta} \frac{\partial^2 Y_{\ell m}}{\partial \varphi^2} = -\ell(\ell+1)Y_{\ell m} \quad \text{with} \quad (2.11)$$

$$Y_{\ell m} = \epsilon_m \sqrt{\frac{(2\ell+1)(\ell-|m|)!}{4\pi(\ell+|m|)!}} P_{\ell m}(\cos \theta) e^{im\varphi},$$

where $P_{\ell m}(\cos \theta)$ are the associated Legendre polynomials and $\epsilon_m = (-1)^m$ for $m > 0$ and $\epsilon_m = 1$ for $m < 0$. The spherical harmonics depend on the angular momentum quantum number ℓ and the azimuthal quantum number m , which take values $\ell = 0, 1, 2, \dots$ and $-\ell \leq m \leq \ell$ [17, pp. 135-139].

However, a decomposition into just the scalar spherical harmonics $Y_{\ell m}$ does not preserve invariance under spatial rotations around the origin $\{t, r, \theta, \varphi\} \rightarrow \{t, r, \theta'(\theta, \varphi), \varphi'(\theta, \varphi)\}$. Under these rotations, the components of the perturbation $h_{\mu\nu}$ transform as scalars, 2-vectors and a 2×2 tensor [11]

$$\begin{aligned} \text{Scalars: } h'_{00} &= h_{00}, & \text{Vectors: } h'_{0a} &= \frac{\partial x^b}{\partial x'^a} h_{0b}, & \text{Tensor: } h'_{ab} &= \frac{\partial x^c}{\partial x'^a} \frac{\partial x^d}{\partial x'^b} h_{cd}. \\ h'_{11} &= h_{11}, & h'_{1a} &= \frac{\partial x^b}{\partial x'^a} h_{1b}. \\ h'_{01} &= h_{01}. \end{aligned} \quad (2.12)$$

Here the latin indices a, b, c take values 2 and 3. The perturbation $h_{\mu\nu}$ must thus be decomposed into tensor harmonics, which are also eigenfunctions of the Laplace operator. Tensor harmonics can be constructed from the spherical harmonics $Y_{\ell m}$ in the form [11, 18]

Scalar tensor harmonic:

$$S_{\ell m} = Y_{\ell m} \quad \text{polar parity } (-1)^\ell, \quad (2.13a)$$

Vector tensor harmonics:

$$1) (\overset{1}{V}_{\ell m})_a = \overset{\gamma_{ab}}{\nabla}_a Y_{\ell m} \quad \text{polar parity } (-1)^\ell, \quad (2.13b)$$

$$2) (\overset{2}{V}_{\ell m})_a = \epsilon_a^b \overset{\gamma_{ab}}{\nabla}_b Y_{\ell m} \quad \text{axial parity } (-1)^{\ell+1}, \quad (2.13c)$$

Second order tensor harmonics:

$$1) (\overset{1}{T}_{\ell m})_{ab} = \overset{\gamma_{ab}}{\nabla}_a \overset{\gamma_{ab}}{\nabla}_b Y_{\ell m} \quad \text{polar parity } (-1)^\ell, \quad (2.13d)$$

$$2) (\overset{2}{T}_{\ell m})_{ab} = \gamma_{ab} Y_{\ell m} \quad \text{polar parity } (-1)^\ell, \quad (2.13e)$$

$$3) (\overset{3}{T}_{\ell m})_{ab} = \frac{1}{2} \left[\epsilon_a^c \overset{\gamma_{ab}}{\nabla}_c \overset{\gamma_{ab}}{\nabla}_b Y_{\ell m} + \epsilon_b^c \overset{\gamma_{ab}}{\nabla}_c \overset{\gamma_{ab}}{\nabla}_a Y_{\ell m} \right] \quad \text{axial parity } (-1)^{\ell+1}, \quad (2.13f)$$

$$4) \quad (T_{\ell m}^4)_{ab} = \epsilon_{ab} Y_{\ell m} \quad \text{axial parity } (-1)^{\ell+1}. \quad (2.13g)$$

Here γ_{ab} is a metric tensor on the unit 2-sphere, $\nabla_a^{\gamma_{ab}}$ is the covariant derivative with respect to this metric and ϵ_{ab} is the totally antisymmetric Levi-Civita tensor

$$\gamma_{ab} = \bar{g}_{ab}/r^2 = \begin{pmatrix} 1 & 0 \\ 0 & \sin^2 \theta \end{pmatrix}, \quad \epsilon_{ab} = \begin{pmatrix} 0 & -\sin \theta \\ \sin \theta & 0 \end{pmatrix}, \quad \epsilon_a{}^b = \begin{pmatrix} 0 & -\frac{1}{\sin \theta} \\ \sin \theta & 0 \end{pmatrix}. \quad (2.14)$$

Each of the tensor harmonics has either axial or polar parity. Parity describes the behaviour of functions under space inversion, which for spherical angles means $(\theta, \varphi) \rightarrow (\pi - \theta, \pi + \varphi)$. A function has 'axial' parity if under such transformation it changes only by a multiplicative factor $(-1)^{\ell+1}$, and it has 'polar' parity if the factor is instead $(-1)^\ell$. This is important, because the background metric and the differential operator in the perturbed field equations are invariant under inversions. This means that the perturbed equations will not mix different parities, and it is possible to distinctly separate [11]

$$h_{\mu\nu} = h_{\mu\nu}^{(\text{axial})} + h_{\mu\nu}^{(\text{polar})}. \quad (2.15)$$

The axial and polar perturbations can be written in terms of the tensor harmonics as [19]

$$h_{\mu\nu}^{(\text{axial})} = \sum_{\ell, m} \begin{pmatrix} 0 & 0 & -h_0(t, r) \frac{1}{\sin \theta} \partial_\varphi & h_0(t, r) \sin \theta \partial_\theta \\ 0 & 0 & -h_1(t, r) \frac{1}{\sin \theta} \partial_\varphi & h_1(t, r) \sin \theta \partial_\theta \\ \text{Sym} & \text{Sym} & \frac{1}{2} h_2(t, r) \frac{1}{\sin \theta} X_{\theta\varphi} & -\frac{1}{2} h_2(t, r) \sin \theta W_{\theta\varphi} \\ \text{Sym} & \text{Sym} & \text{Sym} & -\frac{1}{2} h_2(t, r) \sin \theta X_{\theta\varphi} \end{pmatrix} Y_{\ell m}, \quad (2.16a)$$

$$h_{\mu\nu}^{(\text{polar})} = \sum_{\ell, m} \begin{pmatrix} B(r) H_0(t, r) & H_1(t, r) & c_0(t, r) \partial_\theta & c_0(t, r) \partial_\varphi \\ \text{Sym} & \frac{H_2(t, r)}{B(r)} & c_1(t, r) \partial_\theta & c_1(t, r) \partial_\varphi \\ \text{Sym} & \text{Sym} & r^2 [K(t, r) + G(t, r) \partial_{\theta\theta}] & \frac{1}{2} r^2 G(t, r) X_{\theta\varphi} \\ \text{Sym} & \text{Sym} & \text{Sym} & r^2 \sin^2 \theta [K(t, r) + G(t, r) (\partial_{\theta\theta} - W_{\theta\varphi})] \end{pmatrix} Y_{\ell m}. \quad (2.16b)$$

Here we've defined $X_{\theta\varphi} = 2(\partial_\theta \partial_\varphi - \cot \theta \partial_\varphi)$, $W_{\theta\varphi} = \partial_{\theta\theta} - \cot \theta \partial_\theta - \frac{1}{\sin^2 \theta} \partial_\varphi \partial_\varphi$ and $B(r) = 1 - \frac{2M}{r}$ similarly to [11]. The tensor harmonic $(T_{\ell m}^4)_{ab}$ does not appear in these matrices, because the metric perturbations are symmetric in their indices while the tensor harmonic is antisymmetric.

For the analysis of the quasinormal mode spectrum, one can assume harmonic time dependence $h_0(t, r) = e^{-i\omega t} h_0(r)$ and similarly for all functions of (r, t) . Also, since the problem preserves spherical symmetry, one can restrict the analysis to the case $m = 0$ without loss of generality,

which eliminates φ from the equations [19]. Additionally, the field equations are gauge invariant, which means that they do not change under a coordinate gauge transformation $x'^{\mu} = x^{\mu} + \xi^{\mu}(x^{\alpha})$ with $\xi^{\mu} \ll x^{\alpha}$. Under this coordinate transformation, the perturbation transforms as $h'_{\mu\nu}(x'^{\alpha}) = h_{\mu\nu}(x^{\alpha}) - \nabla_{\nu}\xi_{\mu} - \nabla_{\mu}\xi_{\nu}$. Then, gauge freedom allows a suitable choice of ξ^{μ} to simplify the perturbation [20, p. 967]. The Regge-Wheeler gauge, for axial and polar perturbations respectively, is [11, 19]

$$\xi^{\mu} = (0, 0, \Lambda(t, r)\epsilon^{ab}\partial_b)Y_{\ell m}, \quad \xi^{\mu} = (M_0(t, r), M_1(t, r), M_2(t, r)\gamma^{ab}\partial_b)Y_{\ell m}. \quad (2.17)$$

The factor Λ can be adjusted to annul h_2 and the factors M_0, M_1, M_2 can be adjusted to annul c_0, c_1, G in $h_{\mu\nu}$. Inserting all these assumptions into (2.16), the axial and polar perturbations in the Regge-Wheeler gauge are [19]

$$h_{\mu\nu}^{(\text{axial})} = \sum_{\ell, m} \begin{pmatrix} 0 & 0 & 0 & h_0(r) \sin \theta \partial_{\theta} \\ 0 & 0 & 0 & h_1(r) \sin \theta \partial_{\theta} \\ 0 & 0 & 0 & 0 \\ \text{Sym} & \text{Sym} & 0 & 0 \end{pmatrix} e^{-i\omega t} Y_{\ell m}, \quad (2.18a)$$

$$h_{\mu\nu}^{(\text{polar})} = \sum_{\ell, m} \begin{pmatrix} B(r) H_0(r) & H_1(r) & 0 & 0 \\ \text{Sym} & \frac{H_2(r)}{B(r)} & 0 & 0 \\ 0 & 0 & r^2 K(r) & 0 \\ 0 & 0 & 0 & r^2 \sin^2 \theta K(r) \end{pmatrix} e^{-i\omega t} Y_{\ell m}. \quad (2.18b)$$

2.2 Perturbed field equations

The perturbed field equations can be derived by inserting the $h_{\mu\nu}$ components (2.18) into the field equations (2.10). The axial equations were found and reduced to a one-dimensional wave equation by Regge and Wheeler in [19]. Then, the axial equations were verified and the polar equations corrected by Edelstein and Vishveshwara [21]. Finally, the polar equations were reduced to a one-dimensional wave equation by Zerilli in [22]. This section will summarize the main results of [19], [21] and [22].

The axial case has two unknown functions h_0, h_1 . The perturbed field equations become separable into radial and angular parts

$$\delta R_{\mu\nu} = \delta \mathcal{R}_{\mu\nu}(r) \delta \mathcal{Q}_{\mu\nu}(\theta, \varphi) e^{i\omega t} = 0, \quad (2.19)$$

The axial radial perturbed equations, modified to match earlier notation of this thesis, are

$$\delta\mathcal{R}_{23} = B \frac{dh_1}{dr} + \frac{i\omega}{B} h_0 + \frac{2M_\bullet}{r^2} h_1 \equiv 0, \quad (2.20a)$$

$$\delta\mathcal{R}_{13} = \frac{i\omega}{B} \frac{dh_0}{dr} - \frac{2i\omega}{rB} h_0 + \left[\frac{\ell(\ell+1)}{r^2} - \frac{2}{r^2} - \frac{\omega^2}{B} \right] h_1 \equiv 0, \quad (2.20b)$$

$$\delta\mathcal{R}_{03} = B \frac{d^2 h_0}{dr^2} + i\omega B \frac{dh_1}{dr} - \left[\frac{\ell(\ell+1)}{r^2} - \frac{4M_\bullet}{r^3} \right] h_0 + \frac{2i\omega B}{r} h_1 \equiv 0. \quad (2.20c)$$

The equation $\delta\mathcal{R}_{03} = 0$ can be disregarded as it is a combination of the other two in the form

$$i\omega \delta\mathcal{R}_{03} = \frac{d[B^2 \delta\mathcal{R}_{13}]}{dr} - \frac{(1-3B)B}{r} \delta\mathcal{R}_{13} - \frac{(\ell-1)(\ell+2)B}{r^2} \delta\mathcal{R}_{23}. \quad (2.21)$$

A one-dimensional wave equation can be derived by finding h_0 from $\delta\mathcal{R}_{23} = 0$, and inserting it into $\delta\mathcal{R}_{13} = 0$. To simplify the interpretation of the resulting equation, the radial function h_1 is redefined as

$$\hat{h}_1 \equiv \frac{B h_1}{r}. \quad (2.22)$$

In order to eliminate the first-order derivatives of \hat{h}_1 , the radial coordinate is changed to the so-called tortoise coordinate

$$r_* = r + 2M_\bullet \ln \left(\frac{r}{2M_\bullet} - 1 \right), \quad dr_* = \frac{dr}{B}. \quad (2.23)$$

It has real values only in the relevant coordinate range for quasinormal modes, which is outside the event horizon of the black hole, since the event horizon $r = 2M_\bullet$ is mapped to $r_* = -\infty$ [11].

Following these considerations, the Regge-Wheeler equation is derived as

$$\frac{d^2}{dr_*^2} \hat{h}_1 + (\omega^2 - V_{RW}(r_*)) \hat{h}_1 = 0 \quad \text{with the Regge-Wheeler potential} \quad (2.24)$$

$$V_{RW}(r) = \left(1 - \frac{2M_\bullet}{r} \right) \left(\frac{\ell(\ell+1)}{r^2} - \frac{6M_\bullet}{r^3} \right).$$

We can see that this equation takes the same form as the homogeneous differential equations (1.2), which is used for defining the quasinormal mode solutions.

Now let us turn to the polar field equations. The polar case has four unknown functions H_0 , H_1 , H_2 and K . In order for the angular dependence to factorize in the field equation $\delta R_{22} = 0$, one must impose

$$H_0 = H_2 \equiv H. \quad (2.25)$$

Then, the radial polar perturbed equations are

$$\delta\mathcal{R}_{01} = \frac{dK}{dr} + \frac{\ell(\ell+1)}{2i\omega r^2} H_1 + \frac{r-3M_\bullet}{r^2 B} K - \frac{1}{r} H \equiv 0, \quad (2.26a)$$

$$\delta\mathcal{R}_{02} = B \frac{dH_1}{dr} + \frac{2M_\bullet}{r^2} H_1 + i\omega(K+H) = 0, \quad (2.26b)$$

$$\delta\mathcal{R}_{12} = B \frac{dH}{dr} - B \frac{dK}{dr} + i\omega H_1 + \frac{2M_\bullet}{r^2} H \equiv 0, \quad (2.26c)$$

$$\begin{aligned} \delta\mathcal{R}_{00} = & B^2 \frac{d^2 H}{dr^2} + 2i\omega B \frac{dH_1}{dr} - \frac{2M_\bullet B}{r^2} \frac{dK}{dr} + \frac{2B}{r} \frac{dH}{dr} + \frac{2i\omega(2r-3M_\bullet)}{r^2} H_1 + \\ & - 2\omega^2 K - \left[\omega^2 + \frac{\ell(\ell+1)B}{r^2} \right] H \equiv 0, \end{aligned} \quad (2.26d)$$

$$\begin{aligned} \delta\mathcal{R}_{11} = & B^2 \frac{d^2 H}{dr^2} - 2B^2 \frac{d^2 K}{dr^2} + 2i\omega B \frac{dH_1}{dr} - \frac{2B(2r-3M_\bullet)}{r^2} \frac{dK}{dr} + \frac{2}{r} \frac{dH}{dr} + \\ & + \frac{2i\omega M_\bullet}{r^2} H_1 - \left[\omega^2 - \frac{\ell(\ell+1)B}{r^2} \right] H \equiv 0, \end{aligned} \quad (2.26e)$$

$$\begin{aligned} \delta\mathcal{R}_{22} = & r^2 B \frac{d^2 K}{dr^2} + (4r-6M_\bullet) \frac{dK}{dr} - 2rB \frac{dH}{dr} - 2i\omega r H_1 + \\ & + \left[2 + \frac{\omega^2 r^2}{B} - \ell(\ell+1) \right] K - 2H \equiv 0 \end{aligned} \quad (2.26f)$$

The second order equations can be derived from the first-order equations in the form

$$\begin{aligned} \delta\mathcal{R}_{00} = & \frac{B}{2r^2} \mathcal{A}(r) + B \frac{d(\delta\mathcal{R}_{12})}{dr} + B^2 \frac{d(\delta\mathcal{R}_{01})}{dr} + \frac{3B}{r} \delta\mathcal{R}_{12} + \frac{B(1+3B)}{2r} \delta\mathcal{R}_{01} + \\ & + \left[i\omega + \frac{i\ell(\ell+1)B}{2r^2\omega} \right] \delta\mathcal{R}_{02}, \\ \delta\mathcal{R}_{11} = & -\frac{B}{2r^2} \mathcal{A}(r) + B \frac{d(\delta\mathcal{R}_{12})}{dr} - B^2 \frac{d(\delta\mathcal{R}_{01})}{dr} + \frac{B}{r} \delta\mathcal{R}_{12} - \frac{B(1+3B)}{2r} \delta\mathcal{R}_{01} + \\ & + \left[i\omega - \frac{i\ell(\ell+1)B}{2r^2\omega} \right] \delta\mathcal{R}_{02}, \\ \delta\mathcal{R}_{22} = & -\frac{\mathcal{A}(r)}{2} - r \frac{d(\delta\mathcal{R}_{12})}{dr} + r^2 B \frac{d(\delta\mathcal{R}_{01})}{dr} - \frac{\ell(\ell+1)}{2i\omega} \delta\mathcal{R}_{02} + \frac{r(B+3)}{2} \delta\mathcal{R}_{01}, \end{aligned} \quad (2.27)$$

where $\mathcal{A}(r)$ is the algebraic relation

$$\mathcal{A} = \left[2i\omega r + \frac{\ell(\ell+1)M_\bullet}{i\omega r^2} \right] H_1 + \left[2\lambda + \frac{2M_\bullet(r-3M_\bullet)}{r^2 B} - \frac{2\omega^2 r^2}{B} \right] K - \left[2\lambda + \frac{6M_\bullet}{r} \right] H, \quad (2.28)$$

where $\lambda = \frac{1}{2}(\ell-1)(\ell+2)$. This algebraic relation must vanish, and can be used to replace H in $\delta\mathcal{R}_{01} = 0$ and $\delta\mathcal{R}_{02} = 0$. To obtain a one-dimensional wave equation, the radial coordinate is again changed to the tortoise coordinate and the following redefinitions of H_1 and K are

introduced: $R \equiv H_1/\omega$,

$$\begin{aligned} K &= f(r)\hat{K} + g(r)\hat{R} \quad \text{with} \quad f(r) = \frac{\lambda(\lambda+1)r^2 + 3\lambda M_\bullet r + 6M_\bullet^2}{r^2(\lambda r + 3M_\bullet)}, \quad g(r) = 1, \\ R &= h(r)\hat{K} + k(r)\hat{R} \quad \text{with} \quad h(r) = \frac{i(-\lambda r^2 + 3\lambda M_\bullet r + 3M_\bullet^2)}{(r-2M_\bullet)(\lambda r + 3M_\bullet)}, \quad k(r) = \frac{-ir^2}{(r-2M_\bullet)}. \end{aligned} \quad (2.29)$$

Following these considerations, the Zerilli equation is derived as

$$\begin{aligned} \frac{d^2}{dr_*^2} \hat{K} + (\omega^2 - V_Z(r_*)) \hat{K} &= 0 \quad \text{with the Zerilli potential} \\ V_Z(r) &= \left(1 - \frac{2M_\bullet}{r}\right) \frac{2\lambda^2(\lambda+1)r^3 + 6\lambda^2 M_\bullet r^2 + 18\lambda M_\bullet^2 r + 18M_\bullet^3}{r^3(\lambda r + 3M_\bullet)^2}. \end{aligned} \quad (2.30)$$

2.3 Quasinormal frequencies

The Regge-Wheeler and Zerilli equations actually describe the same physical properties as they are related by the equation [23]

$$\left[\frac{2}{3}\lambda(\lambda+1) - 2M_\bullet i\omega\right] \hat{h}_1 = \left[\frac{2}{3}\lambda(\lambda+1) + \frac{6M_\bullet^2(r-2M_\bullet)}{r^2(\lambda r + 3M_\bullet)}\right] \hat{K} - 2M_\bullet \frac{d^2 \hat{K}}{dr_*^2}. \quad (2.31)$$

Quasinormal frequencies found from equations (2.24) and (2.30) will therefore give the same quasinormal spectrum. So, only the Regge-Wheeler equation can be used for simplicity. There are different techniques for finding quasinormal frequencies, an overview is given in [11]. We will look into two of the most common methods.

A continued fraction method was introduced by Leaver in [24]. The solution to the Regge-Wheeler equation must ensure regularity of the boundary conditions. For the quasinormal problem, the boundary conditions are that $\hat{h}_1 \rightarrow (r-2M_\bullet)^{i\omega}$ as $r \rightarrow 2M_\bullet$ and $\hat{h}_1 \rightarrow r^{-i\omega} e^{-i\omega r}$ as $r \rightarrow \infty$. Adopting a system of units for which $2M_\bullet = 1$, the ansatz satisfying these demands can be written in the form

$$\hat{h}_1 = (r-1)^{i\omega} r^{-2i\omega} e^{-i\omega(r-1)} \sum_{n=0}^{\infty} a_n \left(\frac{r-1}{r}\right)^n, \quad (2.32)$$

where the expansion coefficients a_n are determined recursively by

$$a_0 = 1, \quad (2.33a)$$

$$\alpha_0 a_1 + \beta_0 a_0 = 0, \quad (2.33b)$$

$$\alpha_n a_{n+1} + \beta_n a_n + \gamma_n a_{n-1} = 0 \quad (2.33c)$$

with

$$\begin{aligned}
\alpha_n &= n^2 + (2i\omega + 2)n + 2i\omega + 1, \\
\beta_n &= -[2n^2 + (8i\omega + 2)n - 8\omega^2 + 4i\omega + \ell(\ell + 1) - 3], \\
\gamma_n &= n^2 + 4i\omega n - 4\omega^2 - 4.
\end{aligned} \tag{2.34}$$

To guarantee the convergence of the series in (2.32) at spatial infinity, the coefficients a_n must satisfy an infinite continued fraction relation

$$\frac{a_{n+1}}{a_n} = - \frac{\gamma_{n+1}}{\beta_{n+1} - \frac{\alpha_{n+1} \gamma_{n+2}}{\beta_{n+2} - \frac{\alpha_{n+2} \gamma_{n+3}}{\beta_{n+3} - \dots}}}. \tag{2.35}$$

The quasinormal frequencies ω can be found by evaluating this relation at $n = 0$. The relation (2.33b) gives $a_1/a_0 = -\beta_0/\alpha_0$ and the continued fraction relation at $n = 0$ becomes

$$\beta_0 - \frac{\alpha_0 \gamma_1}{\beta_1 - \frac{\alpha_1 \gamma_2}{\beta_2 - \frac{\alpha_2 \gamma_3}{\beta_3 - \dots}}} = 0. \tag{2.36}$$

Leaver found sixty roots of this equation numerically for $\ell = 2$ and $\ell = 3$ in [24].

Alternatively, a semianalytic approach based on the WKB approximation, used in quantum mechanics to obtain approximate solutions to the static one-dimensional Schrödinger equation [17, p.315], was introduced by Schutz and Will in [25]. The wave equation is in the form

$$\frac{d^2\psi}{dx^2} + Q(x)\psi = 0, \tag{2.37}$$

where the function $-Q(x)$ has a maximum at x_0 and approaches asymptotically a constant value at $x \rightarrow \pm\infty$. Three separate regions are defined: I for (x_2, ∞) , II for (x_1, x_2) and III for $(-\infty, x_1)$, where $Q(x_1) = Q(x_2) = 0$ and $x_1 < x_0 < x_2$. The solutions ψ_I and ψ_{III} are given by zeroth order WKB functions. In region II, $Q(x)$ is expanded in a second-order Taylor series and a solution ψ_{II} is found. Their modified method requires that these solutions are simultaneously matched at x_1 and x_2 , which forms a quantization condition

$$\frac{Q_0}{\sqrt{2Q_0''}} = i\left(n + \frac{1}{2}\right), \quad \text{where } Q_0 = Q(x_0) \quad \text{and} \quad Q_0'' = \left. \frac{d^2Q}{dx^2} \right|_{x=x_0}. \tag{2.38}$$

For Schwarzschild black holes, the potential is $Q(r_*) = \omega^2 - V_{RW}(r_*)$. They calculated the frequencies ω for $\ell = 2, 3, 4$, but only the fundamental mode mode $n = 0$ agreed with the numerical results.

This approach was expanded to third order WKB terms by Will and Iyer in [26], where they

used third order WKB functions for ψ_I and ψ_{III} , and expanded $Q(x)$ into the Taylor series up to sixth order terms. They found the relation

$$i \frac{Q_0}{\sqrt{2Q_0''}} - \Lambda(n) - \Omega(n) = n + \frac{1}{2}, \quad \text{where}$$

$$\Lambda(n) = \frac{1}{\sqrt{2Q_0''}} \left[\frac{1}{8} \left(\frac{Q_0^{(4)}}{Q_0''} \right) \left(\frac{1}{4} + \alpha^2 \right) - \frac{1}{288} \left(\frac{Q_0'''}{Q_0''} \right)^2 (7 + 60\alpha^2) \right],$$

$$\Omega(n) = \frac{\alpha}{2Q_0''} \left[\frac{5}{6912} \left(\frac{Q_0'''}{Q_0''} \right)^4 (77 + 188\alpha^2) - \frac{1}{384} \left(\frac{(Q_0''')^2 Q_0^{(4)}}{(Q_0'')^3} \right) (51 + 100\alpha^2) + \right. \quad (2.39)$$

$$+ \frac{1}{2304} \left(\frac{Q_0^{(4)}}{Q_0''} \right)^2 (67 + 68\alpha^2) + \frac{1}{288} \left(\frac{Q_0''' Q_0^{(5)}}{(Q_0'')^2} \right) (19 + 28\alpha^2) +$$

$$\left. - \frac{1}{288} \left(\frac{Q_0^{(6)}}{Q_0''} \right) (5 + 4\alpha^2) \right] \quad \text{with } \alpha = n + \frac{1}{2}.$$

In [27], Iyer calculated Schwarzschild black hole frequencies for $\ell = 2, 3, 4$ with the 3rd order WKB approximation and compared them to results from [24] and [23]. The accuracy of the WKB method was greatly improved, and it worked especially well for $n \leq \ell$. The results for $\ell = 2$ are displayed in Table 2.1.

n	σ_{Leaver}	σ_{WKB}	Deviation for $\text{Re}(\sigma)$, $\text{Im}(\sigma)$
0	$0.3737 - i0.0890$	$0.3731 - i0.0892$	$(-0.13\%), (-0.22\%)$
1	$0.3467 - i0.2739$	$0.3460 - i0.2749$	$(-0.20\%), (-0.36\%)$
2	$0.3011 - i0.4783$	$0.3029 - i0.4711$	$(0.60\%), (1.5\%)$
3	$0.2515 - i0.7051$	$0.2475 - i0.6730$	$(-1.6\%), (4.6\%)$

Table 2.1: The frequencies $\sigma = \omega M_\bullet$ for $\ell = 2$ found by Leaver and from the 3rd order WKB approximation by Iyer, table from [27].

These frequencies are given in geometrical units, which can be converted into kHz by multiplying with $2\pi \cdot (5142 \text{ Hz}) \cdot (M_\odot/M_\bullet)$, where M_\odot is the Solar mass [10].

Chapter 3

Quasinormal modes in New General Relativity

General relativity is a very successful theory of gravity, and has had much validation from experiments. However, as mentioned above, there are notable shortcomings, which alternative theories of gravity are attempting to resolve. Many theories extend the existing framework of GR by adding higher order curvature invariant or new fields [7]. There are also theories, which take a completely different approach by describing the gravitational field in terms of other properties of spacetime, either in addition to curvature or instead of it [28]. New general relativity (NGR) is one of such theories [29]. In the following, we will introduce the basic ideas necessary for its formulation and define the main features of the theory.

Torsion is an attribute of a general connection $\Gamma^\rho_{\nu\mu}$ in the same way that curvature is. In a torsion-free spacetime, like the Riemannian spacetime of GR, one can infinitesimally parallel transport two vectors to form a closed parallelogram. However, in the presence of torsion, the parallelogram will not close. The torsion tensor is proportional to this lack of closure, and is defined as [28]

$$T^\rho_{\mu\nu} = \Gamma^\rho_{\nu\mu} - \Gamma^\rho_{\mu\nu}. \quad (3.1)$$

In teleparallel theories, the gravitational field is described purely by torsion, which behaves similarly to a force in the field equations. These theories can then be framed as gauge theories with torsion as the field strength. The physical motivation stems from this formulation resembling other fundamental fields, such as electromagnetism, rather than gravity being a purely geometrical effect like in GR [30]. The spacetimes of teleparallel theories have non-vanishing torsion and are metric-compatible, but have zero curvature [31]. It should be emphasised that zero curvature does not automatically yield the Minkowski spacetime, because there torsion vanishes as well [29].

The covariant formulation of teleparallel theories is defined in terms of 1) tetrads $\theta^a = \theta^a_\mu dx^\mu$, which form a dual basis of the tangent space at each point in spacetime, and 2) a flat spin connection $\omega^a_b = \omega^a_{b\mu} dx^\mu = \Lambda^a_c \partial_\mu (\Lambda_b^c) dx^\mu$, which represents inertial effects in a rotated frame. Here Λ^a_b are local Lorentz transformations in the tangent spaces and Latin indices a, b, c represent the Lorentz indices. The inverse of the tetrads are vectors $e_a = e_a^\mu \partial_\mu$ that form a basis

of the tangent space, and so their components satisfy [28, 30]

$$\theta^a{}_{\mu} e_b{}^{\mu} = \delta_b^a, \quad \theta^a{}_{\mu} e_a{}^{\nu} = \delta_{\nu}^{\mu}. \quad (3.2)$$

The spacetime metric $g_{\mu\nu}$ and the tangent space metric, which is the Minkowski metric η_{ab} , are related by the tetrad in the form [30]

$$g_{\mu\nu} = \eta_{ab} \theta^a{}_{\mu} \theta^b{}_{\nu}, \quad g^{\mu\nu} = \eta^{ab} e_a{}^{\mu} e_b{}^{\nu}. \quad (3.3)$$

The spin connection is flat, meaning that it has a vanishing curvature tensor $R^a{}_{b\mu\nu}(\omega^a{}_{b\mu}) = 0$, and metric compatible. It is possible to choose a "proper" frame, where the inertial spin connection vanishes $\omega^a{}_{b\mu} = 0$ with a local Lorentz transformation. This is called the Weitzenböck gauge. The teleparallel affine connection, also called the Weitzenböck connection as it describes the Weitzenböck spacetime, can be defined more generally as $\dot{\Gamma}^{\rho}{}_{\mu\nu} = e_a{}^{\rho}(\partial_{\nu}\theta^a{}_{\mu} + \omega^a{}_{b\nu}\theta^b{}_{\mu})$, and if $\omega^a{}_{b\mu} = 0$ as [29, 30]

$$\dot{\Gamma}^{\rho}{}_{\mu\nu} = e_a{}^{\rho} \partial_{\nu} \theta^a{}_{\mu}. \quad (3.4)$$

This connection defines a vanishing curvature tensor $R^{\rho}{}_{\sigma\mu\nu}(\dot{\Gamma}^{\rho}{}_{\mu\nu}) = 0$, it is metric-compatible $\dot{\nabla}_{\rho} g_{\mu\nu} = 0$, and its torsion tensor is [29]

$$T^{\rho}{}_{\mu\nu} = \dot{\Gamma}^{\rho}{}_{\nu\mu} - \dot{\Gamma}^{\rho}{}_{\mu\nu} = e_a{}^{\rho}(\partial_{\mu}\theta^a{}_{\nu} - \partial_{\nu}\theta^a{}_{\mu}). \quad (3.5)$$

GR can also be written in this teleparallel formulation, called the teleparallel equivalent of general relativity (TEGR) or just teleparallel gravity. This formulation has certain advantages and TEGR was recently used for quasinormal mode calculations to find the quasinormal energy spectrum of Schwarzschild black holes in [32]. However, while GR and TEGR are entirely equivalent, their respective extensions are not. Thus, modified teleparallel theories provide another avenue to explore alternative theories of gravity [33]. One advantage of these theories is, for example, that adding higher order torsion invariants does not change the field equations to higher order differential equations, which happens for curvature based theories [30].

New general relativity (NGR) was introduced by Hayashi and Shirafuji in [29] and is one of the oldest modifications of teleparallel gravity. The torsion tensor is decomposed into vector, axial, tensor irreducible pieces in the form

$$T_{\rho\mu\nu} = \frac{2}{3}(t_{\rho\mu\nu} - t_{\rho\nu\mu}) + \frac{1}{3}(g_{\rho\mu}v_{\nu} - g_{\rho\nu}v_{\mu}) + \epsilon_{\rho\mu\nu\kappa}a^{\kappa}, \quad (3.6)$$

where $\epsilon_{\mu\nu\rho\sigma} = \sqrt{\det(g)}\varepsilon_{\mu\nu\rho\sigma}$ is the totally antisymmetric Levi-Civita tensor with $\varepsilon_{\mu\nu\rho\sigma}$ as the

usual Levi-Civita symbol with values $-1, 0, 1$. The respective irreducible pieces are

$$\mathbf{v}_\mu = T^\rho{}_{\rho\mu}, \quad (3.7a)$$

$$\mathbf{a}_\mu = \frac{1}{6}\epsilon_{\mu\nu\rho\sigma}T^{\nu\rho\sigma}, \quad (3.7b)$$

$$\mathbf{t}_{\mu\nu\rho} = T_{(\mu\nu)\rho} + \frac{1}{3}(g_{\rho(\mu}\mathbf{v}_{\nu)} - g_{\mu\nu}\mathbf{v}_\rho). \quad (3.7c)$$

The gravitational lagrangian density of NGR is defined as

$$\mathcal{L}_G = c_v \mathbf{v}^\mu \mathbf{v}_\mu + c_a \mathbf{a}^\mu \mathbf{a}_\mu + c_t \mathbf{t}^{\rho\mu\nu} \mathbf{t}_{\rho\mu\nu}. \quad (3.8)$$

This simplifies to TEGR if the constants take values $c_v = -\frac{2}{3}$, $c_t = \frac{2}{3}$ and $c_a = \frac{3}{2}$. The NGR field equations are $E_{\mu\nu} = 8\pi T_{\mu\nu}$, where $T_{\mu\nu}$ is the energy-momentum tensor and $E_{\mu\nu}$ is the gravitational part [29, 34]

$$\begin{aligned} 8\pi E_{\mu\nu} = & c_a \left(\frac{1}{2} \mathbf{a}^\rho \mathbf{a}_{(\rho} g_{\mu\nu)} - \frac{4}{9} \epsilon_{\nu\alpha\beta\gamma} \mathbf{a}^\alpha \mathbf{t}_\mu{}^{\beta\gamma} - \frac{2}{9} \epsilon_{\mu\nu\rho\sigma} \mathbf{a}^\rho \mathbf{v}^\sigma - \frac{1}{3} \epsilon_{\mu\nu\rho\sigma} \mathring{\nabla}^\rho \mathbf{a}^\sigma \right) + \\ & + c_t \left(\frac{2}{3} \mathbf{t}_{\alpha[\beta\gamma]} \mathbf{t}^{\alpha\beta\gamma} g_{\mu\nu} - \frac{4}{3} \mathbf{t}_{\mu[\rho\sigma]} \mathbf{t}_\nu{}^{\rho\sigma} + 2 \mathring{\nabla}^\rho \mathbf{t}_{\mu[\nu\rho]} - \frac{2}{3} \mathbf{t}_{\nu[\mu\rho]} \mathbf{v}^\rho + \frac{1}{2} \epsilon_{\mu\alpha\beta\gamma} \mathbf{a}^\alpha \mathbf{t}_\nu{}^{\beta\gamma} \right) + \\ & + c_v \left(\frac{1}{2} \mathbf{v}^\rho \mathbf{v}_{(\rho} g_{\mu\nu)} + \frac{4}{3} \mathbf{t}_{\mu[\rho\nu]} \mathbf{v}^\rho + 2 g_{\mu[\nu} \mathring{\nabla}^\rho \mathbf{v}_{\rho]} - \frac{1}{2} \epsilon_{\mu\nu\rho\sigma} \mathbf{a}^\rho \mathbf{v}^\sigma \right). \end{aligned} \quad (3.9)$$

The field equations in vacuum $E_{\mu\nu} = 0$ are solved by Schwarzschild geometry only if [29]

$$c_t + c_v = 0. \quad (3.10)$$

It is possible to find $c'_t = \frac{2}{3}$ in $\mathcal{L}'_G = m \mathcal{L}_G$, where $m = \text{const}$, for any choice of c_t . As a universal property of lagrangians, multiplication by a constant will not change the field equations. So in spherical symmetry, one can always retrieve the TEGR values for c_t and c_v . Then, only c_a remains a free parameter. The authors called this 1-parameter new general relativity and supported it with observations in [35], where they found that Solar system measurements heavily constrain c_t and c_v to the TEGR values, but c_a is left arbitrary by the measurements. A parameter δc_a can then always be defined so that $c_a = \frac{3}{2} + \delta c_a$. Therefore, to be compatible with observations and have Schwarzschild geometry as a solution, one needs to choose

$$c_t = \frac{2}{3}, \quad c_v = -\frac{2}{3}, \quad c_a = \frac{3}{2} + \delta c_a. \quad (3.11)$$

In [33], the NGR field equations were expanded around a flat Minkowski background to study gravitational wave propagation. They found that gravitational waves in 1-parameter NGR have exactly two polarizations just like in GR. In [36], more general teleparallel modifications of Schwarzschild geometry were examined and corrections to the GR values of the photon sphere, perihelion shift, Shapiro delay and light deflection were found. For the 1-parameter NGR case,

which in the notation of the [36] means taking $\alpha_1 = \alpha_2 = \dots = 0$, all the corrections vanish.

We are going to investigate whether any deviations from GR can be found in the quasinormal modes of Schwarzschild black holes in the 1-parameter NGR theory, following the ideas laid out in Chapter 2. We will first write the tensors appearing in the NGR field equations in terms of linear perturbations. Then, we will explicitly find the background tensor components and ensure that the background field equations vanish, as they should for a Schwarzschild spacetime. Finally, we will find the components of the perturbations and analyse the perturbed field equations.

3.1 Expanding to linear perturbations

We are going to expand the NGR field equations around a general background, which we will later specify to the Schwarzschild background. The equations will hold up to only the linear order, and any higher order terms will be neglected. The general scheme for the tetrad and all quantities defined by the tetrad has been presented in [34]. We are going to follow these ideas and expand the NGR field equations first around a general background. The tetrad is split into an unperturbed background $\bar{\theta}^a{}_\mu$ and a sufficiently small perturbation $\tau^a{}_\mu$:

$$\theta^a{}_\mu = \bar{\theta}^a{}_\mu + \tau^a{}_\mu. \quad (3.12)$$

The inverse tetrad can similarly be split into $e_a{}^\mu = \bar{e}_a{}^\mu + \delta e_a{}^\mu$, and the relation $\theta^a{}_\mu e_a{}^\nu = (\bar{\theta}^a{}_\mu + \tau^a{}_\mu)(\bar{e}_a{}^\nu + \delta e_a{}^\nu) = \delta_\mu^\nu$ in the linear order gives $\delta e_a{}^\mu = -\bar{e}_a{}^\sigma \bar{e}_b{}^\mu \tau^b{}_\sigma$. So we can write

$$e_a{}^\mu = \bar{e}_a{}^\mu - \bar{e}_a{}^\sigma \bar{e}_b{}^\mu \tau^b{}_\sigma. \quad (3.13)$$

A perturbation $\tau_{\mu\nu}$ with only spacetime indices can be defined as

$$\tau_{\mu\nu} = \eta_{ab} \bar{\theta}^a{}_\mu \tau^b{}_\nu, \quad (3.14)$$

where $\bar{g}_{\mu\nu} = \eta_{ab} \bar{\theta}^a{}_\mu \bar{\theta}^b{}_\nu$ is the background metric. The inverse of this relation can be written as

$$\tau^a{}_\mu = \bar{\theta}^a{}_\sigma \bar{g}^{\sigma\kappa} \tau_{\kappa\mu}, \quad \text{which also gives} \quad \delta e_a{}^\mu = -\bar{e}_a{}^\sigma \bar{g}^{\mu\kappa} \tau_{\kappa\sigma}. \quad (3.15)$$

Any arbitrary tensor $A_{\mu\nu}$ can be split into a symmetric part $A_{(\mu\nu)} = \frac{1}{2}(A_{\mu\nu} + A_{\nu\mu})$ and an antisymmetric part $A_{[\mu\nu]} = \frac{1}{2}(A_{\mu\nu} - A_{\nu\mu})$. We can define symmetric and antisymmetric perturbations as $h_{\mu\nu} = 2\tau_{(\mu\nu)}$ and $a_{\mu\nu} = 2\tau_{[\mu\nu]}$ and write

$$\tau_{\mu\nu} = \frac{1}{2}(h_{\mu\nu} + a_{\mu\nu}), \quad (3.16)$$

The metric, defined in terms of the tetrad, expands into

$$g_{\mu\nu} = \eta_{ab}(\bar{\theta}^a{}_{\mu} + \tau^a{}_{\mu})(\bar{\theta}^b{}_{\nu} + \tau^b{}_{\nu}) = \bar{g}_{\mu\nu} + 2\tau_{(\mu\nu)} = \bar{g}_{\mu\nu} + h_{\mu\nu}. \quad (3.17)$$

The inverse metric can similarly be found as $g^{\mu\nu} = \bar{g}^{\mu\nu} - 2\tau^{(\mu\nu)} = \bar{g}^{\mu\nu} - h^{\mu\nu}$. We see that the symmetric part of $\tau_{\mu\nu}$ is just the linear perturbation of the metric. The Levi-Civita tensor $\epsilon_{\mu\nu\rho\sigma}$ expands into

$$\epsilon_{\mu\nu\rho\sigma} = \left(1 + \frac{1}{2}h\right)\bar{\epsilon}_{\mu\nu\rho\sigma}, \quad \text{since} \quad \sqrt{\det(g)} = \left(1 + \frac{1}{2}h\right)\sqrt{\det(\bar{g})} \quad \text{with} \quad h = h_{\mu\nu}\bar{g}^{\mu\nu}. \quad (3.18)$$

The teleparallel connection expands into $\dot{\Gamma}^{\rho}{}_{\mu\nu} = (\bar{e}_a{}^{\rho} - \bar{e}_a{}^{\sigma}\bar{g}^{\rho\kappa}\tau_{\kappa\sigma})\partial_{\nu}(\bar{\theta}^a{}_{\mu} + \bar{\theta}^a{}_{\sigma}\bar{g}^{\sigma\kappa}\tau_{\kappa\mu}) = \dot{\bar{\Gamma}}^{\rho}{}_{\mu\nu} + \delta\dot{\bar{\Gamma}}^{\rho}{}_{\mu\nu}$, where the linear perturbation $\delta\dot{\bar{\Gamma}}^{\rho}{}_{\mu\nu}$ can be found as

$$\begin{aligned} \delta\dot{\bar{\Gamma}}^{\rho}{}_{\mu\nu} &= \bar{e}_a{}^{\rho}\partial_{\nu}(\bar{\theta}^a{}_{\sigma}\bar{g}^{\sigma\kappa}\tau_{\kappa\mu}) - \bar{e}_a{}^{\sigma}\bar{g}^{\rho\kappa}\tau_{\kappa\sigma}\partial_{\nu}\bar{\theta}^a{}_{\mu} = \\ &= \bar{e}_a{}^{\rho}\bar{\theta}^a{}_{\sigma}\partial_{\nu}(\bar{g}^{\sigma\kappa}\tau_{\kappa\mu}) + \bar{g}^{\sigma\kappa}\tau_{\kappa\mu}\bar{e}_a{}^{\rho}\partial_{\nu}\bar{\theta}^a{}_{\sigma} - \bar{g}^{\rho\kappa}\tau_{\kappa\sigma}\bar{e}_a{}^{\sigma}\partial_{\nu}\bar{\theta}^a{}_{\mu} = \\ &= p_{\nu}(\bar{g}^{\rho\kappa}\tau_{\kappa\mu}) + (\bar{g}^{\sigma\kappa}\tau_{\kappa\mu})\dot{\bar{\Gamma}}^{\rho}{}_{\sigma\nu} - (\bar{g}^{\rho\kappa}\tau_{\kappa\sigma})\dot{\bar{\Gamma}}^{\sigma}{}_{\mu\nu} = \dot{\bar{\nabla}}(\bar{g}^{\rho\kappa}\tau_{\kappa\mu}) = \\ &= \bar{g}^{\rho\kappa}\dot{\bar{\nabla}}\tau_{\kappa\mu}. \end{aligned} \quad (3.19)$$

The linear perturbation of the torsion tensor $T^{\rho}{}_{\mu\nu} = \dot{\bar{\Gamma}}^{\rho}{}_{\nu\mu} - \dot{\bar{\Gamma}}^{\rho}{}_{\mu\nu}$ is then

$$\delta T^{\rho}{}_{\mu\nu} = \delta\dot{\bar{\Gamma}}^{\rho}{}_{\nu\mu} - \delta\dot{\bar{\Gamma}}^{\rho}{}_{\mu\nu} = \bar{g}^{\rho\kappa}(\dot{\bar{\nabla}}_{\mu}\tau_{\kappa\nu} - \dot{\bar{\nabla}}_{\nu}\tau_{\kappa\mu}) = \bar{g}^{\rho\kappa}(\dot{\bar{\nabla}}_{[\mu}h_{\nu]\kappa} - \dot{\bar{\nabla}}_{[\mu}a_{\nu]\kappa}). \quad (3.20)$$

Here we have made use of the symmetries $h_{\mu\nu} = h_{\nu\mu}$ and $a_{\mu\nu} = -a_{\nu\mu}$. Inserting the torsion tensor $T^{\rho}{}_{\mu\nu} = \bar{T}^{\rho}{}_{\mu\nu} + \delta T^{\rho}{}_{\mu\nu}$ into definitions (3.7), the vector irreducible $\mathbf{v}_{\mu} = T^{\rho}{}_{\rho\mu}$ becomes

$$\mathbf{v}_{\mu} = \bar{\mathbf{v}}_{\mu} + \bar{g}^{\rho\kappa}\dot{\bar{\nabla}}_{[\rho}h_{\mu]\kappa} - \bar{g}^{\rho\kappa}\dot{\bar{\nabla}}_{[\rho}a_{\mu]\kappa} = \bar{\mathbf{v}}_{\mu} + \delta\mathbf{v}_{\mu}, \quad (3.21)$$

the axial irreducible $\mathbf{a}_{\mu} = \frac{1}{6}\epsilon_{\mu\nu\rho\sigma}\bar{g}^{\rho\alpha}\bar{g}^{\sigma\beta}T^{\nu}{}_{\alpha\beta}$ becomes

$$\begin{aligned} \mathbf{a}_{\mu} &= \bar{\mathbf{a}}_{\mu} + \frac{1}{2}h\bar{\mathbf{a}}_{\mu} - \frac{1}{6}\epsilon_{\mu\nu\rho\sigma}(h^{\rho\alpha}\bar{g}^{\sigma\beta} + \bar{g}^{\rho\alpha}h^{\sigma\beta})\bar{T}^{\nu}{}_{\alpha\beta} + \frac{1}{6}\epsilon_{\mu\nu\rho\sigma}\bar{g}^{\rho\alpha}\bar{g}^{\sigma\beta}\bar{g}^{\gamma\kappa}\dot{\bar{\nabla}}_{[\alpha}h_{\beta]\kappa} + \\ &\quad - \frac{1}{6}\epsilon_{\mu\nu\rho\sigma}\bar{g}^{\rho\alpha}\bar{g}^{\sigma\beta}\bar{g}^{\gamma\kappa}\dot{\bar{\nabla}}_{[\alpha}a_{\beta]\kappa} = \bar{\mathbf{a}}_{\mu} + \delta\mathbf{a}_{\mu}, \end{aligned} \quad (3.22)$$

and the tensor irreducible $\mathbf{t}_{\mu\nu\rho} = \frac{1}{2}(g_{\mu\kappa}T^{\kappa}{}_{\nu\rho} + g_{\nu\kappa}T^{\kappa}{}_{\mu\rho}) + \frac{1}{3}(\mathbf{v}_{(\mu}g_{\nu)\rho} - \mathbf{v}_{\rho}g_{\mu\nu})$ becomes

$$\begin{aligned} \mathbf{t}_{\mu\nu\rho} &= \bar{\mathbf{t}}_{\mu\nu\rho} + h_{\kappa(\mu}\bar{T}^{\kappa}{}_{\nu)\rho} + \frac{1}{3}(\bar{\mathbf{v}}_{(\mu}h_{\nu)\rho} - \bar{\mathbf{v}}_{\rho}h_{\mu\nu}) + \frac{1}{3}(\delta\mathbf{v}_{(\mu}g_{\nu)\rho} - \delta\mathbf{v}_{\rho}g_{\mu\nu}) + \\ &\quad + \frac{1}{2}(\dot{\bar{\nabla}}_{[\nu}h_{\rho]\mu} + \dot{\bar{\nabla}}_{[\mu}h_{\rho]\nu}) - \frac{1}{2}(\dot{\bar{\nabla}}_{[\nu}a_{\rho]\mu} + \dot{\bar{\nabla}}_{[\mu}a_{\rho]\nu}) = \bar{\mathbf{t}}_{\mu\nu\rho} + \delta\mathbf{t}_{\mu\nu\rho}. \end{aligned} \quad (3.23)$$

We have now written all necessary tensors in terms of the symmetric and antisymmetric tetrad perturbations $h_{\mu\nu}$ and $a_{\mu\nu}$. We are also going to lower all indices in the field equations with the metric so that we can directly use all the results found above. In vacuum, the NGR field equations (3.9) with lowered indices and c_t, c_v values from (3.11) are

$$\begin{aligned}
& c_a \left(\frac{1}{2} g^{\rho\alpha} \mathbf{a}_\alpha \mathbf{a}_{(\rho} g_{\mu\nu)} - \frac{4}{9} g^{\kappa\alpha} g^{\beta\rho} g^{\gamma\sigma} \epsilon_{\nu\alpha\beta\gamma} \mathbf{a}_\kappa \mathbf{t}_{\mu\rho\sigma} - \frac{2}{9} g^{\rho\alpha} g^{\sigma\beta} \epsilon_{\mu\nu\rho\sigma} \mathbf{a}_\alpha \mathbf{v}_\beta + \right. \\
& \quad \left. - \frac{1}{3} g^{\rho\alpha} g^{\sigma\beta} \epsilon_{\mu\nu\rho\sigma} \overset{\circ}{\nabla}_\alpha \mathbf{a}_\beta \right) + \\
& + \frac{2}{3} \left(\frac{2}{3} g^{\alpha\kappa} g^{\beta\rho} g^{\gamma\sigma} \mathbf{t}_{\alpha[\beta\gamma]} \mathbf{t}_{\kappa\rho\sigma} g_{\mu\nu} - \frac{4}{3} g^{\rho\alpha} g^{\sigma\beta} \mathbf{t}_{\mu[\rho\sigma]} \mathbf{t}_{\nu\alpha\beta} + 2g^{\rho\alpha} \overset{\circ}{\nabla}_\alpha \mathbf{t}_{\mu[\nu\rho]} + \right. \\
& \quad \left. - \frac{2}{3} g^{\rho\alpha} \mathbf{t}_{\nu[\mu\rho]} \mathbf{v}_\alpha + \frac{1}{2} g^{\alpha\kappa} g^{\beta\rho} g^{\gamma\sigma} \epsilon_{\mu\alpha\beta\gamma} \mathbf{a}_\kappa \mathbf{t}_{\nu\rho\sigma} \right) + \\
& - \frac{2}{3} \left(\frac{1}{2} g^{\rho\alpha} \mathbf{v}_\alpha \mathbf{v}_{(\rho} g_{\mu\nu)} + \frac{4}{3} g^{\rho\alpha} \mathbf{t}_{\mu[\rho\nu]} \mathbf{v}_\alpha + 2g^{\rho\alpha} \overset{\circ}{\nabla}_\alpha \mathbf{v}_{[\rho} g_{\nu]\mu} - \frac{1}{2} g^{\rho\alpha} g^{\sigma\beta} \epsilon_{\mu\nu\rho\sigma} \mathbf{a}_\alpha \mathbf{v}_\beta \right) = 0.
\end{aligned} \tag{3.24}$$

They can be split into background and first-order perturbed field equations

$$E_{\mu\nu} = \bar{E}_{\mu\nu} + \delta E_{\mu\nu} \equiv 0 \tag{3.25}$$

with the linearly perturbed tensors from (3.17) to (3.23). The background field equations \bar{E} are

$$\begin{aligned}
& c_a \left(\frac{1}{2} \bar{g}^{\rho\alpha} \bar{\mathbf{a}}_\alpha \bar{\mathbf{a}}_{(\rho} \bar{g}_{\mu\nu)} - \frac{4}{9} \bar{g}^{\kappa\alpha} \bar{g}^{\beta\rho} \bar{g}^{\gamma\sigma} \bar{\epsilon}_{\nu\alpha\beta\gamma} \bar{\mathbf{a}}_\kappa \bar{\mathbf{t}}_{\mu\rho\sigma} - \frac{2}{9} \bar{g}^{\rho\alpha} \bar{g}^{\sigma\beta} \bar{\epsilon}_{\mu\nu\rho\sigma} \bar{\mathbf{a}}_\alpha \bar{\mathbf{v}}_\beta + \right. \\
& \quad \left. - \frac{1}{3} \bar{g}^{\rho\alpha} \bar{g}^{\sigma\beta} \bar{\epsilon}_{\mu\nu\rho\sigma} \overset{\circ}{\nabla}_\alpha \bar{\mathbf{a}}_\beta \right) + \\
& + \frac{2}{3} \left(\frac{2}{3} \bar{g}^{\alpha\kappa} \bar{g}^{\beta\rho} \bar{g}^{\gamma\sigma} \bar{\mathbf{t}}_{\alpha[\beta\gamma]} \bar{\mathbf{t}}_{\kappa\rho\sigma} \bar{g}_{\mu\nu} - \frac{4}{3} \bar{g}^{\rho\alpha} \bar{g}^{\sigma\beta} \bar{\mathbf{t}}_{\mu[\rho\sigma]} \bar{\mathbf{t}}_{\nu\alpha\beta} + 2\bar{g}^{\rho\alpha} \overset{\circ}{\nabla}_\alpha \bar{\mathbf{t}}_{\mu[\nu\rho]} + \right. \\
& \quad \left. - \frac{2}{3} \bar{g}^{\rho\alpha} \bar{\mathbf{t}}_{\nu[\mu\rho]} \bar{\mathbf{v}}_\alpha + \frac{1}{2} \bar{g}^{\alpha\kappa} \bar{g}^{\beta\rho} \bar{g}^{\gamma\sigma} \bar{\epsilon}_{\mu\alpha\beta\gamma} \bar{\mathbf{a}}_\kappa \bar{\mathbf{t}}_{\nu\rho\sigma} \right) + \\
& - \frac{2}{3} \left(\frac{1}{2} \bar{g}^{\rho\alpha} \bar{\mathbf{v}}_\alpha \bar{\mathbf{v}}_{(\rho} \bar{g}_{\mu\nu)} + \frac{4}{3} \bar{g}^{\rho\alpha} \bar{\mathbf{t}}_{\mu[\rho\nu]} \bar{\mathbf{v}}_\alpha + 2\bar{g}^{\rho\alpha} \overset{\circ}{\nabla}_\alpha \bar{\mathbf{v}}_{[\rho} \bar{g}_{\nu]\mu} - \frac{1}{2} \bar{g}^{\rho\alpha} \bar{g}^{\sigma\beta} \bar{\epsilon}_{\mu\nu\rho\sigma} \bar{\mathbf{a}}_\alpha \bar{\mathbf{v}}_\beta \right) = 0.
\end{aligned} \tag{3.26}$$

and the first-order perturbed equations are $\delta E_{\mu\nu}$ are

$$\begin{aligned}
& c_a \left[\frac{1}{2} \left(\bar{g}^{\rho\alpha} \delta \mathbf{a}_\alpha \bar{\mathbf{a}}_{(\rho} \bar{g}_{\mu\nu)} + \bar{g}^{\rho\alpha} \bar{\mathbf{a}}_\alpha \delta \mathbf{a}_{(\rho} \bar{g}_{\mu\nu)} - h^{\rho\alpha} \bar{\mathbf{a}}_\alpha \bar{\mathbf{a}}_{(\rho} \bar{g}_{\mu\nu)} + \bar{g}^{\rho\alpha} \bar{\mathbf{a}}_\alpha \bar{\mathbf{a}}_{(\rho} h_{\mu\nu)} \right) + \right. \\
& \quad - \frac{4}{9} \left(\bar{g}^{\kappa\alpha} \bar{g}^{\beta\rho} \bar{g}^{\gamma\sigma} \bar{\epsilon}_{\nu\alpha\beta\gamma} (\delta \mathbf{a}_\kappa \bar{\mathbf{t}}_{\mu\rho\sigma} + \bar{\mathbf{a}}_\kappa \delta \mathbf{t}_{\mu\rho\sigma}) + \right. \\
& \quad \quad \left. - \bar{\epsilon}_{\nu\alpha\beta\gamma} \bar{\mathbf{a}}_\kappa \bar{\mathbf{t}}_{\mu\rho\sigma} (h^{\kappa\alpha} \bar{g}^{\beta\rho} \bar{g}^{\gamma\sigma} + \bar{g}^{\kappa\alpha} h^{\beta\rho} \bar{g}^{\gamma\sigma} + \bar{g}^{\kappa\alpha} \bar{g}^{\beta\rho} h^{\gamma\sigma}) \right) + \\
& \quad - \frac{2}{9} \left(\bar{g}^{\rho\alpha} \bar{g}^{\sigma\beta} \bar{\epsilon}_{\mu\nu\rho\sigma} (\delta \mathbf{a}_\alpha \bar{\mathbf{v}}_\beta + \bar{\mathbf{a}}_\alpha \delta \mathbf{v}_\beta) - \bar{\epsilon}_{\mu\nu\rho\sigma} \bar{\mathbf{a}}_\alpha \bar{\mathbf{v}}_\beta (h^{\rho\alpha} \bar{g}^{\sigma\beta} + \bar{g}^{\rho\alpha} h^{\sigma\beta}) \right) + \\
& \quad - \frac{1}{3} \left(\bar{g}^{\rho\alpha} \bar{g}^{\sigma\beta} \bar{\epsilon}_{\mu\nu\rho\sigma} (\overset{\circ}{\nabla}_\alpha \delta \mathbf{a}_\beta - \delta \Gamma^{\rho\lambda}_{\beta\alpha} \bar{\mathbf{a}}_\lambda) - \bar{\epsilon}_{\mu\nu\rho\sigma} \overset{\circ}{\nabla}_\alpha \bar{\mathbf{a}}_\beta (h^{\rho\alpha} \bar{g}^{\sigma\beta} + \bar{g}^{\rho\alpha} h^{\sigma\beta}) \right) + \\
& \quad \left. - \frac{h}{18} \left(4 \bar{g}^{\kappa\alpha} \bar{g}^{\beta\rho} \bar{g}^{\gamma\sigma} \bar{\epsilon}_{\nu\alpha\beta\gamma} \bar{\mathbf{a}}_\kappa \bar{\mathbf{t}}_{\mu\rho\sigma} + \bar{g}^{\rho\alpha} \bar{g}^{\sigma\beta} \bar{\epsilon}_{\mu\nu\rho\sigma} (2 \bar{\mathbf{a}}_\alpha \bar{\mathbf{v}}_\beta + 3 \overset{\circ}{\nabla}_\alpha \bar{\mathbf{a}}_\beta) \right) \right] +
\end{aligned} \tag{3.27a}$$

$$\begin{aligned}
& + \frac{2}{3} \left[\frac{2}{3} \left(\bar{g}^{\alpha\kappa} \bar{g}^{\beta\rho} \bar{g}^{\gamma\sigma} \bar{g}_{\mu\nu} (\delta \mathbf{t}_{\alpha[\beta\gamma]} \bar{\mathbf{t}}_{\kappa\rho\sigma} + \bar{\mathbf{t}}_{\alpha[\beta\gamma]} \delta \mathbf{t}_{\kappa\rho\sigma}) - \bar{\mathbf{t}}_{\alpha[\beta\gamma]} \bar{\mathbf{t}}_{\kappa\rho\sigma} (h^{\alpha\kappa} \bar{g}^{\beta\rho} \bar{g}^{\gamma\sigma} \bar{g}_{\mu\nu} + \right. \right. \\
& \quad \left. \left. + \bar{g}^{\alpha\kappa} h^{\beta\rho} \bar{g}^{\gamma\sigma} \bar{g}_{\mu\nu} + \bar{g}^{\alpha\kappa} \bar{g}^{\beta\rho} h^{\gamma\sigma} \bar{g}_{\mu\nu} - \bar{g}^{\alpha\kappa} \bar{g}^{\beta\rho} \bar{g}^{\gamma\sigma} h_{\mu\nu}) \right) + \right. \\
& \quad - \frac{4}{3} \left(\bar{g}^{\rho\alpha} \bar{g}^{\sigma\beta} (\delta \mathbf{t}_{\mu[\rho\sigma]} \bar{\mathbf{t}}_{\nu\alpha\beta} + \bar{\mathbf{t}}_{\mu[\rho\sigma]} \delta \mathbf{t}_{\nu\alpha\beta}) - (h^{\rho\alpha} \bar{g}^{\sigma\beta} + h^{\rho\alpha} \bar{g}^{\sigma\beta}) \bar{\mathbf{t}}_{\mu[\rho\sigma]} \bar{\mathbf{t}}_{\nu\alpha\beta} \right) + \\
& \quad + 2 \left(\bar{g}^{\rho\alpha} (\bar{\nabla}_{\alpha} \delta \mathbf{t}_{\mu[\nu\rho]} - \delta \mathbf{\Gamma}^{\lambda}_{\mu\alpha} \bar{\mathbf{t}}_{\lambda[\nu\rho]} - \delta \mathbf{\Gamma}^{\lambda}_{\nu\alpha} \bar{\mathbf{t}}_{\mu[\lambda\rho]} - \delta \mathbf{\Gamma}^{\lambda}_{\rho\alpha} \bar{\mathbf{t}}_{\mu[\nu\lambda]}) - h^{\rho\alpha} \bar{\nabla}_{\alpha} \bar{\mathbf{t}}_{\mu[\nu\rho]} \right) + \tag{3.27b} \\
& \quad - \frac{2}{3} \left(\bar{g}^{\rho\alpha} (\delta \mathbf{t}_{\nu[\mu\rho]} \bar{\mathbf{v}}_{\alpha} + \bar{\mathbf{t}}_{\nu[\mu\rho]} \delta \mathbf{v}_{\alpha}) - h^{\rho\alpha} \bar{\mathbf{t}}_{\nu[\mu\rho]} \bar{\mathbf{v}}_{\alpha} \right) + \\
& \quad + \frac{1}{2} \left(\bar{g}^{\alpha\kappa} \bar{g}^{\beta\rho} \bar{g}^{\gamma\sigma} \bar{\epsilon}_{\mu\alpha\beta\gamma} (\delta \mathbf{a}_{\kappa} \bar{\mathbf{t}}_{\nu\rho\sigma} + \bar{\mathbf{a}}_{\kappa} \delta \mathbf{t}_{\nu\rho\sigma}) + \right. \\
& \quad \left. - \bar{\epsilon}_{\mu\alpha\beta\gamma} \bar{\mathbf{a}}_{\kappa} \bar{\mathbf{t}}_{\nu\rho\sigma} (h^{\alpha\kappa} \bar{g}^{\beta\rho} \bar{g}^{\gamma\sigma} + \bar{g}^{\alpha\kappa} h^{\beta\rho} \bar{g}^{\gamma\sigma} + \bar{g}^{\alpha\kappa} \bar{g}^{\beta\rho} h^{\gamma\sigma}) \right) + \\
& \quad \left. + \frac{h}{4} \bar{g}^{\alpha\kappa} \bar{g}^{\beta\rho} \bar{g}^{\gamma\sigma} \bar{\epsilon}_{\mu\alpha\beta\gamma} \bar{\mathbf{a}}_{\kappa} \bar{\mathbf{t}}_{\nu\rho\sigma} \right] +
\end{aligned}$$

$$\begin{aligned}
& - \frac{2}{3} \left[\frac{1}{2} \left(\bar{g}^{\rho\alpha} \delta \mathbf{v}_{\alpha} \bar{\mathbf{v}}_{(\rho} \bar{g}_{\mu\nu)} + \bar{g}^{\rho\alpha} \bar{\mathbf{v}}_{\alpha} \delta \mathbf{v}_{(\rho} \bar{g}_{\mu\nu)} - h^{\rho\alpha} \bar{\mathbf{v}}_{\alpha} \bar{\mathbf{v}}_{(\rho} \bar{g}_{\mu\nu)} + \bar{g}^{\rho\alpha} \bar{\mathbf{v}}_{\alpha} \bar{\mathbf{v}}_{(\rho} h_{\mu\nu)} \right) + \right. \\
& \quad + \frac{4}{3} \left(\bar{g}^{\rho\alpha} (\delta \mathbf{t}_{\mu[\rho\nu]} \bar{\mathbf{v}}_{\alpha} + \bar{\mathbf{t}}_{\mu[\rho\nu]} \delta \mathbf{v}_{\alpha}) - h^{\rho\alpha} \bar{\mathbf{t}}_{\mu[\rho\nu]} \bar{\mathbf{v}}_{\alpha} \right) + \\
& \quad + 2 \left(\bar{g}^{\rho\alpha} (\bar{\nabla}_{\alpha} \delta \mathbf{v}_{[\rho} \bar{g}_{\nu]\mu} - \delta \mathbf{\Gamma}^{\lambda}_{\alpha[\rho} \bar{g}_{\nu]\mu} \bar{\mathbf{v}}_{\lambda}) - h^{\rho\alpha} \bar{\nabla}_{\alpha} \bar{\mathbf{v}}_{[\rho} \bar{g}_{\nu]\mu} + \bar{g}^{\rho\alpha} \bar{\nabla}_{\alpha} \bar{\mathbf{v}}_{[\rho} h_{\nu]\mu} \right) + \tag{3.27c} \\
& \quad - \frac{1}{2} \left(\bar{g}^{\rho\alpha} \bar{g}^{\sigma\beta} \bar{\epsilon}_{\mu\nu\rho\sigma} (\delta \mathbf{a}_{\alpha} \bar{\mathbf{v}}_{\beta} + \bar{\mathbf{a}}_{\alpha} \delta \mathbf{v}_{\beta}) - (h^{\rho\alpha} \bar{g}^{\sigma\beta} + \bar{g}^{\rho\alpha} h^{\sigma\beta}) \bar{\epsilon}_{\mu\nu\rho\sigma} \bar{\mathbf{a}}_{\alpha} \bar{\mathbf{v}}_{\beta} \right) + \\
& \quad \left. - \frac{h}{4} \bar{g}^{\rho\alpha} \bar{g}^{\sigma\beta} \bar{\epsilon}_{\mu\nu\rho\sigma} \bar{\mathbf{a}}_{\alpha} \bar{\mathbf{v}}_{\beta} \right] = 0.
\end{aligned}$$

3.2 Calculating with SymPy in Jupyter Notebook

In order to analyse the NGR field equations, we are going to need to find the background and perturbation components of the relevant tensors and insert them into (3.26) and (3.27) respectively. All following calculations will be done in Python (version 3.7.4) using its SymPy library (version 1.7.1), which is made for symbolic mathematics, in particular mathematical analysis [37]. We will largely make use of their `Tensor` module. It allows one to define tensors with `TensorHead()` and contra- and covariant indices with `TensorIndex()` functions. It is then possible to create new tensor quantities by adding and multiplying tensors together, and SymPy will automatically track the summation indices itself. It is also possible to raise and lower indices automatically with this module, but we don't use that feature and always track the indices by hand. Explicit component expressions can then be found by using the `.replace_with_arrays()` function. It accepts a dictionary, which relates tensors with the appropriate indices and the components given in lists or matrices. This method does not accept the same `TensorHead()` with different index positions if the automatic index raising/lowering is not defined, so we always define "new" tensors for new index positions. For example, `bar_g(mu, nu)` is the metric with lower indices and `bar_G(-mu, -nu)` is the inverse metric with upper indices. Additionally,

we use of the basic options of SymPy a lot, such as defining symbols and symbolic functions with `symbols()` and `Function()`, various simplifying functions like `.subs()`, `cancel()` and `factor()`, and matrix manipulations.

The code is written and run in Jupyter Notebook (version 1.0.0), which is an open-source web application that enables live code, visualization and LaTeX display options [38]. The code can be run in small chunks by splitting the code into cells. This allows great interactivity as the result of each cell can be displayed and checked immediately. Both SymPy and Jupyter understand basic LaTeX syntax, so all calculations can be viewed and presented in an easy to understand format. The notebooks can also be converted to LaTeX files with the built-in options, which how the code formatting displayed in Appendix C was generated.

Appendix C contains the entire code used for finding the perturbed field equations in Section 3.4. The calculations in Section 3.3 use the exact same code up to output [8], but with the

$$C_1, C_5 = \text{Function}('C_1')(r), \text{Function}('C_5')(r)$$

line in output [3] enabled instead. The resulting background field equations were then manipulated to find the necessary solutions to C_1 and C_5 , and the results were incorporated into the code to be included from the beginning.

3.3 Finding the background field equations

In order to find the background field equations, we need to explicitly find the components of the background tensors written in section 3.1. We will do so for a spherically symmetric background. The most general tetrad components in spherical symmetry are [31]

$$\begin{aligned} \bar{\theta}^0 &= C_1 dt + C_2 dr, \\ \bar{\theta}^1 &= (C_3 dt + C_4 dr) \sin \theta \cos \varphi + (C_5 \cos \theta \cos \varphi - C_6 \sin \varphi) d\theta + \\ &\quad - (C_5 \sin \varphi + C_6 \cos \theta \cos \varphi) \sin \theta d\varphi, \\ \bar{\theta}^2 &= (C_3 dt + C_4 dr) \sin \theta \sin \varphi + (C_5 \cos \theta \sin \varphi + C_6 \cos \varphi) d\theta + \\ &\quad + (C_5 \cos \varphi + C_6 \cos \theta \sin \varphi) \sin \theta d\varphi, \\ \bar{\theta}^3 &= (C_3 dt + C_4 dr) \cos \theta - C_5 \sin \theta d\theta + C_6 \sin^2 \theta d\varphi, \end{aligned} \tag{3.28}$$

where $C_1 = C_1(r)$ to $C_6 = C_6(r)$. The resulting non-vanishing metric components are [31]

$$\begin{aligned} g_{00} &= C_3^2 - C_1^2, & g_{11} &= C_4^2 - C_2^2, & g_{22} &= C_5^2 + C_6^2, & g_{33} &= (C_5^2 + C_6^2) \sin^2 \theta, \\ g_{01} &= g_{10} = C_3 C_4 - C_1 C_2. \end{aligned} \tag{3.29}$$

We are interested in Schwarzschild black holes, so we want the background metric to be specifically the Schwarzschild metric. We can write the metric as

$$\bar{g}_{\mu\nu} = \begin{pmatrix} -F^2 & 0 & 0 & 0 \\ 0 & 1/F^2 & 0 & 0 \\ 0 & 0 & r^2 & 0 \\ 0 & 0 & 0 & r^2 \sin^2 \theta \end{pmatrix}, \quad \text{where } F = F(r) = \sqrt{1 - \frac{2M_\bullet}{r}}, \quad (3.30)$$

and, by comparing (3.29) and (3.30), find the following conditions for C_2 , C_3 , C_4 and C_6 :

$$C_2 = \frac{C_3 C_4}{C_1}, \quad C_3 = \sqrt{C_1^2 - F^2}, \quad C_4 = \frac{\sqrt{C_1^2}}{F^2}, \quad C_6 = \sqrt{r^2 - C_5^2}. \quad (3.31)$$

In further calculations, all expressions will be significantly simplified if the square root $\sqrt{C_1^2}$ can be evaluated, and this can only be done if we know the sign of C_1 . We are going to work with the assumption that $C_1 > 0$ in order to write $\sqrt{C_1^2} = C_1$. While this choice influences the exact form of the expressions we find, the general results are unaffected. If $C_1 < 0$, the square root evaluates to $\sqrt{C_1^2} = -C_1$ and the calculations can be done with the code in Appendix C by simply changing the definition of C_4 . We will proceed to detail the results for $C_1 > 0$ and $C_4 = C_1/F^2$.

We can substitute the background tetrad components with the values (3.31) into (3.4) to find the non-vanishing background teleparallel connection $\dot{\Gamma}^\rho_{\mu\nu}$ coefficients as

$$\begin{aligned} \dot{\Gamma}^0_{01} &= -\dot{\Gamma}^1_{11} = \frac{1 - F^2}{2rF^2}, & \dot{\Gamma}^2_{21} &= \dot{\Gamma}^3_{31} = \frac{1}{r}, & \dot{\Gamma}^3_{23} &= \dot{\Gamma}^3_{32} = -\frac{\dot{\Gamma}^2_{33}}{\sin^2 \theta} = \cot \theta, \\ \dot{\Gamma}^1_{01} &= F^4 \dot{\Gamma}^0_{11} = \frac{C_{12}}{C_{11}}, & \dot{\Gamma}^1_{22} &= \frac{\dot{\Gamma}^1_{33}}{\sin^2 \theta} = r^2 F^2 \dot{\Gamma}^2_{12} = -r^2 F^2 \dot{\Gamma}^3_{13} = -C_1 C_5, \\ \dot{\Gamma}^0_{22} &= \frac{\dot{\Gamma}^0_{33}}{\sin^2 \theta} = \frac{r^2}{F^2} \dot{\Gamma}^2_{02} = \frac{r^2}{F^2} \dot{\Gamma}^3_{03} = \frac{C_5 C_{11}}{F^2}, & \dot{\Gamma}^2_{31} &= -\sin^2 \theta \dot{\Gamma}^3_{21} = \frac{C_{52} \sin \theta}{r C_{51}}, \\ \dot{\Gamma}^0_{23} &= -\dot{\Gamma}^0_{32} = \frac{r^2}{F^2} \dot{\Gamma}^2_{03} = -\frac{r^2 \sin^2 \theta}{F^2} \dot{\Gamma}^3_{02} = \frac{C_{11} C_{51} \sin \theta}{F^2}, \\ \dot{\Gamma}^1_{23} &= -\dot{\Gamma}^1_{32} = -r^2 F^2 \dot{\Gamma}^2_{13} = r^2 F^2 \sin^2 \theta \dot{\Gamma}^3_{12} = -C_1 C_{51} \sin \theta, \end{aligned} \quad (3.32)$$

where

$$\begin{aligned}
C_{11}(r) &= \sqrt{C_1^2 - F^2}, \\
C_{12}(r) &= F \left(F \frac{dC_1}{dr} - C_1 \frac{dF}{dr} \right) \quad \text{with} \quad \frac{dF}{dr} = \frac{(1 - F^2)}{2rF}, \\
C_{51}(r) &= \sqrt{r^2 - C_5^2}, \\
C_{52}(r) &= r \frac{dC_5}{dr} - C_5.
\end{aligned} \tag{3.33}$$

The independent non-vanishing background torsion tensor $\bar{T}^\rho{}_{\mu\nu}$ components are then

$$\begin{aligned}
\bar{T}^0{}_{10} &= \frac{1 - F^2}{2rF^2}, \quad \bar{T}^1{}_{10} = \frac{C_{12}}{C_{11}}, \quad \bar{T}^2{}_{20} = \bar{T}^3{}_{30} = \frac{C_5 C_{11}}{r^2}, \\
\bar{T}^1{}_{23} &= 2C_{51} C_1 \sin \theta, \quad \bar{T}^2{}_{12} = \bar{T}^3{}_{13} = \frac{rF^2 - C_1 C_5}{r^2 F^2}, \\
\bar{T}^2{}_{31} &= \sin^2 \theta \bar{T}^3{}_{12} = -\frac{(rF^2 C_{52} - C_1 C_{51}^2) \sin \theta}{r^2 C_{51} F^2}, \\
\bar{T}^0{}_{32} &= \frac{2r^2}{F^2} \bar{T}^2{}_{30} = \frac{2r^2 \sin^2 \theta}{F^2} \bar{T}^3{}_{02} = \frac{2C_{51} C_{11} \sin \theta}{F^2}.
\end{aligned} \tag{3.34}$$

Other non-zero terms come from the symmetry $\bar{T}^\rho{}_{\mu\nu} = -\bar{T}^\rho{}_{\nu\mu}$. The background torsion tensor components can now be used to find the three background irreducibles $\bar{\mathbf{v}}_\mu$, $\bar{\mathbf{a}}_\mu$ and $\bar{\mathbf{t}}_{\mu\nu\rho}$. The non-vanishing background vector irreducible $\bar{\mathbf{v}}_\mu$ components are

$$\bar{\mathbf{v}}_0 = \frac{r^2 C_{12} + 2C_5 C_{11}^2}{r^2 C_{11}}, \quad \bar{\mathbf{v}}_1 = \frac{4C_1 C_5 - 3rF^2 - r}{2r^2 F^2}. \tag{3.35}$$

The non-vanishing components of the background axial irreducible $\bar{\mathbf{a}}_\mu$ are

$$\bar{\mathbf{a}}_0 = -\frac{2(rF^2 C_{52} - 2C_1 C_{51}^2)}{3r^2 C_{51}}, \quad \bar{\mathbf{a}}_1 = \frac{4C_{51} C_{11}}{3r^2 F^2}. \tag{3.36}$$

The independent non-vanishing background tensor irreducible $\bar{\mathbf{t}}_{\mu\nu\rho}$ components are

$$\begin{aligned}
\bar{\mathbf{t}}_{001} &= \frac{2F^2}{r^2} \bar{\mathbf{t}}_{221} = \frac{2F^2}{r^2 \sin^2 \theta} \bar{\mathbf{t}}_{331} = \frac{2C_1 C_5 - 3rF^2 + r}{3r^2}, \\
\bar{\mathbf{t}}_{011} &= \frac{\bar{\mathbf{t}}_{220}}{r^2 F^2} = \frac{\bar{\mathbf{t}}_{330}}{r^2 F^2 \sin^2 \theta} = -\frac{r^2 C_{12} - C_5 C_{11}^2}{3r^2 F^2 C_{11}}, \\
\bar{\mathbf{t}}_{023} &= -\bar{\mathbf{t}}_{032} = \frac{C_{51} C_{11} \sin \theta}{2}, \quad \bar{\mathbf{t}}_{123} = -\bar{\mathbf{t}}_{132} = \frac{(rF^2 C_{52} + C_1 C_{51}^2) \sin \theta}{2F^2 C_{51}}.
\end{aligned} \tag{3.37}$$

Other components can be found from the relation $(\bar{\mathbf{t}}_{\mu\nu\rho} + 2\bar{\mathbf{t}}_{\mu\rho\nu})|_{\mu=\nu} = 0$ and the symmetry $\bar{\mathbf{t}}_{\mu\nu\rho} = \bar{\mathbf{t}}_{\nu\mu\rho}$.

Inserting all the background tensor components found above into the background field equations (3.26), we find the non-trivial equations

$$\bar{E}_{00} = \frac{2\delta c_a F^2}{9r^4 C_{51}^2} [r^2 F^2 C_{52}^2 - 4r C_1 C_{52} + 4C_{51}^4] \equiv 0, \quad \bar{E}_{10} = -\frac{8\delta c_a}{9r^3} C_{52} C_{11} \equiv 0, \quad (3.38a)$$

$$\bar{E}_{11} = \frac{2\delta c_a}{9r^4 F^2 C_{51}^2} [r F C_{52} + 2 C_{51}^2] [r F C_{52} - 2 C_{51}^2] \equiv 0, \quad (3.38b)$$

$$\bar{E}_{22} = \frac{2\delta c_a}{9r C_{51}^2} C_{52} [2C_1 C_{51}^2 - r F^2 C_{52}] \equiv 0, \quad \bar{E}_{33} = \sin^2 \theta \bar{E}_{22}, \quad (3.38c)$$

$$\begin{aligned} \frac{\bar{E}_{23}}{2 \sin \theta} = & -\frac{(3 + \delta c_a)}{9 C_{51}} \left[r F^2 \frac{dC_{52}}{dr} + C_{52} + \frac{F^2 C_5 C_{52}^2}{C_{51}^2} - 2C_{51}^2 \frac{dC_1}{dr} \right] + \frac{4\delta c_a C_5 C_{51}}{9r^2} + \\ & -\frac{2(1 + \delta c_a) C_1 C_{51}}{3r} - \frac{2(3 + 2\delta c_a) C_1 C_5 C_{52}}{9r C_{51}} + \frac{(9 + 5\delta c_a) F^2 C_{52}}{9 C_{51}} \equiv 0. \end{aligned} \quad (3.38d)$$

The immediately obvious solution is to choose $C_5 = \pm r$, which results in $C_{51} = 0$ and $C_{52} = 0$. In this case, all of the background field equations vanish. It may seem like there could be an issue with $C_{51} = 0$, because it appears in the denominators. This is easily resolved by first demanding that $C_{52} = 0$, which gives the condition $C_5 = \pm \kappa_1 r$ with some constant κ_1 . In that case, $C_{51} = r\sqrt{1 - \kappa_1^2}$ cancels out from the denominators and we find the condition $\kappa_1 = \pm 1$.

We are again going to simplify the following calculations by specifying the sign of C_5 to be positive. This choice affects the exact signs in future expressions, but the overall results remain the same. As mentioned above, the code in Appendix C can easily be used to find the results for $C_1 < 0$ and $C_5 = -r$ as well. In this thesis, we are going to explicitly present the results for

$$C_1 > 0 \quad \text{and} \quad C_5 = r. \quad (3.39)$$

However, $C_5 = \pm r$ is not the only way to satisfy the background field equations in vacuum. The equation $\bar{E}_{11} = 0$ contains two differential equations for C_5 , both of which yield the solution

$$C_5 = r \frac{\kappa_1(F^4 + 6F^2 + 1) + 16\kappa_2(F^3 + F)}{4\kappa_2(F^4 + 6F^2 + 1) + 4\kappa_1(F^3 + F)}, \quad \text{where } \kappa_1 \text{ and } \kappa_2 \text{ are constants.} \quad (3.40)$$

Inserting this result into $\bar{E}_{00} = 0$ gives

$$\bar{E}_{00} = \frac{\delta c_a F (F - 1)^4 (F + 1)^4}{9r^2 [\kappa_1(F^3 + F) + \kappa_2(F^4 + 6F^2 + 1)]^2} (\kappa_1^2 - 16\kappa_2^2)(C_1^2 - F^2) \equiv 0. \quad (3.41)$$

All other components also give the condition $(\kappa_1^2 - 16\kappa_2^2)(C_1^2 - F^2) \equiv 0$. The two possible options are

$$\kappa_1 = \pm 4\kappa_2 \quad \text{or} \quad C_1 = \pm F. \quad (3.42)$$

While choosing $\kappa_1 = \pm 4\kappa_2$ means that $C_5 = \pm r$ again, the choice $C_1 = \pm F$ gives us another branch of solutions. This branch is very curious as the background torsion tensor $\bar{T}^\rho{}_{\mu\nu}$ is not reflection symmetric in the case that $C_5 \neq \pm r$. This has significant consequences when it comes to the perturbed field equations. We will discuss this with the final results in Section 3.5.

We are now going to proceed to find the perturbed field equations with the background components found in (3.32) to (3.37) simplified with $C_5 = r$, $C_{52} = 0$ and $C_{51} = 0$.

3.4 Finding the perturbed field equations

In order to find the components of the perturbed field equations, we first need to determine the components of the tetrad perturbations $h_{\mu\nu}$ and $a_{\mu\nu}$. As seen in (3.17), the symmetric perturbation $h_{\mu\nu}$ is the metric perturbation. We may therefore use the same components as found in GR. We will use up our gauge freedom to write them in the Regge-Wheeler gauge (2.18a) and (2.18b).

When we look at the behaviour of the antisymmetric perturbation $a_{\mu\nu}$ under spatial rotations around the origin $(t, r, \theta, \varphi) \rightarrow (t, r, \theta'(\theta, \varphi), \varphi'(\theta, \varphi))$, we see that, similarly to $h_{\mu\nu}$, its components decompose into

$$\begin{aligned}
\text{Scalars: } a'_{00} &= \frac{\partial x^\mu}{\partial x'^0} \frac{\partial x^\nu}{\partial x'^0} a_{\mu\nu} = a_{00} = 0 & \text{Vectors: } a'_{0a} &= \frac{\partial x^\mu}{\partial x'^0} \frac{\partial x^\nu}{\partial x'^a} a_{\mu\nu} = \frac{\partial x^c}{\partial x'^a} a_{0c} \\
a'_{11} &= \frac{\partial x^\mu}{\partial x'^1} \frac{\partial x^\nu}{\partial x'^1} a_{\mu\nu} = a_{11} = 0 & a'_{1a} &= \frac{\partial x^\mu}{\partial x'^1} \frac{\partial x^\nu}{\partial x'^a} a_{\mu\nu} = \frac{\partial x^c}{\partial x'^a} a_{1c} \\
a'_{01} &= \frac{\partial x^\mu}{\partial x'^0} \frac{\partial x^\nu}{\partial x'^1} a_{\mu\nu} = a_{01} & & \\
\text{Tensor: } a'_{ab} &= \frac{\partial x^\mu}{\partial x'^a} \frac{\partial x^\nu}{\partial x'^b} a_{\mu\nu} = \frac{\partial x^c}{\partial x'^a} \frac{\partial x^d}{\partial x'^b} a_{cd}. & &
\end{aligned} \tag{3.43}$$

Our background is spherically symmetric, so we can once again make use of the tensor harmonics defined in (2.13). By choosing tensor harmonics of appropriate parities and index symmetries, we can write

$$a_{\mu\nu}^{(\text{axial})} = \sum_{\ell, m} \begin{pmatrix} 0 & 0 & 0 & a_0(r) \sin \theta \partial_\theta \\ 0 & 0 & 0 & a_1(r) \sin \theta \partial_\theta \\ \text{Sym} & \text{Sym} & 0 & -a_2(r) \sin \theta \\ \text{Sym} & \text{Sym} & \text{Sym} & 0 \end{pmatrix} e^{-i\omega t} Y_{\ell m}, \tag{3.44a}$$

$$a_{\mu\nu}^{(\text{polar})} = \sum_{\ell,m} \begin{pmatrix} 0 & A_0(r) & A_1(r) \partial_\theta & 0 \\ \text{Sym} & 0 & A_2(r) \partial_\theta & 0 \\ \text{Sym} & \text{Sym} & 0 & 0 \\ \text{Sym} & \text{Sym} & 0 & 0 \end{pmatrix} e^{-i\omega t} Y_{\ell m}. \quad (3.44b)$$

It should be noted that $a_{\mu\nu}^{(\text{polar})}$ does not contain second order tensor harmonics, because the only antisymmetric second order tensor harmonic has axial parity. We can now write the total antisymmetric perturbation $a_{\mu\nu}$ as the sum

$$a_{\mu\nu} = a_{\mu\nu}^{(\text{axial})} + a_{\mu\nu}^{(\text{polar})}. \quad (3.45)$$

For our choice of $C_5 = r$, the perturbed field equations are invariant under inversions and the radial functions in (3.44a) and (3.44b) will not appear together in the equations.

The linear perturbations δv_μ , $\delta \alpha_\mu$ and $\delta t_{\mu\nu\rho}$ can be directly calculated with the components of $h_{\mu\nu}$ and $a_{\mu\nu}$. These components are rather lengthy, and explicitly written down in Appendix A. We can now insert all these perturbations into the linearly perturbed field equations (3.27). To simplify the analysis, it is useful to split the perturbed field equations $\delta E_{\mu\nu} = 0$ into symmetric and antisymmetric equations

$$\delta E_{\mu\nu} = \delta E_{(\mu\nu)} + \delta E_{[\mu\nu]}. \quad (3.46)$$

The symmetric and antisymmetric parts must both vanish independently, since $\delta E_{\mu\nu} = 0$ and we can $\delta E_{(\mu\nu)} = \frac{1}{2}(\delta E_{\mu\nu} + \delta E_{\nu\mu})$ and $\delta E_{[\mu\nu]} = \frac{1}{2}(\delta E_{\mu\nu} - \delta E_{\nu\mu})$. The field equations are spherically symmetric, so we can restrict our analysis to $m = 0$. We will also assume harmonic time dependence $e^{-i\omega t}$ like was done in Chapter 2. The symmetric and antisymmetric field equations then separate into radial and angular parts, which we will denote

$$\begin{aligned} \delta E_{(\mu\nu)} &= \delta \mathcal{E}_{(\mu\nu)}(r) \delta \mathcal{Q}_{(\mu\nu)}(\theta, \varphi) e^{i\omega t}, \\ \delta E_{[\mu\nu]} &= \delta \mathcal{E}_{[\mu\nu]}(r) \delta \mathcal{Q}_{[\mu\nu]}(\theta, \varphi) e^{i\omega t}. \end{aligned} \quad (3.47)$$

3.4.1 Axial perturbed equations

We are first going to look at the axial perturbed field equations. The radial axial non-trivial symmetric field equations can be written as

$$\delta \mathcal{E}_{(03)} = 2 \delta \mathcal{R}_{03} + 9 \delta \mathcal{E}_{(03)}^{\delta c_a} \equiv 0, \quad (3.48a)$$

$$\delta \mathcal{E}_{(13)} = 2 \delta \mathcal{R}_{13} + 9 \delta \mathcal{E}_{(13)}^{\delta c_a} \equiv 0, \quad (3.48b)$$

$$\delta \mathcal{E}_{(23)} = \delta \mathcal{R}_{23} \equiv 0, \quad (3.48c)$$

where $\delta\mathcal{R}_{\mu\nu}$ are the axial field equations in Eq. (2.20) from Chapter 2. It turns out that the equations $\delta\mathcal{E}_{(03)}^{\delta c_a}$ and $\delta\mathcal{E}_{(13)}^{\delta c_a}$ are related in the form

$$\delta\mathcal{E}_{(13)}^{\delta c_a} = \mathcal{K}_1 \delta\mathcal{E}_{(03)}^{\delta c_a} \quad \text{with} \quad \mathcal{K}_1(r) = -\frac{2(r\mathcal{C}_{12} - \mathcal{C}_{11}^2)}{F^2 \mathcal{C}_{11}(2\mathcal{C}_1 - 3F^2 + 1)}. \quad (3.49)$$

This means that we can write $\delta\mathcal{E}_{(13)} = \delta\mathcal{R}_{(13)} - \mathcal{K}_1 \delta\mathcal{R}_{(03)} \equiv 0$, which must be satisfied independently of the exact value of \mathcal{K}_1 , so we find $\delta\mathcal{R}_{(13)} = 0$ and $\delta\mathcal{R}_{(03)} = 0$. We therefore retrieve the perturbed GR field equations for the perturbation functions h_0 and h_1

$$\delta\mathcal{R}_{23} = 0, \quad \delta\mathcal{R}_{13} = 0, \quad \delta\mathcal{R}_{03} = 0. \quad (3.50)$$

The one symmetric field equation for the perturbation functions a_0 , a_1 and a_2 is

$$\delta\mathcal{E}_{(03)} = \mathcal{F}_{11}(r) \frac{da_0}{dr} + \mathcal{F}_{12}(r) a_0 + \mathcal{F}_{13}(r) a_1 + \mathcal{F}_{14}(r) h_0 + \mathcal{F}_{15}(r) h_1 \equiv 0, \quad (3.51)$$

where the equation coefficients $\mathcal{F}_{ij}(r)$ are explicitly written in Appendix B.

Now, let's look at the antisymmetric equations. The radial axial non-trivial antisymmetric field equations are

$$\begin{aligned} \delta\mathcal{E}_{[03]} = & \mathcal{F}_{21} \frac{d^2 a_0}{dr^2} + \mathcal{F}_{22} \frac{da_1}{dr} + \mathcal{F}_{23} a_0 + \mathcal{F}_{24} a_1 + \mathcal{F}_{25} a_2 + \mathcal{F}_{26} \frac{dh_0}{dr} + \mathcal{F}_{27} \frac{dh_1}{dr} + \\ & + \mathcal{F}_{28} h_0 + \mathcal{F}_{29} h_1 \equiv 0, \end{aligned} \quad (3.52a)$$

$$\delta\mathcal{E}_{[13]} = \mathcal{F}_{31} \frac{da_0}{dr} + \mathcal{F}_{32} \frac{da_2}{dr} + \mathcal{F}_{33} a_0 + \mathcal{F}_{34} a_1 + \mathcal{F}_{35} a_2 + \mathcal{F}_{36} h_0 + \mathcal{F}_{37} h_1 \equiv 0, \quad (3.52b)$$

$$\delta\mathcal{E}_{[23]} = \mathcal{F}_{41} \frac{d^2 a_2}{dr^2} + \mathcal{F}_{42} \frac{da_1}{dr} + \mathcal{F}_{43} \frac{da_2}{dr} + \mathcal{F}_{44} a_0 + \mathcal{F}_{45} a_1 + \mathcal{F}_{46} a_2 \equiv 0, \quad (3.52c)$$

where $\mathcal{F}_{ij} = \mathcal{F}_{ij}(r)$ can be found in Appendix B. We can use $\delta\mathcal{E}_{(03)} = 0$ to write

$$a_1 = -\frac{1}{\mathcal{F}_{13}} \left(\mathcal{F}_{11} \frac{da_0}{dr} + \mathcal{F}_{12} a_0 + \mathcal{F}_{14} h_0 + \mathcal{F}_{15} h_1 \right). \quad (3.53)$$

Substituting a_1 into $\delta\mathcal{E}_{[03]} = 0$ yields

$$\begin{aligned} a_2 = & -\frac{1}{\mathcal{F}_{35}} \left[\left(\mathcal{F}_{23} - \frac{\mathcal{F}_{12}\mathcal{F}_{24}}{\mathcal{F}_{13}} - \frac{\mathcal{F}_{22} \frac{d\mathcal{F}_{12}}{dr}}{\mathcal{F}_{13}} + \frac{\mathcal{F}_{12}\mathcal{F}_{22} \frac{d\mathcal{F}_{13}}{dr}}{\mathcal{F}_{13}^2} \right) a_0 + \right. \\ & + \left(\mathcal{F}_{28} - \frac{\mathcal{F}_{14}\mathcal{F}_{24}}{\mathcal{F}_{13}} - \frac{\mathcal{F}_{22} \frac{d\mathcal{F}_{14}}{dr}}{\mathcal{F}_{13}} + \frac{\mathcal{F}_{14}\mathcal{F}_{22} \frac{d\mathcal{F}_{13}}{dr}}{\mathcal{F}_{13}^2} \right) h_0 + \\ & \left. + \left(\mathcal{F}_{29} - \frac{\mathcal{F}_{15}\mathcal{F}_{24}}{\mathcal{F}_{13}} - \frac{\mathcal{F}_{22} \frac{d\mathcal{F}_{15}}{dr}}{\mathcal{F}_{13}} + \frac{\mathcal{F}_{15}\mathcal{F}_{22} \frac{d\mathcal{F}_{13}}{dr}}{\mathcal{F}_{13}^2} \right) h_1 \right] \end{aligned} \quad (3.54)$$

We can now substitute both of these into $\delta E_{[13]} = 0$ and get the equation

$$\mathcal{M}_1(r) \frac{da_0}{dr} + \mathcal{M}_2(r) a_0 + \mathcal{M}_3(r) h_0 + \mathcal{M}_4(r) h_1 = 0, \quad (3.55)$$

where

$$\begin{aligned} \mathcal{M}_1(r) &= \frac{\delta c_a \ell(\ell+1)(r\mathcal{C}_{12} - \mathcal{C}_{11}^2)}{r(ir\omega - 2\mathcal{C}_{11})(ir\omega\mathcal{C}_{11} - r\mathcal{C}_{12} - \mathcal{C}_{11}^2)}, \\ \mathcal{M}_2(r) &= -\frac{\delta c_a \ell(\ell+1)}{r^2 F^2} \left[\frac{(2\mathcal{C}_1 - F^2 - 1)\mathcal{C}_{11}}{2(ir\omega\mathcal{C}_{11} - r\mathcal{C}_{12} - \mathcal{C}_{11}^2)} - \frac{2\mathcal{C}_1(ir\omega\mathcal{C}_{11} - r\mathcal{C}_{12} - \mathcal{C}_{11}^2)}{(ir\omega - 2\mathcal{C}_{11})^2 \mathcal{C}_{11}} + \right. \\ &\quad \left. + \frac{2ir\omega(2\mathcal{C}_1 - F^2) - (6\mathcal{C}_1 - F^2 + 1)\mathcal{C}_{11}}{(ir\omega - 2\mathcal{C}_{11})^2} \right], \\ \mathcal{M}_3(r) &= -\frac{\delta c_a \ell(\ell+1)(2\mathcal{C}_1 - 3F^2 + 1)\mathcal{C}_{11}}{2r^2 F^2(ir\omega\mathcal{C}_{11} - r\mathcal{C}_{12} - \mathcal{C}_{11}^2)}, \\ \mathcal{M}_4(r) &= -\frac{\delta c_a \ell(\ell+1)(r\mathcal{C}_{12} - \mathcal{C}_{11}^2)}{r^2(ir\omega\mathcal{C}_{11} - r\mathcal{C}_{12} - \mathcal{C}_{11}^2)}. \end{aligned} \quad (3.56)$$

The function a_0 can be found by integration if $\mathcal{M}_1(r) \neq 0$ and directly from (3.55) if $\mathcal{M}_1(r) = 0$

$$a_0 = -\frac{(\mathcal{M}_3(r) h_0 + \mathcal{M}_4(r) h_1)}{\mathcal{M}_2}, \quad \mathcal{M}_1(r) = 0, \quad (3.57a)$$

$$a_0 = e^{\int \frac{\mathcal{M}_2}{\mathcal{M}_1} dr} \left[\kappa_0 - \int e^{\int \frac{\mathcal{M}_2}{\mathcal{M}_1} dr} \frac{(\mathcal{M}_3 h_0 + \mathcal{M}_4 h_1)}{\mathcal{M}_1} dr \right], \quad \mathcal{M}_1(r) \neq 0. \quad (3.57b)$$

where κ_0 is an integration constant. As all the antisymmetric axial functions a_0 , a_1 and a_2 are defined in terms of h_0 and h_1 , no new independent quasinormal modes appear.

3.4.2 Polar perturbed equations

Now we'll look at the polar perturbed field equations. The radial polar non-trivial symmetric field equations are

$$\delta \mathcal{E}_{(00)} = \delta \mathcal{R}_{00} \equiv 0, \quad \delta \mathcal{E}_{(01)} = \delta \mathcal{R}_{01} \equiv 0, \quad \delta \mathcal{E}_{(11)} = \delta \mathcal{R}_{11} \equiv 0, \quad (3.58a)$$

$$\delta \mathcal{E}_{(22)} = \delta \mathcal{R}_{22} \equiv 0, \quad \delta \mathcal{E}_{(33)} = \delta \mathcal{R}_{33} \equiv 0,$$

$$\delta \mathcal{E}_{(02)} = 2 \delta \mathcal{R}_{02} + 9 \delta \mathcal{E}_{(02)}^{\delta c_a} \equiv 0, \quad (3.58b)$$

$$\delta \mathcal{E}_{(12)} = 2 \delta \mathcal{R}_{12} + 9 \delta \mathcal{E}_{(12)}^{\delta c_a} \equiv 0, \quad (3.58c)$$

where $\delta \mathcal{R}_{\mu\nu}$ are the polar field equations from Chapter 2 in Eq. (2.26).

The radial polar non-trivial antisymmetric field equations are

$$\delta \mathcal{E}_{[01]} = -\frac{\delta c_a}{r^2} \left[\frac{dA_1}{dr} - A_0 + \frac{2\mathcal{C}_1 - F^2 - 1}{2rF^2} A_1 + \left(i\omega - \frac{r\mathcal{C}_{12} + \mathcal{C}_{11}^2}{r\mathcal{C}_{11}} \right) A_2 \right] \equiv 0, \quad (3.59a)$$

$$\delta\mathcal{E}_{[02]} = \frac{d}{dr}(r^2 F^2 \delta\mathcal{E}_{[01]}) - \mathcal{P}_1(r) \delta\mathcal{E}_{[01]}, \quad (3.59b)$$

$$\delta\mathcal{E}_{[12]} = \mathcal{P}_2(r) \delta\mathcal{E}_{[01]}, \quad (3.59c)$$

where

$$\mathcal{P}_1(r) = \frac{r(2C_1 - 3F^2 + 1)}{2} \quad \text{and} \quad \mathcal{P}_2(r) = \frac{i\omega r^2}{F^2} + \frac{r(rC_{12} + C_{11}^2)}{F^2 C_{11}}. \quad (3.60)$$

Additionally, it turns out that $\delta\mathcal{E}_{(02)}^{\delta c_a}$ and $\delta\mathcal{E}_{(12)}^{\delta c_a}$ can be written in terms of $\delta\mathcal{E}_{[01]}$ as well

$$\begin{aligned} \delta\mathcal{E}_{(02)}^{\delta c_a} &= \mathcal{P}_1(r) \delta\mathcal{E}_{[01]}, \\ \delta\mathcal{E}_{(12)}^{\delta c_a} &= \mathcal{P}_3(r) \delta\mathcal{E}_{[01]} \quad \text{with} \quad \mathcal{P}_3(r) = \frac{r(rC_{12} - C_{11}^2)}{F^2 C_{11}}. \end{aligned} \quad (3.61)$$

They must therefore vanish, since $\delta\mathcal{E}_{[01]} = 0$, and we find that $\delta\mathcal{E}_{(02)} = \delta\mathcal{R}_{02}$ and $\delta\mathcal{E}_{(12)} = \delta\mathcal{R}_{12}$. This means that the symmetric perturbation functions H_0, H_1, K are determined by the perturbed GR field equations

$$\delta\mathcal{R}_{01} \equiv 0, \quad \delta\mathcal{R}_{02} \equiv 0, \quad \delta\mathcal{R}_{12} \equiv 0. \quad (3.62)$$

We are left with only one independent equation for A_0, A_1 and A_2 and it is

$$\delta\mathcal{E}_{[01]} = -\frac{\delta c_a}{r^2} \left[\frac{dA_1}{dr} - A_0 + \frac{2C_1 - F^2 - 1}{2rF^2} A_1 + \left(i\omega - \frac{rC_{12} + C_{11}^2}{rC_{11}} \right) A_2 \right] \equiv 0. \quad (3.63)$$

This means that the system remains under-defined and, therefore, quasinormal modes produced by the antisymmetric perturbation $a_{\mu\nu}^{\text{polar}}$ cannot be found.

3.5 Results and discussion

We find that the quasinormal spectrum of the symmetric perturbations $h_{\mu\nu}$ of Schwarzschild black holes in 1-parameter NGR coincides with the GR spectrum at the linear order of perturbations. This holds equally true for both axial and polar parity perturbations. For the antisymmetric perturbations, we find that the radial functions a_0, a_1 and a_2 in the antisymmetric axial perturbation $a_{\mu\nu}^{\text{axial}}$ are fully determined by the metric perturbation functions h_0 and h_1 as

$$a_0 = \mathcal{F}_0(h_0, h_1), \quad a_1 = \mathcal{F}_1(a_0, h_0, h_1), \quad a_2 = \mathcal{F}_2(a_0, h_0, h_1), \quad (3.64a)$$

where the functions $\mathcal{F}_0, \mathcal{F}_1$ and \mathcal{F}_2 take values (3.57), (3.53) and (3.54) respectively if $C_1 > 0$ and $C_5 = r$. This conclusion can be verified for $C_1 < 0$ and $C_5 = -r$ as well by making the appropriate changes in the code in Appendix C. The exact relationship of these perturbations

functions depends on the value of C_1 and C_5 . For example, if $C_1 = F$ and $C_5 = r$, we find that

$$a_0 = -h_0, \quad a_1 = \frac{1}{i\omega} \frac{dh_0}{dr} + \frac{2(1-F)}{ir\omega F} h_0, \quad a_2 = \frac{L(L+1)}{i\omega} h_0. \quad (3.65)$$

The radial functions A_0 , A_1 and A_2 in the antisymmetric polar perturbation $a_{\mu\nu}^{\text{polar}}$ are not fully defined by quasinormal modes alone. The single equation for these three functions is

$$\delta\mathcal{E}_{[01]} = -\frac{\delta c_a}{r^2} \left[\frac{dA_1}{dr} - A_0 + \frac{2C_1 - F^2 - 1}{2rF^2} A_1 + \left(i\omega - \frac{rC_{12} + C_{11}^2}{rC_{11}} \right) A_2 \right] \equiv 0. \quad (3.66)$$

The quasinormal spectrum can be calculated only if additional constraints for these functions are found. It may be possible to find these constraints by investigating other physical observables in terms of these perturbations. However, as mentioned previously, the results in [36] show that several Schwarzschild black hole related quantities do not get corrections in 1-parameter NGR. So it is yet to be determined which physical observables could provide these constraints. If the functions constrained were A_0 and A_2 specifically, and A_1 were left arbitrary, then the polar quasinormal modes could possibly show deviations from GR. This would mean that polar and axial parity quasinormal modes would no longer coincide, making a clear distinction from GR.

The results of this thesis only hold for the linear order of perturbations. Investigations of another general class teleparallel theories, called $f(T)$ theories of gravity, have revealed that some deviations from GR appear only once higher orders of perturbations are taken into account. For example, [39] found that teleparallel perturbations of Schwarzschild black holes lead to corrections to the Shapiro delay and light deflection at fifth order of perturbations. Additionally, [40] found that additional degrees of freedom predicted by $f(T)$ theories appear around the Minkowski background at third order. There is consequently opportunity for further study to determine whether higher orders of perturbations in NGR would lead to corrections to quasinormal spectrum of Schwarzschild black holes.

It's important to note that there is another branch of solutions, which is yet to be investigated. As mentioned before, the background equations also vanish if $C_1 = \pm F$ and C_5 takes the value

$$C_5 = r \frac{\kappa_1(F^4 + 6F^2 + 1) + 16\kappa_2(F^3 + F)}{4\kappa_2(F^4 + 6F^2 + 1) + 4\kappa_1(F^3 + F)}. \quad (3.67)$$

In that case, the torsion tensor is no longer reflection symmetric and the perturbed field equations therefore aren't either. While they do still separate into radial and angular parts thanks to the spherical symmetry, they mix the radial functions from the axial and polar parts of $h_{\mu\nu}$ and $a_{\mu\nu}$, resulting in more complicated relations. For example, the radial antisymmetric field equation $\delta\mathcal{E}_{[12]} = 0$ is

$$\delta\mathcal{E}_{[12]} = \mathcal{N}_1(r) \frac{dA_1}{dr} + \mathcal{N}_2(r) A_0 + \mathcal{N}_3(r) A_1 + \mathcal{N}_4(r) A_2 + \mathcal{N}_5(r) a_0 + \mathcal{N}_6(r) h_0, \quad (3.68)$$

where

$$\begin{aligned}
\mathcal{N}_2 = -\mathcal{N}_1 &= \frac{\mathcal{N}_4}{i\omega} = \frac{\delta c_a i\omega}{F^2}, & \mathcal{N}_3 &= -\frac{\delta c_a i\omega (F-1)^2 (F+1)^2 (\kappa_1 F + 2\kappa_2 F^2 + 2\kappa_2)}{4rF^4 (\kappa_1 (F^3 + F) + \kappa_2 (F^4 + 6\kappa_2 + \kappa_2))}, \\
\mathcal{N}_5 = -\mathcal{N}_6 &= \frac{\delta c_a i\omega (F-1)^2 (F+1)^2}{4rF^3} \sqrt{\frac{(4\kappa_2 - \kappa_1)(4\kappa_2 + \kappa_1)}{(\kappa_1 (F^3 + F) + \kappa_2 (F^4 + 6\kappa_2 + \kappa_2))^2}}.
\end{aligned} \tag{3.69}$$

Whether this branch gives any new quasinormal modes of Schwarzschild black holes in NGR is yet to be determined.

Summary

The ringdown stage of gravitational waves can be described in terms of quasinormal modes, which are characterized by their complex quasinormal frequencies; the real part represents the oscillation frequency and the imaginary part represents the inverse of the damping time. The values of quasinormal frequencies of black holes are fixed by their physical properties. The ringdown signal provides an opportunity to test theories of gravity in the strong field regime, so quasinormal modes can be used to find experimental constraints and highlight fundamental differences between theories.

GR characterizes gravity by curvature, where the gravitational field equations are a set of differential equations for the metric. The quasinormal modes can be analysed in the formalism of linear perturbation theory, where the metric is split into an unperturbed background and a first-order perturbation. The quasinormal modes are then solutions of the perturbed field equations, for which the metric perturbation can be written as a product of functions depending on the radial coordinate, a damped harmonic oscillation in time and a tensor spherical harmonic. These equations can further be separated into axial and polar parity, and analysing them yields two wave equations called the Regge-Wheeler and the Zerilli equations respectively. They possess the same quasinormal spectrum, and their quasinormal frequencies can be derived from the found wave equations, for example, with the Leaver's method or WKB approximation.

Teleparallel theories of gravity characterize the gravitational field by torsion. In this thesis, we consider the teleparallel theory called 1-parameter NGR, where gravitational field equations are given by the irreducible components of said torsion tensor, which are ultimately defined by the tetrad. We follow a similar approach to GR in deriving quasinormal modes. The tetrad is split into an unperturbed background, and first-order symmetric perturbations and antisymmetric perturbations. These define the linear perturbations of the irreducible components of the torsion tensor. The Schwarzschild background leaves only two of the background tetrad functions arbitrary, which we further constrain using the background field equations. This thesis considers one of the two possible branches. The antisymmetric perturbation of the tetrad is defined using the same method as in GR, and the symmetric perturbation is given directly by the metric perturbation. In our branch of solutions, the perturbed field equations once again separate into axial and polar parity. We find that in 1-parameter NGR, the quasinormal spectrum of the symmetric perturbations coincides with the GR spectrum for both parities at the linear order. For the axial antisymmetric perturbations, we find that they completely defined by the axial symmetric perturbations and do not produce any new quasinormal modes. The polar antisymmetric perturbations, on the other hand, cannot be defined by the quasinormal modes alone. So, additional constrains for these functions must be found if the polar quasinormal spectrum is to be evaluated.

Acknowledgements

First and foremost I would like to sincerely thank my supervisors Manuel Hohmann, Christian Pfeifer and João Luís Rosa for their support and guidance. They offered excellent advice and discussions in the making of this thesis, were always quick to help me with whatever issues I faces, and provided invaluable feedback during the writing process. I would also like to thank my fellow students and the academic staff at the University of Tartu without whom this entire experience would not have been so great and memorable. Finally, I wish to express my deepest gratitude to Sulev for never-ending patience and encouragement, and to all of my friends and family for their support and delightful board-game nights. Thank you, thank you, thank you to everyone who has been a part of this!

Helen Asuküla

Bibliography

- [1] S. Weinberg, *Gravitation and Cosmology: Principles and Applications of the General Theory of Relativity* (John Wiley and Sons, New York, 1972).
- [2] C. M. Will, „The Confrontation between General Relativity and Experiment“, *Living Reviews in Relativity* **17**, (2014).
- [3] R. Abbott et al., „GWTC-2: Compact Binary Coalescences Observed by LIGO and Virgo During the First Half of the Third Observing Run“, (2021) arXiv:2010.14527 [gr-qc].
- [4] J. Baker et al., „Space Based Gravitational Wave Astronomy Beyond LISA“, (2019) arXiv:1907.11305 [astro-ph.IM].
- [5] M. Isi et al., „Testing the No-Hair Theorem with GW150914“, *Physical Review Letters* **123**, (2019).
- [6] B. P. Abbott et al. (LIGO Scientific Collaboration and Virgo Collaboration), „Observation of Gravitational Waves from a Binary Black Hole Merger“, *Phys. Rev. Lett.* **116**, 061102 (2016).
- [7] E. Berti et al., „Testing general relativity with present and future astrophysical observations“, *Classical and Quantum Gravity* **32**, 243001 (2015).
- [8] M. Giesler et al., „Black Hole Ringdown: The Importance of Overtones“, *Phys. Rev. X* **9**, 041060 (2019).
- [9] R. Abbott et al. (LIGO Scientific, Virgo), „Tests of General Relativity with Binary Black Holes from the second LIGO-Virgo Gravitational-Wave Transient Catalog“, (Oct. 2020) arXiv:2010.14529 [gr-qc].
- [10] K. D. Kokkotas and B. G. Schmidt, „Quasi-Normal Modes of Stars and Black Holes“, *Living Reviews in Relativity* **2**, (1999).
- [11] H.-P. Nollert, „Quasinormal modes: the characteristic ‘sound’ of black holes and neutron stars“, *Classical and Quantum Gravity* **16**, R159–R216 (1999).
- [12] E. Berti, V. Cardoso, and A. O. Starinets, „Quasinormal modes of black holes and black branes“, *Classical and Quantum Gravity* **26**, 163001 (2009).
- [13] B. P. Abbott et al. (LIGO Scientific and Virgo Collaborations), „Tests of General Relativity with GW150914“, *Phys. Rev. Lett.* **116**, 221101 (2016).
- [14] S. Carroll, *Spacetime and Geometry: An Introduction to General Relativity* (Pearson, 2004).
- [15] C. Bambi, *Black Holes: A Laboratory for Testing Strong Gravity* (Springer, 2017).
- [16] R. M. Wald, *General Relativity* (Chicago Univ. Pr., Chicago, USA, 1984).
- [17] D. Griffiths, *Introduction to Quantum Mechanics*, Pearson international edition (Pearson Prentice Hall, 2005).

- [18] V. D. Sandberg, „Tensor spherical harmonics on S^2 and S^3 as eigenvalue problems“, *Journal of Mathematical Physics* **19**, 2441–2446 (1978).
- [19] T. Regge and J. A. Wheeler, „Stability of a Schwarzschild Singularity“, *Phys. Rev.* **108**, 1063–1069 (1957).
- [20] C. W. Misner, K. S. Thorne, and J. A. Wheeler, *Gravitation* (W. H. Freeman and Company, 1973).
- [21] L. A. Edelman and C. V. Vishveshwara, „Differential equations for perturbations on the schwarzschild metric“, *Phys. Rev. D* **1**, 3514–3517 (1970).
- [22] F. J. Zerilli, „Effective Potential for Even-Parity Regge-Wheeler Gravitational Perturbation Equations“, *Phys. Rev. Lett.* **24**, 737–738 (1970).
- [23] S. Chandrasekhar and S. Detweiler, „The Quasi-Normal Modes of the Schwarzschild Black Hole“, *Proceedings of the Royal Society of London. Series A, Mathematical and Physical Sciences* **344**, 441–452 (1975).
- [24] E. W. Leaver, „An Analytic representation for the quasi normal modes of Kerr black holes“, *Proc. Roy. Soc. Lond. A* **402**, 285–298 (1985).
- [25] B. F. Schutz and C. M. Will, „Black hole normal modes – a semianalytic approach“, *Astrophys. J.; (United States)* **291**, (1985).
- [26] S. Iyer and C. M. Will, „Black-hole normal modes: A WKB approach. I. Foundations and application of a higher-order WKB analysis of potential-barrier scattering“, *Phys. Rev. D* **35**, 3621–3631 (1987).
- [27] S. Iyer, „Black-hole normal modes: A WKB approach. II. Schwarzschild black holes“, *Phys. Rev. D* **35**, 3632–3636 (1987).
- [28] F. W. Hehl et al., „General relativity with spin and torsion: Foundations and prospects“, *Rev. Mod. Phys.* **48**, 393–416 (1976).
- [29] K. Hayashi and T. Shirafuji, „New general relativity“, *Phys. Rev. D* **19**, 3524–3553 (1979).
- [30] M. Krššák et al., „Teleparallel theories of gravity: illuminating a fully invariant approach“, *Classical and Quantum Gravity* **36**, 183001 (2019).
- [31] M. Hohmann et al., „Modified teleparallel theories of gravity in symmetric spacetimes“, *Phys. Rev. D* **100**, 084002 (2019).
- [32] J. W. Maluf et al., „Perturbations of the Gravitational Energy in theTEGR: Quasinormal Modes of the Schwarzschild Black Hole“, *Universe* **7**, 100 (2021), arXiv:2104.08059 [gr-qc].
- [33] M. Hohmann et al., „Propagation of gravitational waves in teleparallel gravity theories“, *Phys. Rev. D* **98**, 124004 (2018).
- [34] M. Hohmann, „Complete classification of cosmological teleparallel geometries“, (2020) arXiv:2008.12186 [gr-qc].

- [35] K. Hayashi and T. Shirafuji, „Addendum to 'New general relativity'“, *Phys. Rev. D* **24**, 3312–3314 (1981).
- [36] S. Bahamonde and C. Pfeifer, „General teleparallel modifications of Schwarzschild geometry“, *International Journal of Geometric Methods in Modern Physics*, 2140001 (2021).
- [37] A. Meurer et al., „SymPy: symbolic computing in Python“, *PeerJ Computer Science* **3**, e103 (2017).
- [38] T. Kluyver et al., „Jupyter Notebooks – a publishing format for reproducible computational workflows“, in *Positioning and Power in Academic Publishing: Players, Agents and Agendas*, edited by F. Loizides and B. Schmidt (IOS Press, 2016), pp. 87–90.
- [39] C. Pfeifer and S. Schuster, „Static spherically symmetric black holes in weak $f(T)$ -gravity“, (2021) arXiv:2104.00116 [gr-qc].
- [40] J. B. Jiménez et al., „Minkowski space in $f(T)$ gravity“, *Physical Review D* **103**, (2021).

Appendix A

Components of $\delta\mathbf{v}_\mu$, $\delta\mathbf{a}_\mu$ and $\delta\mathbf{t}_{\mu\nu\rho}$

The vector, axial and torsion irreducibles of the torsion tensor split into background and linear perturbations

$$\mathbf{v}_\mu = \bar{\mathbf{v}}_\mu + \delta\mathbf{v}_\mu^{(h)} + \delta\mathbf{v}_\mu^{(a)}, \quad \mathbf{a}_\mu = \bar{\mathbf{a}}_\mu + \delta\mathbf{a}_\mu^{(h)} + \delta\mathbf{a}_\mu^{(a)}, \quad \mathbf{t}_{\mu\nu\rho} = \bar{\mathbf{t}}_{\mu\nu\rho} + \delta\mathbf{t}_{\mu\nu\rho}^{(h)} + \delta\mathbf{t}_{\mu\nu\rho}^{(a)}. \quad (\text{A.1})$$

These perturbations play a role in the perturbed field equations (3.27). We will write the components of these perturbations in spherical symmetry explicitly in this appendix.

The calculations are done in spherical symmetry using $h_{\mu\nu} = h_{\mu\nu}^{(\text{axial})} + h_{\mu\nu}^{(\text{polar})}$ with matrices from (2.18) and $a_{\mu\nu} = a_{\mu\nu}^{(\text{axial})} + a_{\mu\nu}^{(\text{polar})}$ with matrices from (3.44).

The non-trivial vector irreducible perturbation components are

$$\begin{aligned} \delta\mathbf{v}_0^{(h)} &= \frac{1}{2} \left[F^2 \frac{dH_1}{dr} - \frac{r\mathcal{C}_{12} + 2\mathcal{C}_{11}^2}{r\mathcal{C}_{11}} H_0 + \frac{2\mathcal{C}_1}{r} H_1 + \left(i\omega - \frac{\mathcal{C}_{12}}{\mathcal{C}_{11}} \right) H_2 + 2 \left(i\omega - \frac{\mathcal{C}_{11}}{r} \right) K \right] \frac{Y_{\ell m}}{e^{i\omega t}}, \\ \delta\mathbf{v}_1^{(h)} &= \frac{1}{2} \left[\frac{dH_0}{dr} - 2 \frac{dK}{dr} + \left(\frac{i\omega}{F^2} - \frac{2r\mathcal{C}_{12} + 2\mathcal{C}_{11}^2}{rF^2\mathcal{C}_{11}} \right) H_1 + \frac{2\mathcal{C}_1}{rF^2} (H_2 - K) \right] \frac{Y_{\ell m}}{e^{i\omega t}}, \\ \delta\mathbf{v}_2^{(h)} &= \frac{1}{2} \left[H_0 - H_2 - K \right] \frac{\partial_\theta Y_{\ell m}}{e^{i\omega t}}, \\ \delta\mathbf{v}_3^{(h)} &= \frac{1}{2} \left[F^2 \frac{dh_1}{dr} + \left(\frac{i\omega}{F^2} - \frac{r\mathcal{C}_{12} + 3\mathcal{C}_{11}^2}{rF^2\mathcal{C}_{11}} \right) h_0 + \frac{6\mathcal{C}_1 - 3F^2 + 1}{2r} h_1 \right] \frac{\sin\theta \partial_\theta Y_{\ell m}}{e^{i\omega t}}. \end{aligned} \quad (\text{A.2})$$

and

$$\begin{aligned} \delta\mathbf{v}_0^{(a)} &= \frac{1}{2} \left[-F^2 \frac{dA_0}{dr} - \frac{2\mathcal{C}_1}{r} A_0 + \frac{\ell(\ell+1)}{r^2} A_1 \right] \frac{Y_{\ell m}}{e^{i\omega t}}, \\ \delta\mathbf{v}_1^{(a)} &= \frac{1}{2} \left[\left(\frac{i\omega}{F^2} - \frac{2\mathcal{C}_{11}}{rF^2} \right) A_0 + \frac{\ell(\ell+1)}{r^2} A_3 \right] \frac{Y_{\ell m}}{e^{i\omega t}}, \\ \delta\mathbf{v}_2^{(a)} &= \frac{1}{2} \left[F^2 \frac{dA_2}{dr} + \left(\frac{i\omega}{F^2} - \frac{r\mathcal{C}_{12} + \mathcal{C}_{11}^2}{rF^2\mathcal{C}_{11}} \right) A_1 + \frac{2\mathcal{C}_1 - 3F^2 + 1}{2r} A_2 \right] \frac{\partial_\theta Y_{\ell m}}{e^{i\omega t}}, \\ \delta\mathbf{v}_3^{(a)} &= \frac{1}{2} \left[F^2 \frac{da_1}{dr} + \left(\frac{i\omega}{F^2} - \frac{r\mathcal{C}_{12} + \mathcal{C}_{11}^2}{rF^2\mathcal{C}_{11}} \right) a_0 + \frac{2\mathcal{C}_1 - 3F^2 + 1}{2r} a_1 - \frac{a_2}{r^2} \right] \frac{\sin\theta \partial_\theta Y_{\ell m}}{e^{i\omega t}}. \end{aligned} \quad (\text{A.3})$$

The non-trivial axial irreducible perturbation components are

$$\delta\mathbf{a}_2^{(h)} = \frac{1}{3} \left[\frac{2\mathcal{C}_1 - 3F^2 + 1}{2rF^2} h_0 + \frac{r\mathcal{C}_{12} - \mathcal{C}_{11}^2}{r\mathcal{C}_{11}} h_1 \right] \frac{\partial_\theta Y_{\ell m}}{e^{i\omega t}}, \quad (\text{A.4})$$

and

$$\begin{aligned}
\delta \mathbf{a}_0^{(a)} &= \frac{1}{3} \left[\frac{F^2}{r^2} \frac{da_2}{dr} - \frac{\ell(\ell+1)F^2}{r^2} a_1 + \frac{2(C_1 - F^2)}{r^3} a_2 \right] \frac{Y_{\ell m}}{e^{i\omega t}}, \\
\delta \mathbf{a}_1^{(a)} &= \frac{1}{3} \left[-\frac{\ell(\ell+1)}{r^2 F^2} a_0 - \left(\frac{i\omega}{r^2 F^2} + \frac{2C_{11}}{r^3 F^2} \right) a_2 \right] \frac{Y_{\ell m}}{e^{i\omega t}}, \\
\delta \mathbf{a}_2^{(a)} &= \frac{1}{3} \left[-\frac{da_0}{dr} - \frac{2C_1 - F^2 - 1}{2rF^2} a_0 - \left(i\omega - \frac{rC_{12} + C_{11}^2}{rC_{11}} \right) a_1 \right] \frac{\partial_\theta Y_{\ell m}}{e^{i\omega t}}, \\
\delta \mathbf{a}_3^{(a)} &= \frac{1}{3} \left[\frac{dA_1}{dr} - A_0 + \frac{2C_1 - F^2 - 1}{2rF^2} A_1 + \left(i\omega - \frac{rC_{12} + C_{11}^2}{rC_{11}} \right) A_2 \right] \frac{\sin \theta \partial_\theta Y_{\ell m}}{e^{i\omega t}}.
\end{aligned} \tag{A.5}$$

The independent non-trivial tensor irreducible perturbation components are

$$\begin{aligned}
\delta t_{001}^{(h)} &= -\frac{1}{3} \left[F^2 \frac{dH_0}{dr} + F^2 \frac{dK}{dr} + \frac{2C_1 - 3F^2 + 1}{r} H_0 + \left(i\omega - \frac{C_{11}}{r} \right) H_1 - \frac{C_1}{r} (H_2 - K) \right] \frac{Y_{\ell m}}{e^{i\omega t}}, \\
\delta t_{221}^{(h)} &= -\frac{1}{6} \left[r^2 \frac{dH_0}{dr} + r^2 \frac{dK}{dr} + r^2 \left(\frac{i\omega}{F^2} - \frac{2rC_{12} - C_{11}^2}{rF^2 C_{11}} \right) H_1 - \frac{rC_1}{F^2} H_2 + (C_1 - 3F^2 - 1) K \right] \frac{Y_{\ell m}}{e^{i\omega t}}, \\
\delta t_{002}^{(h)} &= -\frac{1}{6} \left[2F^2 H_0 + F^2 H_2 + F^2 K \right] \frac{\partial_\theta Y_{\ell m}}{e^{i\omega t}}, \quad \delta t_{012}^{(h)} = -\frac{H_1}{2} \frac{\partial_\theta Y_{\ell m}}{e^{i\omega t}}, \\
\delta t_{112}^{(h)} &= -\frac{1}{6} \left[\frac{1}{F^2} H_0 + \frac{2}{F^2} H_2 - \frac{1}{F^2} K \right] \frac{\partial_\theta Y_{\ell m}}{e^{i\omega t}}, \quad \delta t_{332}^{(h)} = -\left[H_0 - H_2 + 2K \right] \frac{\sin^2 \theta \partial_\theta Y_{\ell m}}{e^{i\omega t}}, \\
\delta t_{003}^{(h)} &= \frac{1}{3} \left[\frac{F^4}{2} \frac{dh_1}{dr} - \left(i\omega - \frac{rC_{12} + C_{11}^2}{2rC_{11}} \right) h_0 + \frac{F^2(6C_1 - 3F^2 + 1)}{4r} h_1 \right] \frac{\partial_\theta Y_{\ell m}}{e^{i\omega t}}, \\
\delta t_{113}^{(h)} &= \frac{1}{3} \left[\frac{dh_1}{dr} - \left(\frac{i\omega}{2F^4} + \frac{2rC_{12} - 3C_{11}^2}{2rF^4 C_{11}} \right) h_0 + \frac{C_1}{2rF^2} h_1 \right] \frac{\sin \theta \partial_\theta Y_{\ell m}}{e^{i\omega t}}, \\
\delta t_{223}^{(h)} &= -\frac{1}{6} \left[F^2 r^2 \frac{dh_1}{dr} + r^2 \left(\frac{i\omega}{F^2} - \frac{C_{12}}{F^2 C_{11}} \right) h_0 - \frac{r(3F^2 - 1)}{2} h_1 \right] \frac{\sin \theta \partial_\theta Y_{\ell m}}{e^{i\omega t}}, \\
\delta t_{011}^{(h)} &= -\frac{1}{6} \left[\frac{dH_1}{dr} - \frac{rC_{12} - C_{11}^2}{rF^2 C_{11}} H_0 + \frac{C_1 - 3F^2 + 1}{rF^2} H_1 + \right. \\
&\quad \left. + \left(\frac{i\omega}{F^2} - \frac{rC_{12} - 2C_{11}^2}{rF^2 C_{11}} \right) H_2 - \left(\frac{i\omega}{F^2} - \frac{C_{11}}{rF^2} \right) K \right] \frac{Y_{\ell m}}{e^{i\omega t}}, \\
\delta t_{220}^{(h)} &= -\frac{1}{6} \left[F^2 r^2 \frac{dH_1}{dr} - \frac{r(rC_{12} - C_{11}^2)}{C_{11}} H_0 - rC_1 H_1 + \right. \\
&\quad \left. + \left(i\omega r^2 - r^2 \frac{C_{12}}{C_{11}} \right) H_2 - \left(i\omega r^2 - \frac{r(2rC_{12} - C_{11}^2)}{C_{11}} \right) K \right] \frac{Y_{\ell m}}{e^{i\omega t}}, \\
\delta t_{013}^{(h)} &= \frac{1}{4} \left[\frac{dh_0}{dr} + \frac{8C_1 + 3F^3 - 5}{6rF^2} h_0 - \left(i\omega - \frac{rC_{12} - 4C_{11}^2}{3rF^2 C_{11}} \right) h_1 \right] \frac{\sin \theta \partial_\theta Y_{\ell m}}{e^{i\omega t}}, \\
\delta t_{031}^{(h)} &= -\frac{1}{2} \left[\frac{dh_0}{dr} + \frac{5C_1 - 6F^2 - 2}{6rF^2} h_0 + \left(\frac{i\omega}{2} - \frac{2rC_{12} + C_{11}^2}{6rC_{11}} \right) h_1 \right] \frac{\sin \theta \partial_\theta Y_{\ell m}}{e^{i\omega t}}, \\
\delta t_{130}^{(h)} &= \frac{1}{4} \left[\frac{dh_0}{dr} + \frac{2C_1 - 15F^2 + 1}{6rF^2} h_0 + \left(2i\omega - \frac{rC_{12} + 5C_{11}^2}{rC_{11}} \right) h_1 \right] \frac{\partial_\theta Y_{\ell m}}{e^{i\omega t}}, \\
\delta t_{230}^{(h)} &= -\frac{\ell(\ell+1)}{4} \frac{h_0}{e^{i\omega t}} \frac{\sin \theta Y_{\ell m}}{e^{i\omega t}} - \frac{h_0}{2} \frac{\cos \theta \partial_\theta Y_{\ell m}}{e^{i\omega t}}, \\
\delta t_{231}^{(h)} &= -\frac{\ell(\ell+1)}{4} \frac{h_1}{e^{i\omega t}} \frac{\sin \theta Y_{\ell m}}{e^{i\omega t}} - \frac{h_1}{2} \frac{\cos \theta \partial_\theta Y_{\ell m}}{e^{i\omega t}}, \\
\delta t_{021}^{(h)} &= \delta t_{120}^{(h)} = -\frac{1}{2} \delta t_{012}^{(h)}, \quad \delta t_{331}^{(h)} = \sin^2 \theta \delta t_{221}^{(h)}, \quad \delta t_{033}^{(h)} = \sin^2 \theta \delta t_{022}^{(h)},
\end{aligned} \tag{A.6}$$

$$\begin{aligned}\delta t_{023}^{(h)} &= \delta t_{230}^{(h)} + h_0 \frac{3 \cos \theta}{4} \frac{\partial_\theta Y_{\ell m}}{e^{i\omega t}}, & \delta t_{032}^{(h)} &= -2 \delta t_{230}^{(h)} - h_0 \frac{3 \cos \theta}{4} \frac{\partial_\theta Y_{\ell m}}{e^{i\omega t}}, \\ \delta t_{123}^{(h)} &= \delta t_{231}^{(h)} + h_1 \frac{3 \cos \theta}{4} \frac{\partial_\theta Y_{\ell m}}{e^{i\omega t}}, & \delta t_{132}^{(h)} &= -2 \delta t_{231}^{(h)} - h_1 \frac{3 \cos \theta}{4} \frac{\partial_\theta Y_{\ell m}}{e^{i\omega t}},\end{aligned}$$

and

$$\begin{aligned}\delta t_{001}^{(a)} &= -\frac{1}{3} \left[\left(i\omega + \frac{C_{11}}{r} \right) A_0 - \frac{\ell(\ell+1)F^2}{2r^2} A_2 \right] \frac{Y_{\ell m}}{e^{i\omega t}}, \\ \delta t_{021}^{(a)} &= \frac{1}{4} \left[A_0 - \frac{C_1}{rF^2} A_1 + \left(i\omega + \frac{C_{11}}{r} \right) A_2 \right] \frac{\partial_\theta Y_{\ell m}}{e^{i\omega t}}, \\ \delta t_{221}^{(a)} &= \frac{1}{6} \left[\left(\frac{i\omega r^2}{2F^2} + \frac{rC_{11}}{2F^2} \right) A_0 - \ell(\ell+1)r^4 A_2 \right] \frac{Y_{\ell m}}{e^{i\omega t}} - \frac{A_2}{4 \tan \theta} \frac{\partial_\theta Y_{\ell m}}{e^{i\omega t}}, \\ \delta t_{331}^{(a)} &= -\frac{1}{6} \left[\left(\frac{i\omega r^2}{F^2} + \frac{rC_{11}}{F^2} \right) A_0 + \ell(\ell+1)r^4 A_2 \right] \frac{\sin^2 \theta Y_{\ell m}}{e^{i\omega t}} - \frac{A_2 \cos \theta \sin \theta}{2} \frac{\partial_\theta Y_{\ell m}}{e^{i\omega t}}, \\ \delta t_{002}^{(a)} &= \frac{1}{3} \left[\frac{F^4}{2} \frac{dA_2}{dr} - \left(i\omega + \frac{rC_{12} + C_{11}^2}{2rC_{11}} \right) A_1 + \frac{(2C_1 - 3F^2 + 1)F^2}{4r} A_2 \right] \frac{\partial_\theta Y_{\ell m}}{e^{i\omega t}}, \\ \delta t_{112}^{(a)} &= \frac{1}{3} \left[\frac{dA_2}{dr} - \left(\frac{i\omega}{2F^4} - \frac{2rC_{12} - C_{11}^2}{2rF^4 C_{11}} \right) A_1 - \frac{C_1 + 3F^2 - 1}{6rF^2} A_2 \right] \frac{\partial_\theta Y_{\ell m}}{e^{i\omega t}}, \\ \delta t_{332}^{(a)} &= -\frac{1}{6} \left[F^2 r^2 \frac{dA_2}{dr} + \left(\frac{i\omega r^2}{F^2} - \frac{r(rC_{12} - 2C_{11}^2)}{F^2 C_{11}} \right) A_1 - \frac{r(4C_1 + 3F^2 - 1)}{2} A_2 \right] \frac{\sin^2 \theta \partial_\theta Y_{\ell m}}{e^{i\omega t}}, \\ \delta t_{003}^{(a)} &= \frac{1}{3} \left[\frac{F^4}{2} \frac{da_1}{dr} - \left(i\omega + \frac{rC_{12} + C_{11}^2}{2rC_{11}} \right) a_0 + \frac{(2C_1 - 3F^2 + 1)F^2}{4r} a_1 - \frac{F^2}{2r^2} a_2 \right] \frac{\sin \theta \partial_\theta Y_{\ell m}}{e^{i\omega t}}, \\ \delta t_{113}^{(a)} &= \frac{1}{3} \left[\frac{da_1}{dr} - \left(\frac{i\omega}{2F^4} - \frac{2rC_{12} - C_{11}^2}{2rF^4 C_{11}} \right) a_0 - \frac{C_1 + 3F^2 - 1}{6rF^2} a_1 \right] \frac{\sin \theta \partial_\theta Y_{\ell m}}{e^{i\omega t}}, \\ \delta t_{223}^{(a)} &= -\frac{1}{6} \left[F^2 r^2 \frac{da_1}{dr} + \left(\frac{i\omega r^2}{F^2} - \frac{r(rC_{12} - 2C_{11}^2)}{F^2 C_{11}} \right) a_0 + \right. \\ &\quad \left. - \frac{r(4C_1 + 3F^2 - 1)}{2} a_1 + 2a_2 \right] \frac{\sin \theta \partial_\theta Y_{\ell m}}{e^{i\omega t}}, \\ \delta t_{011}^{(a)} &= \frac{1}{6} \left[\frac{dA_0}{dr} - \frac{C_1}{rF^2} A_0 + \frac{\ell(\ell+1)}{2r^2 F^2} A_1 \right] \frac{Y_{\ell m}}{e^{i\omega t}}, \\ \delta t_{220}^{(a)} &= \frac{1}{3} \left[\frac{F^2 r^2}{2} \frac{dA_0}{dr} - \frac{rC_1}{2} A_0 + \ell(\ell+1)r^4 A_1 \right] \frac{Y_{\ell m}}{e^{i\omega t}} + \frac{A_1}{2 \tan \theta} \frac{\partial_\theta Y_{\ell m}}{e^{i\omega t}}, \\ \delta t_{330}^{(a)} &= \frac{1}{6} \left[F^2 r^2 \frac{dA_0}{dr} - rC_1 A_0 - \ell(\ell+1)r^4 A_1 \right] \frac{\sin^2 \theta Y_{\ell m}}{e^{i\omega t}} - \frac{A_1 \cos \theta \sin \theta}{2} \frac{\partial_\theta Y_{\ell m}}{e^{i\omega t}}, \\ \delta t_{012}^{(a)} &= \frac{1}{4} \left[\frac{dA_1}{dr} - \frac{F^2 - 1}{2rF^2} A_1 - \left(i\omega + \frac{C_{12}}{C_{11}} \right) A_2 \right] \frac{\partial_\theta Y_{\ell m}}{e^{i\omega t}}, \\ \delta t_{120}^{(a)} &= -\frac{1}{4} \left[\frac{dA_1}{dr} - A_0 - \frac{2C_1 + F^2 + 1}{2rF^2} A_1 - \frac{rC_{12} - C_{11}^2}{rC_{11}} A_2 \right] \frac{\partial_\theta Y_{\ell m}}{e^{i\omega t}}, \\ \delta t_{013}^{(a)} &= \frac{1}{4} \left[\frac{da_0}{dr} - \frac{F^2 - 1}{2rF^2} a_0 - \left(i\omega + \frac{C_{12}}{C_{11}} \right) a_1 \right] \frac{\sin \theta \partial_\theta Y_{\ell m}}{e^{i\omega t}}, \\ \delta t_{130}^{(a)} &= -\frac{1}{4} \left[\frac{da_0}{dr} - \frac{2C_1 + F^2 + 1}{2rF^2} a_0 - \frac{rC_{12} - C_{11}^2}{rC_{11}} a_1 \right] \frac{\sin \theta \partial_\theta Y_{\ell m}}{e^{i\omega t}}, \\ \delta t_{023}^{(a)} &= -\frac{1}{4} \left[\ell(\ell+1) a_0 - \left(i\omega + \frac{C_{11}}{r} \right) a_2 \right] \frac{\sin \theta \partial_\theta Y_{\ell m}}{e^{i\omega t}} - \frac{a_0 \cos \theta}{4} \frac{\partial_\theta Y_{\ell m}}{e^{i\omega t}},\end{aligned} \tag{A.7}$$

$$\begin{aligned}
\delta t_{031}^{(a)} &= -\frac{1}{4} \left[\frac{C_1}{4rF^2} a_0 - \left(i\omega + \frac{C_{11}}{r} \right) a_1 \right] \frac{\sin \theta \partial_\theta Y_{\ell m}}{e^{i\omega t}}, \\
\delta t_{032}^{(a)} &= -\frac{1}{4} \left(i\omega + \frac{C_{11}}{r} \right) a_2 \frac{Y_{\ell m}}{e^{i\omega t}} - \frac{a_0 \cos \theta \partial_\theta Y_{\ell m}}{4 e^{i\omega t}}, \\
\delta t_{230}^{(a)} &= \frac{\ell(\ell+1) a_0 \sin \theta Y_{\ell m}}{4 e^{i\omega t}} + \frac{a_0 \cos \theta \partial_\theta Y_{\ell m}}{2 e^{i\omega t}}, \\
\delta t_{231}^{(a)} &= \frac{\ell(\ell+1) a_1 \sin \theta Y_{\ell m}}{4 e^{i\omega t}} + \frac{a_1 \cos \theta \partial_\theta Y_{\ell m}}{2 e^{i\omega t}}, \\
\delta t_{132}^{(a)} &= \frac{1}{4} \left[\frac{da_2}{dr} - \frac{C_1 + 2F^2}{rF^2} a_2 \right] \frac{\sin \theta Y_{\ell m}}{e^{i\omega t}} - \frac{a_1 \cos \theta \partial_\theta Y_{\ell m}}{4 e^{i\omega t}}, \\
\delta t_{123}^{(a)} &= -\frac{1}{4} \left[\frac{da_2}{dr} + \ell(\ell+1) a_1 - \frac{C_1 + 2F^2}{rF^2} a_2 \right] \frac{\sin \theta Y_{\ell m}}{e^{i\omega t}} - \frac{a_1 \cos \theta \partial_\theta Y_{\ell m}}{4 e^{i\omega t}}.
\end{aligned}$$

Other components of the tensor irreducible perturbation can be found from the symmetry $\delta t_{\mu\nu\rho} = \delta t_{\nu\mu\rho}$ and the relation $(\delta t_{\mu\nu\rho} + 2\delta t_{\mu\rho\nu} = 0)|_{\mu=\nu}$.

Appendix B

Equation coefficients $\mathcal{F}_{ij}(r)$

The function coefficients in the axial perturbed field equations $\delta\mathcal{E}_{(03)}$ in (3.51) are

$$\begin{aligned}
 \mathcal{F}_{11}(r) &= \delta c_a \frac{2C_1 - 3F^2 + 1}{2r}, \\
 \mathcal{F}_{12}(r) &= \delta c_a \frac{(2C_1 - 3F^2 + 1)(2C_1 - F^2 - 1)}{4r^2 F^2}, \\
 \mathcal{F}_{13}(r) &= \frac{\mathcal{F}_{11}\mathcal{F}_{22}}{\mathcal{F}_{21}}, \quad \mathcal{F}_{14}(r) = \frac{\mathcal{F}_{11}^2}{\mathcal{F}_{21}}, \quad \mathcal{F}_{15}(r) = \frac{\mathcal{F}_{11}\mathcal{F}_{27}}{\mathcal{F}_{21}}.
 \end{aligned} \tag{B.1}$$

The function coefficients in the axial perturbed field equations $\delta\mathcal{E}_{[03]}$ in (3.52a) are

$$\begin{aligned}
 \mathcal{F}_{21}(r) &= -\delta c_a F^2, \\
 \mathcal{F}_{22}(r) &= -\delta c_a F^2 \left(i\omega - \frac{r\mathcal{C}_{12} + \mathcal{C}_{11}^2}{\mathcal{C}_{11}} \right), \\
 \mathcal{F}_{23}(r) &= \delta c_a \frac{4\ell(\ell+1)F^2 - 4(r\mathcal{C}_{12} - \mathcal{C}_{11}^2) - 2C_1(F^2 + 1) - F^2(F^2 - 6) - 1}{4r^2 F^2}, \\
 \mathcal{F}_{24}(r) &= \delta c_a \left(\frac{i\omega(2C_1 - F^2 - 1)}{2r} + \frac{F^2}{\mathcal{C}_{11}} \frac{d\mathcal{C}_{12}}{dr} - \frac{C_1(r^2\mathcal{C}_{12}^2 + \mathcal{C}_{11}^4)}{r\mathcal{C}_{11}^3} + \right. \\
 &\quad \left. + \frac{F^2(r\mathcal{C}_{12} - \mathcal{C}_{11}^2)}{r^2\mathcal{C}_{11}} + \frac{\mathcal{C}_{11}}{r^2} \right), \\
 \mathcal{F}_{25}(r) &= \frac{\delta c_a}{r^2} \left(i\omega - \frac{2\mathcal{C}_{11}}{r} \right), \\
 \mathcal{F}_{26}(r) &= \mathcal{F}_{11}, \\
 \mathcal{F}_{27}(r) &= \delta c_a F^2 \frac{r\mathcal{C}_{12} - \mathcal{C}_{11}^2}{r\mathcal{C}_{11}}, \\
 \mathcal{F}_{28}(r) &= \delta c_a \frac{4(r\mathcal{C}_{12} - \mathcal{C}_{11}^2) + 2C_1(3F^2 - 1) + F^2(3F^2 - 6) - 1}{4r^2 F^2}, \\
 \mathcal{F}_{29}(r) &= \delta c_a \left(\frac{F^2}{\mathcal{C}_{11}} \frac{d\mathcal{C}_{12}}{dr} - \frac{C_1(r^2\mathcal{C}_{12}^2 - \mathcal{C}_{11}^4)}{r^2\mathcal{C}_{11}^3} - \frac{\mathcal{C}_{12}(2C_1 - F^2)}{r\mathcal{C}_{11}} + \frac{\mathcal{C}_{11}(F^2 - 1)}{r^2} \right).
 \end{aligned} \tag{B.2}$$

The function coefficients in the axial perturbed field equations $\delta\mathcal{E}_{[13]}$ in (3.52b) are

$$\begin{aligned}
\mathcal{F}_{31}(r) &= \frac{\delta c_a}{F^2} \left(i\omega + \frac{r\mathcal{C}_{12} + \mathcal{C}_{11}^2}{r\mathcal{C}_{11}} \right), \\
\mathcal{F}_{32}(r) &= -\frac{\delta c_a}{r^2}, \\
\mathcal{F}_{33}(r) &= \frac{\mathcal{F}_{12}\mathcal{F}_{31}}{\mathcal{F}_{11}}, \\
\mathcal{F}_{34}(r) &= \delta c_a \left(\frac{\ell(\ell+1)}{r^2} - \frac{\omega^2}{F^2} - \frac{(r\mathcal{C}_{12} + \mathcal{C}_{11}^2)^2}{r^2 F^2 \mathcal{C}_{11}^2} \right) \\
\mathcal{F}_{35}(r) &= -\delta c_a \frac{2(\mathcal{C}_1 - F^2)}{r^3 F^2}, \\
\mathcal{F}_{36}(r) &= \frac{\mathcal{F}_{11}\mathcal{F}_{31}}{\mathcal{F}_{21}}, \quad \mathcal{F}_{37}(r) = \frac{\mathcal{F}_{27}\mathcal{F}_{31}}{\mathcal{F}_{21}}.
\end{aligned} \tag{B.3}$$

The function coefficients in the axial perturbed field equations $\delta\mathcal{E}_{[23]}$ in (3.52c) are

$$\begin{aligned}
\mathcal{F}_{41}(r) &= -\mathcal{F}_{21}, \\
\mathcal{F}_{42}(r) &= -\delta c_a \ell(\ell+1)F^2, \\
\mathcal{F}_{43}(r) &= -\delta c_a \frac{3F^2 - 1}{r}, \\
\mathcal{F}_{44}(r) &= -\delta c_a \frac{\ell(\ell+1)}{F^2} \left(i\omega + \frac{2\mathcal{C}_{11}}{r} \right), \\
\mathcal{F}_{45}(r) &= \delta c_a \ell(\ell+1) \frac{2\mathcal{C}_1 + F^2 - 1}{r}, \\
\mathcal{F}_{46}(r) &= \delta c_a \frac{r^2\omega^2 + 2r\mathcal{C}_{12} + \mathcal{C}_1(F^2 + 1) + F^2(4F^2 - 6)}{r^2 F^2}.
\end{aligned} \tag{B.4}$$

Appendix C

SymPy code in Jupyter Notebook

The following is the SymPy code used to find background and perturbed field equations in Chapter 3. Runtime is displayed for cells that take longer than 1 minute.

```
[1]: from sympy import *

import sympy.tensor.tensor as st
from sympy.tensor.operators import PartialDerivative

from IPython.display import Latex, Math
init_printing()
```

```
[2]: #Rationalize floats:
def R(n): return nsimplify(n)

#Symmetric and antisymmetric brackets:
def symb(T, m, n): return R(1/2)*(T + T.subs({m:i0, n:i1}).subs({i0:n, i1:m}))
def asymb(T, m, n): return R(1/2)*(T - T.subs({m:i0, n:i1}).subs({i0:n, i1:m}))

#Partial derivative:
def PD(A, x):
    i, iA = x.get_indices()[0], A.get_indices()

    PD = st.TensorHead('∂'+A.components[0].name, [ST]*(len(iA)+1))

    iA_dict = [[i1,i2,i3][k] if iA[k].is_up==False else -[i1,i2,i3][k] for k in range(len(iA))]
    if i.is_up==True:
        tensor_dict.update({PD(i0, *iA_dict): PartialDerivative(A, x).replace_with_arrays(tensor_dict)})
    elif i.is_up==False:
        tensor_dict.update({PD(-i0, *iA_dict): PartialDerivative(A, x).replace_with_arrays(tensor_dict)})

    return PD(-i, *iA)

#Covariant derivative:
def bar_nabla(i, T, connection='GR'):
    iT = T.get_indices()

    if connection=='GR': Gamma=bar_Gamma_ring
    elif connection=='TG': Gamma=bar_Gamma_dot

    covariantD = PD(T, coord(-i))

    l = st.TensorIndex('l', ST, is_up=False)
    for k in range(len(iT)):
        if iT[k].is_up==True: covariantD += Gamma(iT[k], l, i)*T.subs(iT[k], -l)
        elif iT[k].is_up==False: covariantD += -Gamma(-l, iT[k], i)*T.subs(iT[k], l)

    return covariantD
```

```
[3]: #Coordinates:
t, r = symbols('t,r',positive=True)
theta, phi = symbols('theta,phi',real=True)

#Lagrangian constants:
c_a, c_t, c_v = R(3/2), R(2/3), -R(2/3)
dca = symbols('δc_a')
```

```

#Schwarzschild:
M_bullet, omega = symbols('M_{\bullet}', positive=True), symbols('\omega')

F = Function('F', positive=True)(r)
B, B_func = Function('B', positive=True)(r), 1-2*M_bullet/r

dF_subs = {diff(F,r): (1-F**2)/(2*r*F),
            diff(F,r,2): diff((1-F**2)/(2*r*F)).doit().subs(diff(F,r),(1-F**2)/(2*r*F))}

#Spherical harmonics:
L, M = symbols('L', nonnegative=True, integer=True), symbols('M', integer=True)

Y_LM = Function('Y_{LM}', real=True)(theta,phi)
YLM_diff_rules = {diff(Y_LM,theta,2): -1/tan(theta)*diff(Y_LM,theta) - (L*(L+1)-M**2/sin(theta)**2)*Y_LM,
                  diff(Y_LM,phi): I*M*Y_LM,
                  diff(Y_LM,phi,2): -M**2*Y_LM,
                  M:0}

#Tetrad functions:
#C_1, C_5 = Function('C_1')(r), Function('C_5')(r)
C_1, C_5 = Function('C_1')(r), r

C_4= C_1/F**2 #C_4= -C_1/F**2 if C_1 < 0
C_3, C_6 = sqrt(C_1**2-F**2), sqrt(r**2-C_5**2)
C_2 = C_3*C_4/C_1

```

```

[4]: #Spacetime indices:
ST = st.TensorIndexType('SpaceTime', dummy_name='lambda', dim=4)

mu, nu = st.TensorIndex('mu', ST, is_up=False), st.TensorIndex('nu', ST, is_up=False)
rho, sigma = st.TensorIndex('rho', ST, is_up=False), st.TensorIndex('sigma', ST, is_up=False)
alpha, beta = st.TensorIndex('alpha', ST, is_up=False), st.TensorIndex('beta', ST, is_up=False)
gamma, kappa = st.TensorIndex('gamma', ST, is_up=False), st.TensorIndex('kappa', ST, is_up=False)

i0, i1 = st.TensorIndex('i0', ST, is_up=False), st.TensorIndex('i1', ST, is_up=False)
i2, i3 = st.TensorIndex('i2', ST, is_up=False), st.TensorIndex('i3', ST, is_up=False)

#Lorentz indices:
LZ = st.TensorIndexType('Lz', dummy_name='c', dim=4)

b0, b1 = st.TensorIndex('b0', LZ, is_up=True), st.TensorIndex('b1', LZ, is_up=True)
c0, c1 = st.TensorIndex('c0', LZ, is_up=True), st.TensorIndex('c1', LZ, is_up=True)

#Tensors:
coord = st.TensorHead('x', [ST])
eta_down, eta_up = st.TensorHead('\eta_{down}', [ST]*2), st.TensorHead("\eta_{up}", [ST]*2)

tensor_dict = {coord(-i0): [t,r,theta,phi], eta_down(c0,c1): diag(-1,1,1,1), eta_up(-c0,-c1):
↳diag(-1,1,1,1)}

```

1 Background equations

```

[5]: #Define tensors:
bar_tet = st.TensorHead('\overline{\theta}', [LZ,ST])
bar_e = st.TensorHead('\overline{e}', [LZ,ST])

bar_g = st.TensorHead('\overline{g}', [ST]*2)
bar_G = st.TensorHead('\overline{G}', [ST]*2)
bar_eps = st.TensorHead('\overline{e}', [ST]*4)

bar_Gamma_dot = st.TensorHead('\dot{\overline{\Gamma}}', [ST]*3)
bar_Gamma_ring = st.TensorHead('\mathring{\overline{\Gamma}}', [ST]*3)

bar_T = st.TensorHead('\overline{T}', [ST]*3)

```

```

bar_mfv = st.TensorHead('\overline{\mathfrak{v}}', [ST])
bar_mfa = st.TensorHead('\overline{\mathfrak{a}}', [ST])
bar_mft = st.TensorHead('\overline{\mathfrak{t}}', [ST]*3)

```

```

[6]: #Tetrad:
bg_tet = Matrix([[C_1, C_2, 0, 0],
                 [C_3*sin(theta)*cos(phi), C_4*sin(theta)*cos(phi),
                  C_5*cos(theta)*cos(phi)-C_6*sin(phi), -(C_5*sin(phi)+C_6*cos(theta)*cos(phi))*sin(theta)],
                 [C_3*sin(theta)*sin(phi), C_4*sin(theta)*sin(phi),
                  C_5*cos(theta)*sin(phi)+C_6*cos(phi), (C_5*cos(phi)-C_6*cos(theta)*sin(phi))*sin(theta)],
                 [C_3*cos(theta), C_4*cos(theta), -C_5*sin(theta), C_6*sin(theta)**2]])

bg_e = (bg_tet.T).inv()

tensor_dict.update({bar_tet(c0,i0): bg_tet, bar_e(-c0,-i0): bg_e})

#Metric:
bg_g = eta_up(-b0,-b1)*bar_tet(b0,mu)*bar_tet(b1,nu)
bg_g = bg_g.replace_with_arrays(tensor_dict, [mu,nu]).tomatrix().applyfunc(simplify)

bg_G = eta_down(b0,b1)*bar_e(-b0,-mu)*bar_e(-b1,-nu)
bg_G = bg_G.replace_with_arrays(tensor_dict, [-mu,-nu]).tomatrix().applyfunc(simplify)

tensor_dict.update({bar_g(i0,i1): bg_g, bar_G(-i0,-i1): bg_G})

#Levi-Civita symbol:
sqrt_det_bg_g = sqrt(abs(det(bg_g))).subs(abs(sin(theta)),sin(theta))
bg_eps = [[[[sqrt_det_bg_g*LeviCivita(i,j,k,m) for m in range(4)] for k in range(4)] for j in range(4)] for i in range(4)]

tensor_dict.update({bar_eps(i0,i1,i2,i3): bg_eps})

#Connections:
bg_Gamma_dot = bar_e(-b0,-rho)*PD(bar_tet(b0,mu),coord(-nu))
bg_Gamma_dot = bg_Gamma_dot.replace_with_arrays(tensor_dict, [-rho,mu,nu]).applyfunc(simplify)

bg_Gamma_ring = R(1/2)*bar_G(-rho,-alpha)*(PD(bar_g(nu,alpha),coord(-mu)) + PD(bar_g(mu,alpha),coord(-nu))\
- PD(bar_g(mu,nu),coord(-alpha)))
bg_Gamma_ring = bg_Gamma_ring.replace_with_arrays(tensor_dict, [-rho,mu,nu]).applyfunc(simplify)

tensor_dict.update({bar_Gamma_dot(-i0,i1,i2): bg_Gamma_dot,
                    bar_Gamma_ring(-i0,i1,i2): bg_Gamma_ring})

#Torsion:
bg_T = bar_Gamma_dot(-rho,nu,mu) - bar_Gamma_dot(-rho,mu,nu)
bg_T = bg_T.replace_with_arrays(tensor_dict, [-rho,mu,nu]).applyfunc(simplify)

tensor_dict.update({bar_T(-i0,i1,i2): bg_T})

#Tensors \mf{v}, \mf{a}, \mf{t}:
bg_mfv = bar_T(-alpha,alpha,mu)
bg_mfv = bg_mfv.replace_with_arrays(tensor_dict, [mu]).applyfunc(simplify)

bg_mfa = R(1/6)*bar_eps(mu,kappa,rho,sigma)*bar_G(-alpha,-rho)*bar_G(-beta,-sigma)*bar_T(-kappa,alpha,beta)
bg_mfa = bg_mfa.replace_with_arrays(tensor_dict, [mu]).applyfunc(simplify)

bg_mft = symb(bar_g(mu,alpha)*bar_T(-alpha,nu,rho),mu,nu) \
+R(1/3)*(symb(bar_T(-alpha,alpha,mu)*bar_g(nu,rho),mu,nu)-bar_T(-alpha,alpha,rho)*bar_g(mu,nu))
bg_mft = bg_mft.replace_with_arrays(tensor_dict, [mu,nu,rho]).applyfunc(simplify)

tensor_dict.update({bar_mfv(i0): bg_mfv,
                    bar_mfa(i0): bg_mfa,
                    bar_mft(i0,i1,i2): bg_mft})

```

```

[7]: #For running speed:
bar_MFT = st.TensorHead('\overline{\mathfrak{t}}', [ST]*3)

```

```

bg_MFT = (bar_mft(mu,beta,gamma)*bar_G(-beta,-nu)*bar_G(-gamma,-rho)).replace_with_arrays(tensor_dict,
↳[mu,-nu,-rho]).applyfunc(simplify)

bar_EPS = st.TensorHead('\overline{\mathcal{e}}', [ST]*4)
bg_EPS = (bar_eps(mu,nu,alpha,beta)*bar_G(-alpha,-rho)*bar_G(-beta,-sigma)).
↳replace_with_arrays(tensor_dict, [mu,nu,-rho,-sigma]).applyfunc(simplify)

tensor_dict.update({bar_MFT(i0,-i1,-i2): bg_MFT,
                    bar_EPS(i0,i1,-i2,-i3): bg_EPS})

```

```

[8]: #Background field equations:
bg_Eq \
= (c_a+dca)*(R(1/6)*bar_G(-rho,-alpha)*bar_mfa(alpha)*(bar_mfa(rho)*bar_g(mu,nu)+bar_mfa(mu)*bar_g(rho,nu)\
+ bar_mfa(nu)*bar_g(rho,mu)) \
-R(4/9)*bar_eps(nu,alpha,beta,gamma)*bar_G(-alpha,-kappa)*bar_mfa(kappa)\
*bar_MFT(mu,-beta,-gamma) \
-R(2/9)*bar_EPS(mu,nu,-alpha,-beta)*bar_mfa(alpha)*bar_mfv(beta) \
+R(1/3)*bar_EPS(mu,nu,-alpha,-beta)*bar_nabla(alpha, bar_mfa(beta))) + \
+ c_t*(R(2/3)*asymb(bar_mft(alpha,beta,gamma),beta,gamma)*bar_G(-alpha,-kappa)\
*bar_MFT(kappa,-beta,-gamma)*bar_g(mu,nu) \
-R(4/3)*asymb(bar_mft(mu,rho,sigma),rho,sigma)*bar_MFT(nu,-rho,-sigma) \
+2*bar_G(-rho,-alpha)*asymb(bar_nabla(alpha, bar_mft(mu,nu,rho)),nu,rho) \
-R(2/3)*asymb(bar_mft(nu,mu,rho),mu,rho)*bar_G(-rho,-alpha)*bar_mfv(alpha) \
+R(1/2)*bar_eps(mu,alpha,beta,gamma)*bar_G(-alpha,-kappa)*bar_mfa(kappa)*bar_MFT(nu,-beta,-gamma))\
+ c_v*(R(1/6)*bar_G(-rho,-alpha)*bar_mfv(alpha)*bar_mfv(rho)*bar_g(mu,nu)+bar_mfv(mu)*bar_g(rho,nu)\
+ bar_mfv(nu)*bar_g(mu,rho)) \
+R(4/3)*asymb(bar_mft(mu,rho,nu),rho,nu)*bar_G(-rho,-alpha)*bar_mfv(alpha) \
+2*bar_G(-rho,-alpha)*asymb(bar_nabla(alpha, bar_mfv(rho))*bar_g(nu,mu),rho,nu) \
-R(1/2)*bar_EPS(mu,nu,-alpha,-beta)*bar_mfa(alpha)*bar_mfv(beta))

bg_fieldEq = cancel(simplify(bg_Eq.replace_with_arrays(tensor_dict, [mu,nu]).tomatrix()))
bg_fieldEq = trigsimp(cancel(expand(bg_fieldEq.subs(dF_subs).doit())))
bg_fieldEq

```

```

[8]: 
$$\begin{bmatrix} 0 & 0 & 0 & 0 \\ 0 & 0 & 0 & 0 \\ 0 & 0 & 0 & 0 \\ 0 & 0 & 0 & 0 \end{bmatrix}$$


```

2 Perturbed equations

```

[9]: #Define tensors:
h = st.TensorHead('h', [ST]*2)
dh_mfv = st.TensorHead('\delta\mathfrak{v}(h)', [ST])
dh_mfa = st.TensorHead('\delta\mathfrak{a}(h)', [ST])
dh_mft = st.TensorHead('\delta\mathfrak{t}(h)', [ST]*3)
dh_Gamma_ring = st.TensorHead('\delta\mathring{\overline{\Gamma}}', [ST]*3)

a = st.TensorHead('a', [ST]*2)
da_mfv = st.TensorHead('\delta\mathfrak{v}(a)', [ST])
da_mfa = st.TensorHead('\delta\mathfrak{a}(a)', [ST])
da_mft = st.TensorHead('\delta\mathfrak{t}(a)', [ST]*3)

```

```

[10]: #Symmetric perturbations:
h_0, h_1 = Function('h_0', real=True), Function('h_1', real=True)
H_0, H_1, H_2, K = Function('H_0', real=True), Function('H_1', real=True), Function('H_2', real=True),
↳Function('K', real=True)

h_ax_02, h_ax_03 = 0, h_0(t,r)*sin(theta)*diff(Y_LM, theta)
h_ax_12, h_ax_13 = 0, h_1(t,r)*sin(theta)*diff(Y_LM, theta)

h_pol_01 = H_1(t,r)*Y_LM
h_pol_00, h_pol_11 = H_0(t,r)*F**2*Y_LM, H_2(t,r)*1/F**2*Y_LM
h_pol_22, h_pol_33 = K(t,r)*r**2*Y_LM, K(t,r)*r**2*sin(theta)**2*Y_LM

```

```

h_axial = Matrix([[0,0,h_ax_02,h_ax_03],[0,0,h_ax_12,h_ax_13],[h_ax_02,h_ax_12,0,0],[h_ax_03,h_ax_13,0,0]])
h_polar = Matrix([[h_pol_00,h_pol_01,0,0],[h_pol_01,h_pol_11,0,0],[0,0,h_pol_22,0],[0,0,0,h_pol_33]])

tensor_dict.update({h(i0,i1): h_axial+h_polar})

H = st.TensorHead('\mathcal{h}', [ST]*2)
tensor_dict.update({H(-i0,-i1): (h(rho,sigma)*bar_G(-rho,-mu)*bar_G(-sigma,-nu)).
→replace_with_arrays(tensor_dict, [-mu,-nu]).applyfunc(simplify)})

h_trace = simplify((h(mu,nu)*bar_G(-mu,-nu)).replace_with_arrays(tensor_dict))

#Antisymmetric perturbations:
a_0, a_1, a_2 = Function('a_0', real=True), Function('a_1', real=True), Function('a_2', real=True)
A_0, A_1, A_2 = Function('A_0', real=True), Function('A_1', real=True), Function('A_2', real=True)

a_ax_02, a_ax_03 = 0, a_0(t,r)*sin(theta)*diff(Y_LM, theta)
a_ax_12, a_ax_13 = 0, a_1(t,r)*sin(theta)*diff(Y_LM, theta)
a_ax_23 = -a_2(t,r)*sin(theta)*Y_LM

a_pol_01 = A_0(t,r)*Y_LM
a_pol_02, a_pol_03 = A_1(t,r)*diff(Y_LM, theta), 0
a_pol_12, a_pol_13 = A_2(t,r)*diff(Y_LM, theta), 0

a_axial = Matrix([[0,0,a_ax_02,a_ax_03],[0,0,a_ax_12,a_ax_13],
[-a_ax_02,-a_ax_12,0,a_ax_23],[-a_ax_03,-a_ax_13,-a_ax_23,0]])
a_polar = Matrix([[0,a_pol_01,a_pol_02,a_pol_03],[-a_pol_01,0,a_pol_12,a_pol_13],
[-a_pol_02,-a_pol_12,0,0],[-a_pol_03,-a_pol_13,0,0]])

tensor_dict.update({a(i0,i1): a_axial+a_polar})

```

2.1 Defining field equations:

```

[11]: %%time
#Perturbation of \mf{v}
delta_mfv_h = asymb(bar_nabla(sigma,h(mu,kappa),'TG'),sigma,mu)*bar_G(-kappa,-sigma)
delta_mfv_h = (delta_mfv_h.replace_with_arrays(tensor_dict, [mu])).subs(YLM_diff_rules).doit().
→applyfunc(cancel)

delta_mfv_a = -asymb(bar_nabla(sigma,a(mu,kappa),'TG'),sigma,mu)*bar_G(-kappa,-sigma)
delta_mfv_a = (delta_mfv_a.replace_with_arrays(tensor_dict, [mu])).subs(YLM_diff_rules).doit().
→applyfunc(cancel)

tensor_dict.update({dh_mfv(i0): delta_mfv_h, da_mfv(i0): delta_mfv_a})

#Perturbation of \mf{a}
delta_mfa_h = R(1/2)*h_trace*bar_mfa(mu)\
-R(1/6)*bar_eps(mu,nu,rho,sigma)*(bar_G(-alpha,-rho)*H(-beta,-sigma)\
+ H(-alpha,-rho)*bar_G(-beta,-sigma))*bar_T(-nu,alpha,beta)\
+R(1/6)*asymb(bar_nabla(alpha,h(beta,kappa),'TG'),alpha,beta)*bar_EPS(mu,nu,-alpha,-beta)\
*bar_G(-kappa,-nu)
delta_mfa_h = (delta_mfa_h.replace_with_arrays(tensor_dict, [mu])).subs(YLM_diff_rules).doit().
→applyfunc(cancel)

delta_mfa_a = -R(1/6)*asymb(bar_nabla(alpha,a(beta,kappa),'TG'),alpha,beta)*bar_EPS(mu,nu,-alpha,-beta)\
*bar_G(-kappa,-nu)
delta_mfa_a = (delta_mfa_a.replace_with_arrays(tensor_dict, [mu])).subs(YLM_diff_rules).doit().
→applyfunc(cancel)

tensor_dict.update({dh_mfa(i0): delta_mfa_h, da_mfa(i0): delta_mfa_a})

#Perturbation of \mf{t}
delta_mft_h = symb(h(sigma,mu)*bar_T(-sigma,nu,rho),mu,nu)\
+symb(asymb(bar_nabla(nu,h(rho,mu),'TG'),nu,rho),nu,mu)\
+R(1/3)*(symb(bar_mfv(mu)*h(nu,rho),mu,nu) - bar_mfv(rho)*h(mu,nu))\
+R(1/3)*(symb(dh_mfv(mu)*bar_g(nu,rho),mu,nu) - dh_mfv(rho)*bar_g(mu,nu))

```

```

delta_mft_h = (delta_mft_h.replace_with_arrays(tensor_dict, [mu,nu,rho])).subs(YLM_diff_rules).doit().
→applyfunc(cancel)

delta_mft_a = -symb(asymb(bar_nabla(nu,a(rho,mu),'TG'),nu,rho),nu,mu)\
+R(1/3)*(symb(da_mfv(mu)*bar_g(nu,rho),mu,nu) - da_mfv(rho)*bar_g(mu,nu))
delta_mft_a = (delta_mft_a.replace_with_arrays(tensor_dict, [mu,nu,rho])).subs(YLM_diff_rules).doit().
→applyfunc(cancel)

tensor_dict.update({dh_mft(i0,i1,i2): delta_mft_h, da_mft(i0,i1,i2): delta_mft_a})

#Perturbtion of the Christoffel symbols:
delta_Gamma_ring = R(1/2)*bar_G(-rho,-kappa)*(bar_nabla(mu,h(nu,kappa)) + bar_nabla(nu,h(mu,kappa))\
- bar_nabla(kappa,h(mu,nu)))
delta_Gamma_ring = (delta_Gamma_ring.replace_with_arrays(tensor_dict, [-rho,mu,nu])).applyfunc(cancel)

tensor_dict.update({dh_Gamma_ring(-i0,i1,i2): delta_Gamma_ring})

```

CPU times: user 1min 27s, sys: 767 ms, total: 1min 28s
Wall time: 1min 29s

```

[12]: #For checking the TEGR perturbed field equations:
dh_Riemann = st.TensorHead('δ\mathcal{R}', [ST]*4)
delta_Riemann = PD(dh_Gamma_ring(-rho,nu,sigma),coord(-mu)) - PD(dh_Gamma_ring(-rho,mu,sigma),coord(-nu)) \
+ bar_Gamma_ring(-rho,mu,alpha)*dh_Gamma_ring(-alpha,nu,sigma) \
+ dh_Gamma_ring(-rho,mu,alpha)*bar_Gamma_ring(-alpha,nu,sigma) \
- bar_Gamma_ring(-rho,nu,alpha)*dh_Gamma_ring(-alpha,mu,sigma) \
- dh_Gamma_ring(-rho,nu,alpha)*bar_Gamma_ring(-alpha,mu,sigma)
delta_Riemann = delta_Riemann.replace_with_arrays(tensor_dict, [-rho,sigma,mu,nu]).applyfunc(expand)

tensor_dict.update({dh_Riemann(-i0,i1,i2,i3): delta_Riemann})

dh_Ein = (dh_Riemann(-kappa,mu,kappa,nu) \
- R(1/2)*(bar_g(mu,nu)*bar_G(-rho,-sigma)*dh_Riemann(-kappa,rho,kappa,sigma)))
→replace_with_arrays(tensor_dict, [mu,nu]).tomatrix()
dh_Ein = expand(dh_Ein).subs(YLM_diff_rules).doit().subs(YLM_diff_rules).doit()
dh_Ein = cancel(trigsimp(dh_Ein.subs(dF_subs).doit()))

```

```

[13]: #For running speed:
bar_mft_hG_Gh = st.TensorHead('(\overline{G}+\overline{G}h)\overline{\mathfrak{t}}', [ST]*3)
bg_mft_hG_Gh = (H(-nu,-alpha)*bar_G(-rho,-beta) + bar_G(-nu,-alpha)*H(-rho,-beta))*bar_mft(mu,alpha,beta)
bg_mft_hG_Gh = bg_mft_hG_Gh.replace_with_arrays(tensor_dict, [mu,-nu,-rho]).applyfunc(simplify)
tensor_dict.update({bar_mft_hG_Gh(i0,-i1,-i2): bg_mft_hG_Gh})

```

```

[14]: %%time
#Field equations with h:
tens_Eq_TEGR_h \
= c_a*(R(1/6)*(bar_G(-rho,-alpha)*dh_mfa(alpha)*(bar_mfa(rho)*bar_g(mu,nu) + bar_mfa(mu)*bar_g(rho,nu)\
+ bar_mfa(nu)*bar_g(rho,mu))\
+ bar_G(-rho,-alpha)*bar_mfa(alpha)*(dh_mfa(rho)*bar_g(mu,nu) + dh_mfa(mu)*bar_g(rho,nu)\
+ dh_mfa(nu)*bar_g(rho,mu))\
- H(-rho,-alpha)*bar_mfa(alpha)*(bar_mfa(rho)*bar_g(mu,nu) + bar_mfa(mu)*bar_g(rho,nu)\
+ bar_mfa(nu)*bar_g(rho,mu))\
+ bar_G(-rho,-alpha)*bar_mfa(alpha)*(bar_mfa(rho)*h(mu,nu) + bar_mfa(mu)*h(rho,nu)\
+ bar_mfa(nu)*h(rho,mu))\
-R(4/9)*(bar_G(-kappa,-alpha)*bar_EPS(nu,alpha,-rho,-sigma)*(dh_mfa(kappa)*bar_mft(mu,rho,sigma)\
+ bar_mfa(kappa)*dh_mft(mu,rho,sigma))\
- bar_mfa(kappa)*bar_mft(mu,rho,sigma)*(bar_EPS(nu,alpha,-rho,-sigma)*H(-kappa,-alpha)\
- bar_EPS(nu,beta,-kappa,-sigma)*H(-beta,-rho)\
+ bar_EPS(nu,gamma,-kappa,-rho)*H(-gamma,-sigma)))\
-R(2/9)*(bar_EPS(mu,nu,-alpha,-beta)*(dh_mfa(alpha)*bar_mfv(beta) + bar_mfa(alpha)*dh_mfv(beta))\
- bar_eps(mu,nu,rho,sigma)*bar_mfa(alpha)*bar_mfv(beta)\
*(H(-rho,-alpha)*bar_G(-sigma,-beta)\
+ bar_G(-rho,-alpha)*H(-sigma,-beta)))\
-R(1/3)*(bar_EPS(mu,nu,-alpha,-beta)*(bar_nabla(alpha,dh_mfa(beta))\
- dh_Gamma_ring(-kappa,beta,alpha)*bar_mfa(kappa))\
- bar_eps(mu,nu,rho,sigma)*bar_nabla(alpha,bar_mfa(beta))\

```

```

*(H(-rho,-alpha)*bar_G(-sigma,-beta)\
+ bar_G(-rho,-alpha)*H(-sigma,-beta))\
-R(1/18)*h_trace*(4*bar_EPS(nu,alpha,-rho,-sigma)*bar_G(-kappa,-alpha)*bar_mfa(kappa)\
*bar_mft(mu,rho,sigma)\
+ bar_EPS(mu,nu,-alpha,-beta)*(2*bar_mfa(alpha)*bar_mfv(beta)\
+ 3*bar_nabla(alpha,bar_mfa(beta))))\
+ c_t*(R(2/3)*(bar_G(-alpha,-kappa)\
*bar_g(mu,nu)*(asymb(dh_mft(alpha,beta,gamma),beta,gamma)*bar_MFT(kappa,-beta,-gamma)\
+ asymb(bar_MFT(alpha,-rho,-sigma),-rho,-sigma)*dh_mft(kappa,rho,sigma))\
- asymb(bar_mft(alpha,beta,gamma),beta,gamma)\
*bar_g(mu,nu)*(bar_MFT(kappa,-beta,-gamma)*H(-alpha,-kappa)\
+ bar_G(-alpha,-kappa)*bar_mft_hG_Gh(kappa,-beta,-gamma))\
+ asymb(bar_mft(alpha,beta,gamma),beta,gamma)*bar_G(-alpha,-kappa)\
*bar_MFT(kappa,-beta,-gamma)*h(mu,nu))\
-R(4/3)*(asymb(dh_mft(mu,rho,sigma),rho,sigma)*bar_MFT(nu,-rho,-sigma)\
+ asymb(bar_MFT(mu,-alpha,-beta),-alpha,-beta)*dh_mft(nu,alpha,beta)\
- asymb(bar_mft(mu,rho,sigma),rho,sigma)*bar_mft_hG_Gh(nu,-rho,-sigma))\
+2*(bar_G(-rho,-alpha)*(asymb(bar_nabla(alpha,dh_mft(mu,nu,rho)),nu,rho)\
- dh_Gamma_ring(-kappa,mu,alpha)*asymb(bar_mft(kappa,nu,rho),nu,rho)\
- dh_Gamma_ring(-kappa,nu,alpha)*asymb(bar_mft(mu,kappa,rho),kappa,rho)\
- dh_Gamma_ring(-kappa,rho,alpha)*asymb(bar_mft(mu,nu,kappa),nu,kappa))\
- H(-rho,-alpha)*asymb(bar_nabla(alpha,bar_mft(mu,nu,rho)),nu,rho))\
-R(2/3)*(bar_G(-rho,-alpha)*(asymb(dh_mft(nu,mu,rho),mu,rho)*bar_mfv(alpha)\
+ asymb(bar_mft(nu,mu,rho),mu,rho)*dh_mfv(alpha))\
- H(-rho,-alpha)*asymb(bar_mft(nu,mu,rho),mu,rho)*bar_mfv(alpha))\
+R(1/2)*(bar_G(-alpha,-kappa)*bar_EPS(mu,alpha,-rho,-sigma)*(dh_mfa(kappa)*bar_mft(nu,rho,sigma)\
+ bar_mfa(kappa)*dh_mft(nu,rho,sigma))\
- bar_mfa(kappa)*bar_mft(nu,rho,sigma)*(bar_EPS(mu,alpha,-rho,-sigma)*H(-alpha,-kappa)\
- bar_EPS(mu,beta,-kappa,-sigma)*H(-beta,-rho)\
+ bar_EPS(mu,gamma,-kappa,-rho)*H(-gamma,-sigma)))\
+R(1/4)*h_trace*bar_EPS(mu,alpha,-rho,-sigma)*bar_G(-alpha,-kappa)*bar_mfa(kappa)\
*bar_mft(nu,rho,sigma))\
+ c_v*(R(1/6)*(bar_G(-rho,-alpha)*dh_mfv(alpha)*(bar_mfv(rho)*bar_g(mu,nu) + bar_mfv(mu)*bar_g(rho,nu)\
+ bar_mfv(nu)*bar_g(rho,mu))\
+ bar_G(-rho,-alpha)*bar_mfv(alpha)*(dh_mfv(rho)*bar_g(mu,nu) + dh_mfv(mu)*bar_g(rho,nu)\
+ dh_mfv(nu)*bar_g(rho,mu))\
- H(-rho,-alpha)*bar_mfv(alpha)*(bar_mfv(rho)*bar_g(mu,nu) + bar_mfv(mu)*bar_g(rho,nu)\
+ bar_mfv(nu)*bar_g(rho,mu))\
+ bar_G(-rho,-alpha)*bar_mfv(alpha)*(bar_mfv(rho)*h(mu,nu) + bar_mfv(mu)*h(rho,nu)\
+ bar_mfv(nu)*h(rho,mu))\
+R(4/3)*(bar_G(-rho,-alpha)*(asymb(dh_mft(mu,rho,nu),rho,nu)*bar_mfv(alpha)\
+ asymb(bar_mft(mu,rho,nu),rho,nu)*dh_mfv(alpha))\
- H(-rho,-alpha)*asymb(bar_mft(mu,rho,nu),rho,nu)*bar_mfv(alpha))\
+2*(bar_G(-rho,-alpha)*(asymb(bar_nabla(alpha,dh_mfv(rho))*bar_g(nu,mu),rho,nu)\
- asymb(dh_Gamma_ring(-kappa,alpha,rho)*bar_g(nu,mu),rho,nu)*bar_mfv(kappa))\
- H(-rho,-alpha)*asymb(bar_nabla(alpha,bar_mfv(rho))*bar_g(nu,mu),rho,nu)\
+ bar_G(-rho,-alpha)*asymb(bar_nabla(alpha,bar_mfv(rho))*h(nu,mu),rho,nu))\
-R(1/2)*(bar_EPS(mu,nu,-alpha,-beta)*(dh_mfa(alpha)*bar_mfv(beta) + bar_mfa(alpha)*dh_mfv(beta))\
- bar_eps(mu,nu,rho,sigma)*bar_mfa(alpha)*bar_mfv(beta)\
*(H(-rho,-alpha)*bar_G(-sigma,-beta)\
+ bar_G(-rho,-alpha)*H(-sigma,-beta))\
-R(1/4)*h_trace*bar_EPS(mu,nu,-alpha,-beta)*bar_mfa(alpha)*bar_mfv(beta)

tens_Eq_dca_h \
= dca*(R(1/6)*(bar_G(-rho,-alpha)*dh_mfa(alpha)*(bar_mfa(rho)*bar_g(mu,nu) + bar_mfa(mu)*bar_g(rho,nu)\
+ bar_mfa(nu)*bar_g(rho,mu))\
+ bar_G(-rho,-alpha)*bar_mfa(alpha)*(dh_mfa(rho)*bar_g(mu,nu) + dh_mfa(mu)*bar_g(rho,nu)\
+ dh_mfa(nu)*bar_g(rho,mu))\
- H(-rho,-alpha)*bar_mfa(alpha)*(bar_mfa(rho)*bar_g(mu,nu) + bar_mfa(mu)*bar_g(rho,nu)\
+ bar_mfa(nu)*bar_g(rho,mu))\
- bar_G(-rho,-alpha)*bar_mfa(alpha)*(bar_mfa(rho)*h(mu,nu) + bar_mfa(mu)*h(rho,nu)\
+ bar_mfa(nu)*h(rho,mu))\
-R(4/9)*(bar_G(-kappa,-alpha)*bar_EPS(nu,alpha,-rho,-sigma)*(dh_mfa(kappa)*bar_mft(mu,rho,sigma)\
+ bar_mfa(kappa)*dh_mft(mu,rho,sigma))\
- bar_mfa(kappa)*bar_mft(mu,rho,sigma)*(bar_EPS(nu,alpha,-rho,-sigma)*H(-kappa,-alpha)\
- bar_EPS(nu,beta,-kappa,-sigma)*H(-beta,-rho)\
+ bar_EPS(nu,gamma,-kappa,-rho)*H(-gamma,-sigma)))\

```

```

-R(2/9)*(bar_EPS(mu,nu,-alpha,-beta)*(dh_mfa(alpha)*bar_mfv(beta) + bar_mfa(alpha)*dh_mfv(beta))\
- bar_eps(mu,nu,rho,sigma)*bar_mfa(alpha)*bar_mfv(beta)\
      *(H(-rho,-alpha)*bar_G(-sigma,-beta)\
      + bar_G(-rho,-alpha)*H(-sigma,-beta)))\
-R(1/3)*(bar_EPS(mu,nu,-alpha,-beta)*(bar_nabla(alpha,dh_mfa(beta))\
      + dh_Gamma_ring(-kappa,beta,alpha)*bar_mfa(kappa))\
- bar_eps(mu,nu,rho,sigma)*bar_nabla(alpha,bar_mfa(beta))\
      *(H(-rho,-alpha)*bar_G(-sigma,-beta)\
      + bar_G(-rho,-alpha)*H(-sigma,-beta)))\
-R(1/18)*h_trace*(4*bar_EPS(nu,alpha,-rho,-sigma)*bar_G(-kappa,-alpha)\
      *bar_mfa(kappa)*bar_mft(mu,rho,sigma)\
      + bar_EPS(mu,nu,-alpha,-beta)*(2*bar_mfa(alpha)*bar_mfv(beta)\
      + 3*bar_nabla(alpha,bar_mfa(beta))))

```

CPU times: user 1min 19s, sys: 535 ms, total: 1min 20s
Wall time: 1min 21s

```

[15]: #Field equations with a:
tens_Eq_TEGR_a \
= c_a*(R(1/6)*(bar_G(-rho,-alpha)*da_mfa(alpha)*(bar_mfa(rho)*bar_g(mu,nu) + bar_mfa(mu)*bar_g(rho,nu)\
      + bar_mfa(nu)*bar_g(rho,mu))\
      + bar_G(-rho,-alpha)*bar_mfa(alpha)*(da_mfa(rho)*bar_g(mu,nu) + da_mfa(mu)*bar_g(rho,nu)\
      + da_mfa(nu)*bar_g(rho,mu)))\
-R(4/9)*bar_G(-kappa,-alpha)*bar_EPS(nu,alpha,-rho,-sigma)*(da_mfa(kappa)*bar_mft(mu,rho,sigma)\
      + bar_mfa(kappa)*da_mft(mu,rho,sigma))\
-R(2/9)*bar_EPS(mu,nu,-alpha,-beta)*(da_mfa(alpha)*bar_mfv(beta) + bar_mfa(alpha)*da_mfv(beta))\
-R(1/3)*bar_EPS(mu,nu,-alpha,-beta)*bar_nabla(alpha,da_mfa(beta))\
+ c_t*(R(2/3)*bar_G(-alpha,-kappa)\
      *(asymb(da_mft(alpha,beta,gamma),beta,gamma)*bar_MFT(kappa,-beta,-gamma)\
      + asymb(bar_MFT(alpha,-rho,-sigma),-rho,-sigma)*da_mft(kappa,rho,sigma))*bar_g(mu,nu)\
-R(4/3)*(asymb(da_mft(mu,rho,sigma),rho,sigma)*bar_MFT(nu,-rho,-sigma)\
      + asymb(bar_MFT(mu,-alpha,-beta),-alpha,-beta)*da_mft(nu,alpha,beta))\
+2*bar_G(-rho,-alpha)*asymb(bar_nabla(alpha,da_mft(mu,nu,rho)),nu,rho)\
-R(2/3)*bar_G(-rho,-alpha)*(asymb(da_mft(nu,mu,rho),mu,rho)*bar_mfv(alpha)\
      + asymb(bar_mft(nu,mu,rho),mu,rho)*da_mfv(alpha))\
+R(1/2)*bar_G(-alpha,-kappa)*bar_EPS(mu,alpha,-rho,-sigma)*(da_mfa(kappa)*bar_mft(nu,rho,sigma)\
      + bar_mfa(kappa)*da_mft(nu,rho,sigma)))\
+ c_v*(R(1/6)*(bar_G(-rho,-alpha)*da_mfv(alpha)*(bar_mfv(rho)*bar_g(mu,nu) + bar_mfv(mu)*bar_g(rho,nu)\
      + bar_mfv(nu)*bar_g(rho,mu))\
      + bar_G(-rho,-alpha)*bar_mfv(alpha)*(da_mfv(rho)*bar_g(mu,nu) + da_mfv(mu)*bar_g(rho,nu)\
      + da_mfv(nu)*bar_g(rho,mu)))\
+R(4/3)*bar_G(-rho,-alpha)*(asymb(da_mft(mu,rho,nu),rho,nu)*bar_mfv(alpha)\
      + asymb(bar_mft(mu,rho,nu),rho,nu)*da_mfv(alpha))\
+2*bar_G(-rho,-alpha)*asymb(bar_nabla(alpha,da_mfv(rho))*bar_g(nu,mu),rho,nu)\
-R(1/2)*bar_EPS(mu,nu,-alpha,-beta)*(da_mfa(alpha)*bar_mfv(beta) + bar_mfa(alpha)*da_mfv(beta))

tens_Eq_dca_a \
= dca*(R(1/6)*(bar_G(-rho,-alpha)*da_mfa(alpha)*(bar_mfa(rho)*bar_g(mu,nu) + bar_mfa(mu)*bar_g(rho,nu)\
      + bar_mfa(nu)*bar_g(rho,mu))\
      + bar_G(-rho,-alpha)*bar_mfa(alpha)*(da_mfa(rho)*bar_g(mu,nu) + da_mfa(mu)*bar_g(rho,nu)\
      + da_mfa(nu)*bar_g(rho,mu)))\
-R(4/9)*bar_G(-kappa,-alpha)*bar_EPS(nu,alpha,-rho,-sigma)*(da_mfa(kappa)*bar_mft(mu,rho,sigma)\
      + bar_mfa(kappa)*da_mft(mu,rho,sigma))\
-R(2/9)*bar_EPS(mu,nu,-alpha,-beta)*(da_mfa(alpha)*bar_mfv(beta) + bar_mfa(alpha)*da_mfv(beta))\
-R(1/3)*bar_EPS(mu,nu,-alpha,-beta)*bar_nabla(alpha,da_mfa(beta))

```

2.2 Finding field equations

```

[16]: %%time
Eq_TEGR_h = tens_Eq_TEGR_h.replace_with_arrays(tensor_dict, [mu,nu]).tomatrix()
Eq_TEGR_a = tens_Eq_TEGR_a.replace_with_arrays(tensor_dict, [mu,nu]).tomatrix()

Eq_dca_h = tens_Eq_dca_h.replace_with_arrays(tensor_dict, [mu,nu]).tomatrix()
Eq_dca_a = tens_Eq_dca_a.replace_with_arrays(tensor_dict, [mu,nu]).tomatrix()

```

CPU times: user 5min 56s, sys: 2.76 s, total: 5min 59s

Wall time: 6min 3s

```
[17]: %%time
Eq_TEGR_h = expand(Eq_TEGR_h).subs(YLM_diff_rules).doit().subs(YLM_diff_rules).doit()
Eq_TEGR_a = expand(Eq_TEGR_a).subs(YLM_diff_rules).doit().subs(YLM_diff_rules).doit()

Eq_dca_h = expand(Eq_dca_h).subs(YLM_diff_rules).doit().subs(YLM_diff_rules).doit()
Eq_dca_a = expand(Eq_dca_a).subs(YLM_diff_rules).doit().subs(YLM_diff_rules).doit()
```

CPU times: user 2min 43s, sys: 1.03 s, total: 2min 44s
Wall time: 2min 46s

```
[18]: %%time
Eq_TEGR_h = cancel(trigsimp(Eq_TEGR_h.subs(dF_subs).doit()))
Eq_TEGR_a = cancel(trigsimp(Eq_TEGR_a.subs(dF_subs).doit()))
display((trigsimp(expand_trig(cancel(dh_Ein-Eq_TEGR_h))), Eq_TEGR_a))
```

$$\left(\begin{array}{cccc} 0 & 0 & 0 & 0 \\ 0 & 0 & 0 & 0 \\ 0 & 0 & 0 & 0 \\ 0 & 0 & 0 & 0 \end{array} \right), \left(\begin{array}{cccc} 0 & 0 & 0 & 0 \\ 0 & 0 & 0 & 0 \\ 0 & 0 & 0 & 0 \\ 0 & 0 & 0 & 0 \end{array} \right)$$

CPU times: user 2min 42s, sys: 1.08 s, total: 2min 43s
Wall time: 2min 45s

```
[19]: %%time
Eq_dca_h = cancel(trigsimp(Eq_dca_h.subs(dF_subs).doit()))
Eq_dca_a = cancel(trigsimp(Eq_dca_a.subs(dF_subs).doit()))
```

CPU times: user 4min 28s, sys: 1.69 s, total: 4min 30s
Wall time: 4min 33s

```
[20]: %%time
Eq_total = cancel(Eq_TEGR_h + Eq_TEGR_a + Eq_dca_h + Eq_dca_a)

Eq_trace = trigsimp(expand(trace(bg_G*Eq_total)))
Eq_total = cancel(Eq_total - R(1/2)*bg_g*Eq_trace)

sym_fieldEq = ones(4)
asym_fieldEq = ones(4)

ij = [(0,0),(0,1),(0,2),(0,3),(1,1),(1,2),(1,3),(2,2),(2,3),(3,3)]

for i,j in ij:
    sym_fieldEq[i,j] = factor(expand(R(1/2)*(Eq_total[i,j] + Eq_total[j,i])))
    sym_fieldEq[j,i] = sym_fieldEq[i,j]

    asym_fieldEq[i,j] = factor(expand(R(1/2)*(Eq_total[i,j] - Eq_total[j,i])))
    asym_fieldEq[j,i] = -asym_fieldEq[i,j]
```

CPU times: user 1min 14s, sys: 470 ms, total: 1min 14s
Wall time: 1min 15s

```
[21]: #Simplifying equations:
harmonic_time_dep = {h_0(t,r): h_0(r)*exp(-I*t*omega), h_1(t,r): h_1(r)*exp(-I*t*omega),
                    H_0(t,r): H_0(r)*exp(-I*t*omega), H_1(t,r): H_1(r)*exp(-I*t*omega),
                    H_2(t,r): H_2(r)*exp(-I*t*omega), K(t,r): K(r)*exp(-I*t*omega),
                    a_0(t,r): a_0(r)*exp(-I*t*omega), a_1(t,r): a_1(r)*exp(-I*t*omega),
                    a_2(t,r): a_2(r)*exp(-I*t*omega), A_0(t,r): A_0(r)*exp(-I*t*omega),
                    A_1(t,r): A_1(r)*exp(-I*t*omega), A_2(t,r): A_2(r)*exp(-I*t*omega)}

def my_fieldeq_simplify(Eq, times=1):
    #Find radial equation:
    non_radial_Eq = 1
    for arg in Eq.args:
        if ('theta' in str(arg)) or (arg.is_rational==True) or (str(arg)=='L') or (str(arg)=='L+1'):
            non_radial_Eq = arg*non_radial_Eq
    new_Eq = expand(cancel(times*Eq/non_radial_Eq))
```

```

if str((t,r)) in str(new_Eq):
    new_Eq = expand(new_Eq.subs(harmonic_time_dep).doit()*exp(I*t*omega))

new_Eq = collect(new_Eq, {h_0(r),h_1(r),a_0(r),a_1(r),a_2(r),H_0(r),H_1(r),H_2(r),K(r),
    A_0(r),A_1(r),A_2(r)})

#Simplify coefficients:
Eq_coeffs = [diff(h_0(r),r,2), diff(h_0(r)), h_0(r), diff(h_1(r),r,2), diff(h_1(r)), h_1(r),
    diff(a_0(r),r,2), diff(a_0(r)), a_0(r), diff(a_1(r),r,2), diff(a_1(r)), a_1(r),
    diff(a_2(r),r,2), diff(a_2(r)), a_2(r), diff(H_0(r),r,2), diff(H_0(r)), H_0(r),
    diff(H_1(r),r,2), diff(H_1(r)), H_1(r), diff(H_2(r),r,2), diff(H_2(r)), H_2(r),
    diff(K(r),r,2), diff(K(r)), K(r), diff(A_0(r),r,2), diff(A_0(r)), A_0(r),
    diff(A_1(r),r,2), diff(A_1(r)), A_1(r), diff(A_2(r),r,2), diff(A_2(r)), A_2(r)]

for arg in Eq_coeffs:
    new_Eq = new_Eq.subs(new_Eq.coeff(arg)*arg, cancel(new_Eq.coeff(arg))*arg)

return new_Eq

Q_11 = Function('Q_{11}') (r) #Q_11 = sqrt(C_1**2 - F**2)
Q_12 = Function('Q_{12}') (r) #Q_12 = F*(F*diff(C_1) - C_1*diff(F))

Q_subs = {diff(C_1): (Q_12/F**2 + C_1*diff(F)/F).subs(dF_subs),
    sqrt(C_1**2-F**2): Q_11, sqrt((C_1-F)*(C_1+F)): Q_11, (C_1-F)*(C_1+F): Q_11**2,
    C_1**2: Q_11**2+F**2, C_1**3: C_1*(Q_11**2+F**2), C_1**5: C_1**3*(Q_11**2+F**2),
    C_1**7: C_1**5*(Q_11**2+F**2), C_1**9: C_1**7*(Q_11**2+F**2), C_1**11: C_1**9*(Q_11**2+F**2)}

```

2.3 Polar pertubed field equations

```

[22]: %%time
display(Latex('Component $\delta E_{[01]}/2$:'))
asym_fieldEq_01 = my_fieldeq_simplify(asym_fieldEq[0,1], times=R(1/2))
asym_fieldEq_01 = asym_fieldEq_01.subs(asym_fieldEq_01.coeff(A_2(r)),\
    cancel(apart(asym_fieldEq_01.coeff(A_2(r)),sqrt(C_1**2-F**2))))
display(Math(latex(collect(my_fieldeq_simplify(asym_fieldEq_01.subs(Q_subs)),dca))+'\equiv 0.'))

display(Latex('Component $\delta E_{(12)}^{\delta c_a}/4$:'))
sym_fieldEq_12_dca = factor(dca*expand(sym_fieldEq[1,2]).coeff(dca,1))
sym_fieldEq_12_dca = my_fieldeq_simplify(sym_fieldEq_12_dca, times=R(1/4))
#Write using dE_{01}
P_3 = cancel(sym_fieldEq_12_dca.coeff(diff(A_1(r)))/asym_fieldEq_01.coeff(diff(A_1(r))))
display(Math('\delta E_{(12)}^{\delta c_a} - P_3(r) \delta E_{[01]} = ' \
    + latex(cancel(sym_fieldEq_12_dca - P_3*asym_fieldEq_01)) \
    + ',\quad P_3(r) = ' + latex(factor(cancel(P_3.subs(Q_subs)))))

display(Latex('Component $\delta E_{(02)}^{\delta c_a}/4$:'))
sym_fieldEq_02_dca = factor(dca*expand(sym_fieldEq[0,2]).coeff(dca,1))
sym_fieldEq_02_dca = my_fieldeq_simplify(sym_fieldEq_02_dca, times=R(1/4))
#Write using dE_{01}
P_1 = cancel(sym_fieldEq_02_dca.coeff(diff(A_1(r)))/asym_fieldEq_01.coeff(diff(A_1(r))))
display(Math('\delta E_{(02)}^{\delta c_a} - P_1(r) \delta E_{[01]} = ' \
    + latex(cancel(sym_fieldEq_02_dca - P_1*asym_fieldEq_01)) \
    + ',\quad P_1(r) = ' + latex(factor(cancel(P_1.subs(Q_subs)))))

display(Latex('(This means that $\delta E_{(12)}^{\delta c_a} \equiv 0$ and $\delta E_{(02)}^{\delta c_a} \equiv 0$.'))

display(Latex('Component $\delta E_{[02]}/4$:'))
asym_fieldEq_02 = my_fieldeq_simplify(asym_fieldEq[0,2], times=R(1/4))
#Write using dE_{01}
P_4 = cancel(asym_fieldEq_02.coeff(diff(A_1(r),r,2))/asym_fieldEq_01.coeff(diff(A_1(r),r)))
P_5 = cancel(expand(asym_fieldEq_02-(diff(P_4*asym_fieldEq_01,r).doit()).subs(dF_subs)).coeff(A_1(r))\
    asym_fieldEq_01.coeff(A_1(r)))
display(Math('\delta E_{[02]} - d_r(P_4(r))\delta E_{[01]} - P_5(r) \delta E_{[01]} = ' + \
    latex(cancel(asym_fieldEq_02 - diff(P_4*asym_fieldEq_01,r).doit()).subs(dF_subs) \
    - P_5*asym_fieldEq_01)) \
    + ',\quad P_4(r) = ' + latex(factor(cancel(P_4.subs(Q_subs))))) \

```

```
+ ',\quad P_5(r)=' + latex(factor(cancel(P_5.subs(Q_subs))))))
```

```
display(Latex('Component $\delta E_{[12]}/4$:'))
asym_fieldEq_12 = my_fieldeq_simplify(asym_fieldEq[1,2], times=R(1/4))
#Write using dE_{01}
P_2 = cancel(asym_fieldEq_12.coeff(diff(A_1(r)))/asym_fieldEq_01.coeff(diff(A_1(r))))
display(Math('\delta E_{[12]} - P_2(r) \delta E_{[01]} = ' \
+ latex(cancel(asym_fieldEq_12 - P_2*asym_fieldEq_01)) \
+ ',\quad P_2(r) = '+latex(factor(cancel(P_2.subs(Q_subs))))))
```

Component $\delta E_{[01]}/2$:

$$\delta c_a \left(\frac{A_0(r)}{r^2} - \frac{d}{dr} \frac{A_1(r)}{r^2} + \frac{(-ir\omega Q_{11}(r) + rQ_{12}(r) + Q_{11}^2(r))A_2(r)}{r^3 Q_{11}(r)} + \frac{(-2C_1(r) + F^2(r) + 1)A_1(r)}{2r^3 F^2(r)} \right) \equiv 0.$$

Component $\delta E_{(12)}^{\delta c_a}/4$:

$$\delta E_{(12)}^{\delta c_a} - P_3(r)\delta E_{[01]} = 0, \quad P_3(r) = \frac{r(rQ_{12}(r) - Q_{11}^2(r))}{F^2(r)Q_{11}(r)}$$

Component $\delta E_{(02)}^{\delta c_a}/4$:

$$\delta E_{(02)}^{\delta c_a} - P_1(r)\delta E_{[01]} = 0, \quad P_1(r) = \frac{r(2C_1(r) - 3F^2(r) + 1)}{2}$$

(This means that $\delta E_{(12)}^{GR} \equiv 0$ and $\delta E_{(02)}^{GR} \equiv 0$.)

Component $\delta E_{[02]}/4$:

$$\delta E_{[02]} - d_r(P_4(r)\delta E_{[01]}) - P_5(r)\delta E_{[01]} = 0, \quad P_4(r) = r^2 F^2(r), \quad P_5(r) = -\frac{r(2C_1(r) - 3F^2(r) + 1)}{2}$$

Component $\delta E_{[12]}/4$:

$$\delta E_{[12]} - P_2(r)\delta E_{[01]} = 0, \quad P_2(r) = \frac{ir(r\omega Q_{11}(r) - irQ_{12}(r) - iQ_{11}^2(r))}{F^2(r)Q_{11}(r)}$$

CPU times: user 2min 13s, sys: 776 ms, total: 2min 13s
Wall time: 2min 18s

```
[23]: display(Latex('Component $\delta E_{(01)}/(-2i\omega)$:'))
sym_fieldEq_01 = sym_fieldEq[0,1].subs(H_2(t,r),H_0(t,r)).doit()
sym_fieldEq_01 = my_fieldeq_simplify(sym_fieldEq_01, times=1/(-2*I*omega))
display(Math(latex(sym_fieldEq_01.subs(F**2,B))+'\equiv 0. '))

display(Latex('Component $\delta E_{(02)}^{\delta c_a}$:'))
sym_fieldEq_02_TEGR = factor(cancel(expand(sym_fieldEq[0,2]).coeff(dca,0)).subs(H_2(t,r),H_0(t,r)).doit())
sym_fieldEq_02_TEGR = my_fieldeq_simplify(sym_fieldEq_02_TEGR)
display(Math(latex(sym_fieldEq_02_TEGR.subs(F**2,B))+'\equiv 0. '))

display(Latex('Component $\delta E_{(12)}^{\delta c_a} \cdot B/2$:'))
sym_fieldEq_12_TEGR = factor(cancel(expand(sym_fieldEq[1,2]).coeff(dca,0)).subs(H_2(t,r),H_0(t,r)).doit())
sym_fieldEq_12_TEGR = my_fieldeq_simplify(sym_fieldEq_12_TEGR, times=F**2/2)
display(Math(latex(sym_fieldEq_12_TEGR.subs(F**2,B))+'\equiv 0. '))

display(Latex('Component $\delta E_{(00)}/2$:'))
sym_fieldEq_00 = sym_fieldEq[0,0].subs(H_2(t,r),H_0(t,r)).doit()
sym_fieldEq_00 = my_fieldeq_simplify(sym_fieldEq_00, times=R(1/2))
display(Math(latex(sym_fieldEq_00.subs(F**2,B))+'\equiv 0. '))

display(Latex('Component $\delta E_{(11)} \cdot B^2/2$:'))
sym_fieldEq_11 = sym_fieldEq[1,1].subs(H_2(t,r),H_0(t,r)).doit()
sym_fieldEq_11 = my_fieldeq_simplify(sym_fieldEq_11, times=F**4/2)
display(Math(latex(sym_fieldEq_11.subs(F**2,B))+'\equiv 0. '))

display(Latex('Component $\delta E_{(22)}$:'))
sym_fieldEq_22 = factor(sym_fieldEq[2,2].subs(H_2(t,r),H_0(t,r)).doit())
sym_fieldEq_22 = my_fieldeq_simplify(sym_fieldEq_22)
```

```
display(Math(latex(sym_fieldEq_22.subs(F**2,B))+'\equiv 0.'))
```

Component $\delta E_{(01)}/(-2i\omega)$:

$$\frac{d}{dr}K(r) + \frac{(3B(r)-1)K(r)}{2rB(r)} - \frac{H_0(r)}{r} + \frac{(-iL^2 - iL)H_1(r)}{2r^2\omega} \equiv 0.$$

Component $\delta E_{(02)}^{GR}$:

$$-i\omega H_0(r) - i\omega K(r) - B(r)\frac{d}{dr}H_1(r) + \frac{(B(r)-1)H_1(r)}{r} \equiv 0.$$

Component $\delta E_{(12)}^{GR} \cdot B/2$:

$$\frac{i\omega H_1(r)}{2} + \frac{B(r)\frac{d}{dr}H_0(r)}{2} - \frac{B(r)\frac{d}{dr}K(r)}{2} + \frac{(1-B(r))H_0(r)}{2r} \equiv 0.$$

Component $\delta E_{(00)}/2$:

$$\begin{aligned} & -2\omega^2 K(r) + 2i\omega B(r)\frac{d}{dr}H_1(r) + B^2(r)\frac{d^2}{dr^2}H_0(r) + \frac{(3i\omega B(r) + i\omega)H_1(r)}{r} + \frac{(B^2(r) - B(r))\frac{d}{dr}K(r)}{r} + \frac{2B(r)\frac{d}{dr}H_0(r)}{r} + \\ & \frac{(-L^2 B(r) - LB(r) - r^2\omega^2)H_0(r)}{r^2} \equiv 0. \end{aligned}$$

Component $\delta E_{(11)} \cdot B^2/2$:

$$\begin{aligned} & 2i\omega B(r)\frac{d}{dr}H_1(r) + B^2(r)\frac{d^2}{dr^2}H_0(r) - 2B^2(r)\frac{d^2}{dr^2}K(r) + \frac{(-i\omega B(r) + i\omega)H_1(r)}{r} + \frac{(-3B^2(r) - B(r))\frac{d}{dr}K(r)}{r} + \frac{2B(r)\frac{d}{dr}H_0(r)}{r} + \\ & \frac{(L^2 B(r) + LB(r) - r^2\omega^2)H_0(r)}{r^2} \equiv 0. \end{aligned}$$

Component $\delta E_{(22)}$:

$$r^2 B(r)\frac{d^2}{dr^2}K(r) - 2ir\omega H_1(r) - 2rB(r)\frac{d}{dr}H_0(r) + (3rB(r) + r)\frac{d}{dr}K(r) + \frac{(-L^2 B(r) - LB(r) + r^2\omega^2 + 2B(r))K(r)}{B(r)} - 2H_0(r) \equiv 0.$$

2.4 Axial perturbed field equations

```
[24]: %%time
sym_fieldEq_13_dca = factor(cancel(dca*expand(sym_fieldEq[1,3]).coeff(dca)))
sym_fieldEq_13_dca = my_fieldeq_simplify(sym_fieldEq_13_dca, times=R(1/4))

sym_fieldEq_03_dca = factor(cancel(dca*expand(sym_fieldEq[0,3]).coeff(dca)))
sym_fieldEq_03_dca = my_fieldeq_simplify(sym_fieldEq_03_dca, times=R(1/4))

display(Latex('We can find that'))

kappa_ax = cancel(sym_fieldEq_13_dca.coeff(diff(a_0(r)))/sym_fieldEq_03_dca.coeff(diff(a_0(r))))
display(Math('\delta E_{(13)}^{\delta c_a} - \kappa_{ax}\delta E_{(03)}^{\delta c_a} = ' \
+ latex(cancel(sym_fieldEq_13_dca - kappa_ax*sym_fieldEq_03_dca)) \
+ ', \quad \kappa_{ax} = ' + latex(factor(cancel(kappa_ax.subs(Q_subs))))))
display(Latex('This means that $R_{(13)}^{GR} - \kappa_{ax}R_{(03)}^{GR} \equiv 0$, \
so $R_{(13)}^{GR} \equiv 0$ and $R_{(03)}^{GR} \equiv 0$.'))
```

We can find that

$$\delta E_{(13)}^{\delta c_a} - \kappa_{ax}\delta E_{(03)}^{\delta c_a} = 0, \quad \kappa_{ax} = -\frac{2(rQ_{12}(r) - Q_{11}^2(r))}{(2C_1(r) - 3F^2(r) + 1)F^2(r)Q_{11}(r)}$$

This means that $R_{(13)}^{GR} - \kappa_{ax}R_{(03)}^{GR} \equiv 0$, so $R_{(13)}^{GR} \equiv 0$ and $R_{(03)}^{GR} \equiv 0$.

CPU times: user 1min 3s, sys: 152 ms, total: 1min 3s

Wall time: 1min 4s

```
[25]: display(Latex('Component $\delta E_{(23)}$:$'))
sym_fieldEq_23 = my_fieldeq_simplify(sym_fieldEq[2,3], times=-1)
display(Math(latex(sym_fieldEq_23.subs(F**2,B))+'\equiv 0.'))

display(Latex('Component $\delta E_{(13)}^{GR}$:$'))
sym_fieldEq_13_TEGR = factor(cancel(expand(sym_fieldEq[1,3]).coeff(dca,0)))
sym_fieldEq_13_TEGR = my_fieldeq_simplify(sym_fieldEq_13_TEGR, times=-1)
```

```

display(Math(latex(sym_fieldEq_13_TEGR.subs(F**2,B))+'\equiv 0.'))

display(Latex('\delta E_{(03)}^{-GR}'))
sym_fieldEq_03_TEGR = factor(cancel(expand(sym_fieldEq[0,3]).coeff(dca,0)))
sym_fieldEq_03_TEGR = my_fieldeq_simplify(sym_fieldEq_03_TEGR)
display(Math(latex(sym_fieldEq_03_TEGR.subs(F**2,B))+'\equiv 0.'))

```

Component $\delta E_{(23)}$:

$$\frac{i\omega h_0(r)}{B(r)} + B(r) \frac{d}{dr} h_1(r) + \frac{(1-B(r))h_1(r)}{r} \equiv 0.$$

Component $\delta E_{(13)}^{GR}$:

$$\frac{i\omega \frac{d}{dr} h_0(r)}{B(r)} - \frac{2i\omega h_0(r)}{rB(r)} + \frac{(L^2 B(r) + LB(r) - r^2 \omega^2 - 2B(r))h_1(r)}{r^2 B(r)} \equiv 0.$$

Component $\delta E_{(03)}^{GR}$:

$$i\omega B(r) \frac{d}{dr} h_1(r) + B(r) \frac{d^2}{dr^2} h_0(r) + \frac{2i\omega B(r)h_1(r)}{r} + \frac{(-L^2 - L - 2B(r) + 2)h_0(r)}{r^2} \equiv 0.$$

```

[26]: %%time
F_11, F_12, F_13, F_14, F_15 = Function('F_{11}')(r), Function('F_{12}')(r), Function('F_{13}')(r),
    ↪Function('F_{14}')(r), Function('F_{15}')(r)
F_21, F_22, F_23, F_24, F_25, F_26, F_27, F_28, F_29 = Function('F_{21}')(r), Function('F_{22}')(r),
    ↪Function('F_{23}')(r), Function('F_{24}')(r), Function('F_{25}')(r), Function('F_{26}')(r),
    ↪Function('F_{27}')(r), Function('F_{28}')(r), Function('F_{29}')(r)
F_31, F_32, F_33, F_34, F_35, F_36, F_37 = Function('F_{31}')(r), Function('F_{32}')(r),
    ↪Function('F_{33}')(r), Function('F_{34}')(r), Function('F_{35}')(r), Function('F_{36}')(r),
    ↪Function('F_{37}')(r)
F_41, F_42, F_43, F_44, F_45, F_46 = Function('F_{41}')(r), Function('F_{42}')(r), Function('F_{43}')(r),
    ↪Function('F_{44}')(r), Function('F_{45}')(r), Function('F_{46}')(r)

myfieldEq_values = {}

display(Latex('\delta E_{(03)}^{-\delta c_a}/4$'))

myfieldEq1 = sym_fieldEq_03_dca
for func, arg in {F_11:diff(a_0(r)), F_12:a_0(r), F_13:a_1(r), F_14:h_0(r), F_15:h_1(r)}.items():
    myfieldEq_values.update({func: factor(myfieldEq1.coeff(arg))})
    myfieldEq1 = myfieldEq1.subs(myfieldEq1.coeff(arg)*arg, func*arg)
display(Math(latex(myfieldEq1)))

display(Latex('\delta E_{[03]}/4$'))
asym_fieldEq_03 = my_fieldeq_simplify(asym_fieldEq[0,3], times=R(1/4))

myfieldEq2 = asym_fieldEq_03
for func, arg in {F_21:diff(a_0(r),r,2), F_22:diff(a_1(r)), F_23:a_0(r), F_24:a_1(r), F_25:a_2(r), F_26:
    ↪diff(h_0(r)), F_27:diff(h_1(r)), F_28:h_0(r), F_29:h_1(r)}.items():
    myfieldEq_values.update({func: factor(myfieldEq2.coeff(arg))})
    myfieldEq2 = myfieldEq2.subs(myfieldEq2.coeff(arg)*arg, func*arg)
display(Math(latex(myfieldEq2)))

display(Latex('\delta E_{[13]}/4$'))
asym_fieldEq_13 = my_fieldeq_simplify(asym_fieldEq[1,3], times=R(1/4))

myfieldEq3 = asym_fieldEq_13
for func, arg in {F_31:diff(a_0(r)), F_32:diff(a_2(r)), F_33:a_0(r), F_34:a_1(r), F_35:a_2(r), F_36:h_0(r),
    ↪F_37:h_1(r)}.items():
    myfieldEq_values.update({func: factor(myfieldEq3.coeff(arg))})
    myfieldEq3 = myfieldEq3.subs(myfieldEq3.coeff(arg)*arg, func*arg)
display(Math(latex(myfieldEq3)))

display(Latex('\delta E_{[23]}/4$'))
asym_fieldEq_23 = my_fieldeq_simplify(asym_fieldEq[2,3], times=R(1/4))

myfieldEq4 = asym_fieldEq_23

```

```

for func, arg in {F_41:diff(a_2(r),r,2), F_42:diff(a_1(r)), F_43:diff(a_2(r)), F_44:a_0(r), F_45:a_1(r),
↳F_46:a_2(r)}.items():
    myfieldEq_values.update({func: factor(myfieldEq4.coeff(arg))})
myfieldEq4 = myfieldEq4.subs(myfieldEq4.coeff(arg)*arg, func*arg)
display(Math(latex(myfieldEq4)))

```

Component $\delta E_{(03)}^{\delta c_a} / 4$

$$F_{11}(r) \frac{d}{dr} a_0(r) + F_{12}(r) a_0(r) + F_{13}(r) a_1(r) + F_{14}(r) h_0(r) + F_{15}(r) h_1(r)$$

Component $\delta E_{[03]} / 4$

$$F_{21}(r) \frac{d^2}{dr^2} a_0(r) + F_{22}(r) \frac{d}{dr} a_1(r) + F_{23}(r) a_0(r) + F_{24}(r) a_1(r) + F_{25}(r) a_2(r) + F_{26}(r) \frac{d}{dr} h_0(r) + F_{27}(r) \frac{d}{dr} h_1(r) + F_{28}(r) h_0(r) + F_{29}(r) h_1(r)$$

Component $\delta E_{[13]} / 4$

$$F_{31}(r) \frac{d}{dr} a_0(r) + F_{32}(r) \frac{d}{dr} a_2(r) + F_{33}(r) a_0(r) + F_{34}(r) a_1(r) + F_{35}(r) a_2(r) + F_{36}(r) h_0(r) + F_{37}(r) h_1(r)$$

Component $\delta E_{[23]} / 4$

$$F_{41}(r) \frac{d^2}{dr^2} a_2(r) + F_{42}(r) \frac{d}{dr} a_1(r) + F_{43}(r) \frac{d}{dr} a_2(r) + F_{44}(r) a_0(r) + F_{45}(r) a_1(r) + F_{46}(r) a_2(r)$$

CPU times: user 8min 22s, sys: 2.32 s, total: 8min 24s

Wall time: 8min 30s

[27]: Q_myfieldEq_values = {}

```

for func, val in myfieldEq_values.items():
    new_val = cancel(cancel(val).subs(Q_subs).doit()).subs(dF_subs)
    new_val = factor(cancel(new_val.subs(Q_subs)))
    Q_myfieldEq_values.update({func: new_val})

for func in [F_12, F_14]:
    Q_myfieldEq_values.update({func: factor(Q_myfieldEq_values[func].subs(Q_11**2,C_1**2-F**2))})

```

[28]: a1_from_Eq1 = solve(myfieldEq1, a_1(r))[0]

```

myfieldEq2_subs = collect(expand(myfieldEq2.subs(a_1(r), a1_from_Eq1).doit()),{a_0(r),a_2(r),h_0(r),h_1(r)})
for arg in [diff(a_0(r),r,2),diff(a_0(r)),diff(h_0(r)),diff(h_1(r))]:
    myfieldEq2_subs = myfieldEq2_subs.subs(myfieldEq2_subs.coeff(arg)*arg, \
        arg*cancel(myfieldEq2_subs.coeff(arg).subs(myfieldEq_values).doit()).subs(dF_subs)))

a2_from_Eq2 = solve(myfieldEq2_subs, a_2(r))[0]

myfieldEq3_subs = collect(expand(myfieldEq3.subs(a_1(r), a1_from_Eq1).subs(a_2(r), a2_from_Eq2).doit()),
    {a_0(r),h_0(r),h_1(r)})
for arg in [diff(h_0(r),r,2),diff(h_1(r),r,2),diff(h_0(r)),diff(h_1(r))]:
    myfieldEq3_subs = myfieldEq3_subs.subs(myfieldEq3_subs.coeff(arg)*arg, \
        arg*cancel(myfieldEq3_subs.coeff(arg).subs(myfieldEq_values).doit()).subs(dF_subs)))

```

[29]:

```

%%time
M_1, M_2, M_3, M_4 = Function('M_1')(r), Function('M_2')(r), Function('M_3')(r), Function('M_4')(r)
M_funcs = {}

for func, arg in {M_1:diff(a_0(r)), M_2:a_0(r), M_3:h_0(r), M_4:h_1(r)}.items():
    Mi_top, Mi_bottom = fraction(together(myfieldEq3_subs.coeff(arg).subs(myfieldEq_values).doit()))
    #Bottom:
    Mi_bottom = expand(expand(expand(Mi_bottom.subs(Q_subs)).subs(Q_subs)).subs(Q_subs))
    #Top:
    Mi_top = expand(expand(Mi_top.subs(Q_subs).doit()).subs(Q_subs))
    Mi_top = expand(Mi_top.subs(dF_subs).doit()).subs(dF_subs)
    Mi_top = expand(expand(Mi_top.subs(Q_subs).doit()).subs(Q_subs))

M_funcs.update({func: together(Mi_top/Mi_bottom)})

```

CPU times: user 10min 42s, sys: 5.42 s, total: 10min 47s
Wall time: 11min 6s

```
[30]: M_funcs[M_1] = factor(cancel(M_funcs[M_1]))

P = Function('P')(r) #P = I*r*omega*Q_11 - r*Q_12 - Q_11**2
#Change to P = I*r*omega*Q_11 + r*Q_12 - Q_11**2 if C_1 < 0

M2_top=expand(fraction(M_funcs[M_2])[0].subs(Q_12,-(P-I*r*omega*Q_11+Q_11**2)/r))
M2_bot=factor(fraction(M_funcs[M_2])[1].subs(Q_12,-(P-I*r*omega*Q_11+Q_11**2)/r)).subs(Q_11**2,C_1**2-F**2)

new_M2 = 0
for i in range(5):
    M2_top_Pi = factor(factor(factor(M2_top.coeff(P,i)*P**i).subs(Q_11,sqrt(C_1**2-F**2))).subs(Q_subs))
    new_M2 += factor(M2_top_Pi/M2_bot)

M_funcs[M_2] = new_M2
M_funcs[M_3] = factor(cancel(factor(cancel(M_funcs[M_3])).subs(Q_11**2, C_1**2-F**2)).subs(Q_subs))
M_funcs[M_4] = factor(cancel(M_funcs[M_4]))

display(Math(latex(M_1)+'= '+latex(M_funcs[M_1])))
display(Math(latex(M_2)+'= '+latex(M_funcs[M_2])))
display(Math(latex(M_3)+'= '+latex(M_funcs[M_3])))
display(Math(latex(M_4)+'= '+latex(M_funcs[M_4])))
```

$$M_1(r) = \frac{L\delta c_a(L+1)(rQ_{12}(r) - Q_{11}^2(r))}{r(r\omega + 2iQ_{11}(r))(r\omega Q_{11}(r) + irQ_{12}(r) + iQ_{11}^2(r))}$$

$$M_2(r) = -\frac{L\delta c_a(L+1)(2C_1(r) - F^2(r) - 1)Q_{11}(r)}{2r^2F^2(r)P(r)} - \frac{iL\delta c_a(L+1)(4r\omega C_1(r) - 2r\omega F^2(r) + 6iC_1(r)Q_{11}(r) - iF^2(r)Q_{11}(r) - iQ_{11}(r))}{r^2(r\omega + 2iQ_{11}(r))^2F^2(r)} + \frac{2L\delta c_a(L+1)C_1(r)P(r)}{r^2(r\omega + 2iQ_{11}(r))^2F^2(r)Q_{11}(r)}$$

$$M_3(r) = -\frac{iL\delta c_a(L+1)(2C_1(r) - 3F^2(r) + 1)Q_{11}(r)}{2r^2(r\omega Q_{11}(r) + irQ_{12}(r) + iQ_{11}^2(r))F^2(r)}$$

$$M_4(r) = -\frac{iL\delta c_a(L+1)(rQ_{12}(r) - Q_{11}^2(r))}{r^2(r\omega Q_{11}(r) + irQ_{12}(r) + iQ_{11}^2(r))}$$

```
[31]: a0_from_Eq3 = dsolve(M_1*diff(a_0(r))+M_2*a_0(r)+M_3*h_0(r)+M_4*h_1(r), a_0(r),
hint='almost_linear_Integral')
display(a0_from_Eq3)
```

$$a_0(r) = \left(C_1 + \int \frac{(-M_3(r)h_0(r) - M_4(r)h_1(r))e^{\int \frac{M_2(r)}{M_1(r)} dr}}{M_1(r)} dr \right) e^{-\int \frac{M_2(r)}{M_1(r)} dr}$$

```
[32]: a0_for_C1equalsF = myfieldEq3_subs
for func, arg in {M_1:diff(a_0(r)), M_2:a_0(r), M_3:h_0(r), M_4:h_1(r)}.items():
    new_coeff = factor(M_funcs[func].subs(P,I*r*omega*Q_11 + r*Q_12 - Q_11**2).subs(Q_12,0))
    new_coeff = factor(new_coeff.subs(Q_11,0))
    a0_for_C1equalsF = a0_for_C1equalsF.subs(a0_for_C1equalsF.coeff(arg)*arg, new_coeff*arg)
a0_for_C1equalsF = solve(a0_for_C1equalsF,a_0(r))[0]

display(Latex('If $C_1=F$, then'))

display(Math('a_0='+latex(a0_for_C1equalsF)))

a1_for_C1equalsF = together(expand(a1_from_Eq1.subs(Q_myfieldEq_values).subs(Q_12,0).doit()))
a1_for_C1equalsF = factor(a1_for_C1equalsF.subs(Q_11,0).doit())
a1_for_C1equalsF = factor(a1_for_C1equalsF.subs(a_0(r),a0_for_C1equalsF).subs(C_1,F).doit()).subs(dF_subs))
display(Math('a_1='+latex(a1_for_C1equalsF)))

a2_for_C1equalsF = together(expand(a2_from_Eq2.subs(Q_myfieldEq_values).subs(Q_12,0).doit()))
```

```

a2_for_C1equalsF = factor(a2_for_C1equalsF.subs(Q_11,0).doit())
a2_for_C1equalsF = factor(a2_for_C1equalsF.subs(a_0(r),a0_for_C1equalsF).subs(C_1,F).doit()).subs(dF_subs))
display(Math('a_2=' + latex(a2_for_C1equalsF)))

```

If $C_1 = F$, then

$$a_0 = -h_0(r)$$

$$a_1 = -\frac{i\left(rF(r)\frac{d}{dr}h_0(r) - 2F(r)h_0(r) + 2h_0(r)\right)}{r\omega F(r)}$$

$$a_2 = -\frac{iL(L+1)h_0(r)}{\omega}$$

Lihtlitsents lõputöö reprodutseerimiseks ja üldsusele kättesaadavaks tegemiseks

Mina, Helen Asuküla,

1. annan Tartu Ülikoolile tasuta loa (lihtlitsentsi) minu loodud teose

Quasinormal modes of Schwarzschild black holes in 1-parameter New General Relativity,

mille juhendajad on Manuel Hohmann, PhD, Christian Pfeifer, PhD ja João Luís Rosa, PhD, reprodutseerimiseks eesmärgiga seda säilitada, sealhulgas lisada digitaalarhiivi DSpace kuni autoriõiguse kehtivuse lõppemiseni.

2. Annan Tartu Ülikoolile loa teha punktis 1 nimetatud teos üldsusele kättesaadavaks Tartu Ülikooli veebikeskkonna, sealhulgas digitaalarhiivi DSpace kaudu Creative Commons'i litsentsiga CC BY NC ND 3.0, mis lubab autorile viidates teost reprodutseerida, levitada ja üldsusele suunata ning keelab luua tuletatud teost ja kasutada teost ärieesmärgil, kuni autoriõiguse kehtivuse lõppemiseni.
3. Olen teadlik, et punktides 1 ja 2 nimetatud õigused jäävad alles ka autorile.
4. Kinnitan, et lihtlitsentsi andmisega ei riku ma teiste isikute intellektuaalomandi ega isikuandmete kaitse õigusaktidest tulenevaid õigusi.

Helen Asuküla

3. juuni 2021. a.